Architecture of A Cognitive Non-Line-of-Sight Backhaul for 5G Outdoor Urban Small cells

BY

Bessie Malila

A thesis submitted for the degree of

Doctor of Philosophy

in the Department of Electrical Engineering,

Faculty of Engineering and the Built Environment, University of Cape Town

July 2017

Supervisors: Associate Professor Olabisi Falowo, Mr. Neco Ventura

I, the undersigned, Bessie Malila, hereby, attests that the research exposed in this thesis titled "Architecture of A Cognitive Non-Line-of-Sight Backhaul for 5G Outdoor Urban Small cells", is original and that it has not been and will not be used to pursue or attain any other academic degree of any level at any other academic institution, be it foreign or South African.

Signature:_____

Date :24/07/2017

Dedication

To my late beloved husband, Sonke Malila Ndebele, who encouraged me to pursue my dream of undertaking PhD studies. Will forever miss you.

To my supportive parents, Mr. Oliver Majuru and Mrs Violet Tagarira Majuru, who have always raised the academic performance bar for us, their children, from the tender age of primary school.

To my brothers and sisters for being there for me through their financial and moral support during the studies: Erica Uzanda and Rambayi Majuru; and my boys: Victor Malila, Vusani Malila and Jacob Malila .

Acknowledgements

First and foremost, I would like to thank God for giving me the strength to continuously work hard throughout, the wisdom to make the right decisions and the courage to face and overcome the many challenges that I faced during the PhD journey.

I am greatly indebted to my supervisors, Associate Professor Olabisi Falowo and the Head of the Centre for Broadband Networks, Mr. Neco Ventura. Their supervision and mentorship throughout the study period was of great value and encouragement in shaping my research work.

My sincere appreciation is extended to the MimoTech research team who have shared their valuable suggestions and evaluations throughout the course of this work.

My appreciation also goes to the 2013-2017 CRG research team for their technical support, comments and compliments throughout my studies.

Finally, a very special thank you to my family for your unwavering support; my late husband Sonke Malila Ndebele and my boys Victor Malila, Vusani Malila and Jacob Malila; my dear parents, Mr. and Mrs Oliver Majuru and the Malila family for their support during the tragic passing on of my husband during my studies and their continued support throughout the rest of study period.

Contents

Abstract

Densely deployed small cell networks will address the growing demand for broadband mobile connectivity, by increasing access network capacity and coverage. However, most potential small cell base station (SCBS) locations do not have existing telecommunication infrastructure. Providing backhaul connectivity to core networks is therefore a challenge. Millimeter wave (mmW) technologies operated at 30-90GHz are currently being considered to provide low-cost, flexible, high-capacity and reliable backhaul solutions using existing roof-mounted backhaul aggregation sites. Using intelligent mmW radio devices and massive multiple-input multiple-output (MIMO), for enabling point-to-multipoint (PtMP) operation, is considered in this research.

The core aim of this research is to develop an architecture of an intelligent non-line-sight (NLOS) small cell backhaul (SCB) system based on mmW and massive MIMO technologies, and supporting intelligent algorithms to facilitate reliable NLOS street-to-rooftop NLOS SCB connectivity. In the proposed architecture, diffraction points are used as signal anchor points between backhaul radio devices. In the new architecture the integration of these technologies is considered. This involves the design of efficient artificial intelligence algorithms to enable backhaul radio devices to autonomously select suitable NLOS propagation paths, find an optimal number of links that meet the backhaul performance requirements and determine an optimal number of diffractions points capable of covering predetermined SCB locations. Throughout the thesis, a number of algorithms are developed and simulated using the MATLAB application.

This thesis mainly investigates three key issues: First, a novel intelligent NLOS SCB architecture, termed the cognitive NLOS SCB (CNSCB) system is proposed to enable street-to-rooftop NLOS connectivity using predetermined diffraction points located on roof edges. Second, an algorithm to enable the autonomous creation

of multiple-paths, evaluate the performance of each link and determine an optimal number of possible paths per backhaul link is developed. Third, an algorithm to determine the optimal number of diffraction points that can cover an identified SCBS location is also developed. Also, another investigated issue related to the operation of the proposed architecture is its energy efficiency, and its performance is compared to that of a point-to-point (PtP) architecture.

The proposed solutions were examined using analytical models, simulations and experimental work to determine the strength of the street-to-rooftop backhaul links and their ability to meet current and future SCB requirements. The results obtained showed that reliable multiple NLOS links can be achieved using device intelligence to guide radio signals along the propagation path. Furthermore, the PtMP architecture is found to be more energy efficient than the PtP architecture. The proposed architecture and algorithms offer a novel backhaul solution for outdoor urban small cells.

Finally, this research shows that traditional techniques of addressing the demand for connectivity, which consisted of improving or evolving existing solutions, may no-longer be applicable in emerging communication technologies. There is therefore need to consider new ways of solving the emerging challenges.

List of Abbreviations

3GPP	3rd Generation Partnership Project
5G	5th Generation
5GPPP	5th Generation Public Private Partnership Project
ABR	Aggregation Backhaul Radio
AN	Aggregator node
API	Application Programming Interface
BBU	Base Band Unit
CAPEX	Capital Expenditure
CMOS	Complementary Metal Oxide Semiconductor
C-RAN	Cloud Radio Access Network
D2D	Device to Device
DSL	digital Subscriber Line
DPP	Disjoint Path Problem
eICIC	enhanced Inter-cell Interference Coordination
eNB	evolved Node B
feICIC	further enhanced Inter-cell Interference Coordination
GA	Genetic Algorithm
Gbps	Gigabits per second
GHz	Gigahertz
HBR	Hub Backhaul Radio

HetNet	Heterogeneous Networks
HSPA	High Speed Packet Access
ICIC	Inter-cell Interference Coordination
IoT	Internet of Things
LoS	LoS of Sight
LTE	Long Term Evolution
MBS	Macro-cell Base Station
MHz	Megahertz
MIMO	Multiple-input Multiple-output
mmW	Millimeter wave
NGMN	Next Generation Mobile Network
NLOS	Non-Line-of-sight
OPEX	Operational Expenditure
PtMP	Point-to-Multipoint
PtP	Point-to-Point
QoE	Quality of Experience
QoS	Quality of Service
RAT	Radio access Technology
RRU	Remote Radio Unit
SBR	Street Backhaul Radio
SCB	Small Cell Backbone
SCBS	Small Cell Base Station
SCF	Small Cell Forum
SDN	Software Defined Networking
SINR	Signal-to-Interference plus Noise Ratio
SKED	Siingle Knife Edge Diffraction
SON	Self-organising Network

SPF	Shortest Path First
SPP	Shortest Path Problem
SWMN	Self-organising Wireless Mesh Network
UDN	Ultra-dense Network
UE	User equipment

List of Tables

List of Figures

Chapter 1

Introduction

1.1 Research Background

Mobile network operators are currently faced by unprecedented demand for mobile broadband connectivity, with network traffic forecast to reach ten times current levels by 2020 [1]. Emerging technologies such as devices-to-device (D2D) communications, machine-to-machine (M2M) communications and Internet of things (IoT) are expected to be dominant as networks evolve to the fifth generation cellular systems (5G)[2]. These technologies are expected to generate additional traffic, thus, increasing the demand for connectivity on the access networks. The increase in network traffic is, being accompanied by decline in revenues, as users opt for low-cost data-based communications enabled by applications such as WhatsApp and Skype. Network operators are therefore faced with the challenge of finding strategies to increase network capacity and coverage while keeping capital and operational costs low.

A number of strategies have been adopted to address this challenge on the access network [3]. Coverage and capacity gains have been achieved by adding more sectors per base station, increasing the number of base stations and accessing new

spectrum. In addition to this, the use of advanced antenna technologies such as multiple-input-multiple-output (MIMO), increasing transmitter/receiver order of diversity and using higher order modulation techniques, have also been implemented on existing systems [3]. However, these improvements have technological and physical limitations. For example, use of higher order MIMO is constrained by the physical size of equipment, power consumption, and implementation costs. Furthermore, increasing the number of macro base stations can only be done to a certain extent, since it becomes increasingly difficult and expensive as the number of required base stations increases. For example in urban areas, the space becomes a problem for large numbers of macro base stations.

The introduction of new technologies by the third generation partnership project (3GPP) such as high-speed packet access (HSPA), long-term evolution (LTE) and LTE-advanced (LTE-A) was also aimed at improving data rates on the access networks. In addition to this, heterogeneous access networks (HetNets) consisting of different radio access technologies have also been introduced to cost-effectively increase network capacity and provide ubiquitous coverage. HetNets provide seamless network coverage to different zones ranging from indoor, office buildings, homes and open outdoor spaces. Most popular among these are densely deployed small cell networks. Small cell networks are operator-managed mobile networks consisting of low-power, low-cost base stations, operated in licensed spectrum bands [4]. They have the same functionalities as macro base stations but have a much smaller form factor. Small cell technologies include Femto, Pico and Micro cell, in order of increasing base station power, with base station coverage radius of up to 10m, 200m and 2000m respectively [4]. Since they use the same interfaces as macro base stations, i.e. S1, X2, Iub and Iuh [5], small cells can be easily integrated with existing macro base stations. Outdoor small cells will be deployed in traffic hotspots to enhance network capacity,

traffic not-spots - to provide coverage in locations not covered by macro base stations - and at macro base station cell edges to enhance cell edge performance [5].

Small cell deployment is already underway with many operators adopting them due to their flexibility and lower maintenance costs [5]. According to recent market reports, small cell shipments grew by 280% in 2015, of which 66% was for non-residential deployments [6]. Forecasts for 2016 included 270% growth in enterprise shipments and 150% growth in urban small cell shipments. The revenue from small cells is estimated to reach $6B by 2020 [6].

These developments point to overwhelming acceptance of small cell technologies. However, backhauling small cell traffic to core networks has been identified as one of the challenges in fully realizing the benefits of small cell networks, especially in outdoor urban environments. This research proposes a non-line-of-sight (NLOS) solution for backhauling traffic from outdoor urban small cell base stations (SCBSs) to core networks using existing backhaul aggregation sites located on roof tops. Termed the cognitive NLOS Small Cell Backhaul (CNSCB) system, the solution is based on emerging millimeter wave (mmW) technologies which operate in the 30-300GHz spectrum bands, artificial intelligence and can provide reliable street to rooftop NLOS backhaul connectivity to SCBSs deployed at street level.

1.2 Research Motivation

Besides the benefits of improved network capacity and coverage, ultra-dense deployment of small cell networks at street-level brings the mobile network closer to users, allowing them to experience Gbps data rates that have not been possible with traditional roof-mounted base stations. By allowing more users and devices to access the network, small cells enable network operators to realize more revenues at a fraction of the current capital and operational costs [5].

For mobile networks, the end-to-end connectivity consists of the radio interface, which is the user device to base station segment, the backhaul segment which connects the base station to an aggregation site and the core transport segment which connects the aggregation site to the core and services networks. This is illustrated in Fig. 1.1. Of all the network segments, the small cell backhaul, which consists of two devices, one mounted on the aggregation site and another collocated with a SCBS on the street light pole, is the most difficult to realise. The proposed use of mmW technologies presents a challenge since the radio signals are susceptible to blockage. There is strong motivation to develop NLOS SCB solutions at mmW frequencies in order to realise Gbps, flexible and scalable wireless backhaul links.

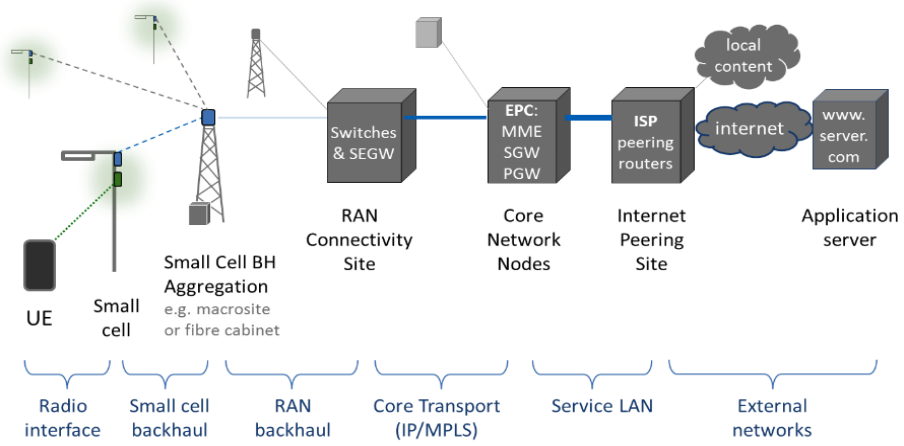

Figure 1.1: End-to-end transport network segments for providing services using small cell networks [4]

The 3GPP has focused on enhancing the radio inteface, and network operators have invested heavily on the radio access network (RAN) backhaul and core network transport segments. However, little attention has been paid to the SCB segment. In industry, several product vendors have proposed possible SCB solutions, building on their expertise on the RAN backhaul [7]. Currently, products that fully address the capacity, coverage, cost-effectiveness and flexibility required in outdoor urban SCB deployments remain elusive. In the research community, work on wireless outdoor

SCB solutions has focused on NLOS propagation measurements at mmW frequencies aimed at determining the feasilibity of using such technologies as high capacity NLOS SCB solutions in urban environments, and positive results have been recorded [8]. However, the results were based on the ability of the roof-mounted transmitters to illuminate areas in the general direction of small cell deployment areas, which may not be with the specific deployment areas required by network operators. Unlike indoor small cell deployments which will be random and deployed by end-users, outdoor small cells will be deployed by network operators to address access requirements in specific areas. NLOS SCB solutions in which the mmW radio frequency energy (RF) can be concentrated in a specific direction are therefore required. This way, backhaul coverage can be provided at the exact SCBS locations where it is required, even when such a location is not visible from an aggregation site.

Such a solution, based on the concept of the single knife edge diffraction (SKED) model has been proposed by researchers at Ericsson and is illustrated in Fig. 1.2 [9]. The hub represents a backhaul aggregation site located on the top of a building. The RF beam is manually pointed to a diffraction point such that the signal is detected at the SCBS location on the side of a building. The solution is based

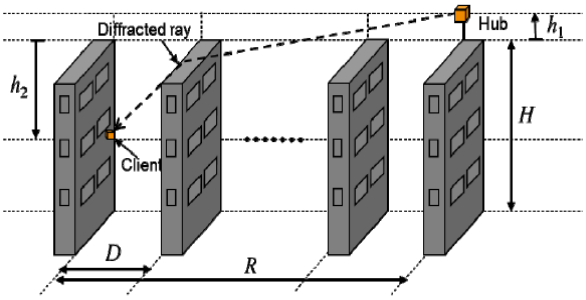

Figure 1.2: End-to-end transport network segments for providing services using small cell networks [9]

on manual determination of the diffraction points to be used for directing signals from aggregation sites to SCBS locations. Implementation of such a solution in dense

network deployment scenarios will not be cost-effective since installation teams would be required at each installation site to manually search the a path with the dominant beam. However, the need for automated beam steering to simplify the antenna alignment process is highlighted as a key requirement. Adding devices intelligence to radio devices has been proposed by 3GPP to enable self-organising network (SON) capabilities on access networks to reduce operational costs by minimizing human intervention in device configuration and network performance optimization processes. The same benefits can be achieved by adopting SON on the SCB segment. Furthermore, the RF beam strength can change depending on the environment and physical changes in the blocking objects, intelligent, continuous beam-searching achieved through SON can improve system reliability.

Ultra-dense network (UDN) deployment expected in 5G access networks will require large numbers of backhaul links and increased network complexity on the backhaul segment. Furthermore, energy consumption, which has been previously negligible in traditional mobile wireless backhaul links, will no-longer be negligible, due to the large numbers of deployed devices and resultant backhaul traffic requiring encoding and decoding in the backhaul nodes. In addition to minimizing human intervention in the installation processes, SON can also reduce operational costs associated with backhaul network management and optimization. SON is also being proposed to manage energy consumption on the access network by implementing sleep modes. The motivation for introducing SON on the SCB segment to address these issues is therefore increasing. This can be achieved by adding artificial intelligence algorithms in the backhaul radio devices. Artificial intelligence algorithms that can be implemented in SCB radio devices are developed in this research to address some of these challenges.

The motivation behind this research is to address backhaul coverage of outdoor small cells under NLOS conditions using mmW, massive MIMO and cognitive technologies.

The goal is to provide high-capacity, low-cost, scalable and reliable backhaul coverage to specific SCBS locations identified by network operators for provision of broadband mobile access to end-users. This provides a backhaul solution that interconnects small cells to core networks and enable networks operators to offer reliable broandband connectivity to end-users and the emerging myriad of M2M, D2D and IoT devices.

1.3 Problem Statement

There are many obstacles and challenges that must be resolved in order to provide suitable backhaul solutions for small cell networks. This thesis deals with providing backhaul coverage to SCBS deployed 3-6m above ground in outdoor urban environments. Specifically, the research addresses the problem of NLOS backhaul coverage at specific SCBS locations at mmW frequency bands, as well as energy efficiency aspects under UDN backhaul deployment scenarios. The main problem to be addressed is how to provide reliable street-to-rooftop backhaul connectivity to outdoor small cells using intelligent radio devices operated at mmW technologies under NLOS conditions.

Small cell networks will be deployed in both indoor and outdoor environments to provide mobile broadband connectivity to a large number of people and devices. Backhauling indoor small cells, i.e. Femto cells, will not be a challenge since most buildings have existing wired connectivity, which was previously used for fixed telecommunication services, and is readily available for use as backhaul. However, deployment locations for outdoor small cells, i.e. Pico and Micro cells, do not have existing telecommunications infrastructure. Backhauling these small cells is a challenge because rolling out new wired backhaul connectivity will be time-consuming and expensive. Furthermore, the backhaul capacity requirements for small cells, which is set at a minimum of 180Mbps, far exceeds the 2Mbps of existing microwave backhaul solutions [6]. In addition to this, 5G transport network requirements

include support for up to 1Gbps data rates on the backhaul segment [5]. Low-cost, high-capacity backhaul solutions are therefore required.

Another challenge posed by the deployment strategy of outdoor urban small cells is the need to provide backhaul connectivity to core networks using existing roof-mounted mobile backhaul aggregation sites that were traditionally used to provide clear line-of-sight (LoS) backhaul connectivity to macro cell base stations. This will reduce operational costs for the network operators. Deployment of wired solutions will negatively impact network operators' revenues and could also slow down small cell deployment since the process is time-consuming. Deployment of inherently capacity-limited existing microwave solutions will lead to poor quality of service (QoS) and user quality of experience (QoE), and eventually loss of revenues by the network operators. In the absence of low-cost and reliable connectivity to the aggregation sites, it will not be possible to deliver outdoor small cell traffic to core networks.

Wireless systems operated in mmW spectrum bands, i.e. 30-300GHz, are currently being proposed to provide high capacity, flexible, scalable and quick to deploy SCB solutions due to the inherent wide bandwidths, which translate to channel capacity in the ranges of Gbps [10]. However, using them for street-to-rooftop backhaul deployments will be a challenge due to signal blockage. Like all wireless systems operated above 6GHz, mmW systems require clear LoS for proper operation.

Fig. 1.3. illustrates a typical deployment scenario for SCBS. Two types backhaul are possible. Street-to-street backhaul links assume availability of wired connectivity, which will be limited in most small cell deployments. Street-to-rooftop links would be desirable since they connect the SCBSs to core networks via well established backhaul aggregation sites. But establish such links will be a challenge since most small cells will not have direct LoS with the aggregation sites. Macro base stations are collocated with backhaul radio devices, with LoS microwave backhaul links connecting the base

stations to aggregation sites where they connect to the core and services networks using high speed fibre optic cables.

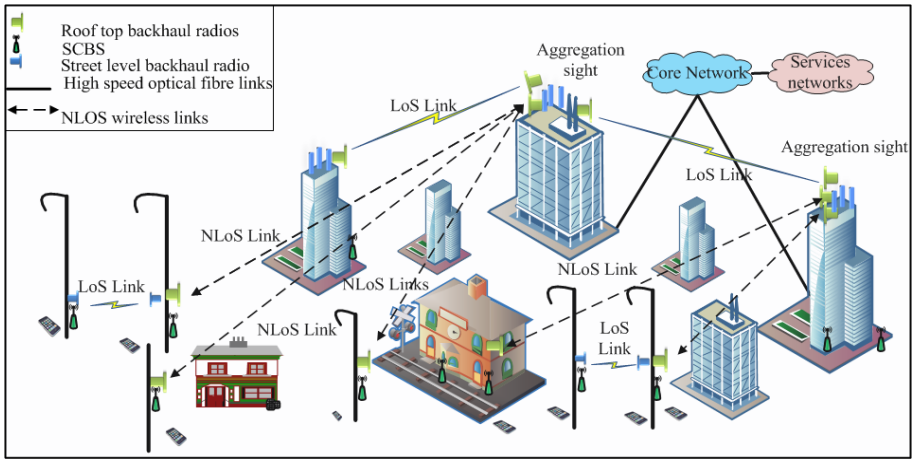

Figure 1.3: Typical heterogeneous network deployment in urban environments.

The other challenge faced in small cell network deployments is the increased number of SCB links required to connect the SCBSs to aggregation sites, which will result in increased network complexity [11]. SON techniques have successfully been used on access networks to reduce network implementation and management costs [12]. The use of SON on the backhaul segment is expected to achieve the same. Emerging requirements for 5G systems include dynamic, flexible and scalable backhaul systems and device intelligence [13]. While the former can be achieved using SON technologies, the cognitive engine (CE), which is the source of intelligence in cognitive radio technologies (CRT) provides a platform for developing algorithms that can enable implementation of intelligence in backhaul radio devices. However, algorithms related to adding intelligence to backhaul radio devices still need to be developed.

The energy consumption in mobile networks is growing and its contribution to global warming is rising [14]. The expected increase in backhaul links will results in the deployment of large numbers of devices and large volumes of traffic on the backhaul segment. This will in turn lead to increased energy consumption compared to

traditional microwave backhaul solutions. Determination of the energy consumed on the SCB segment is therefore necessary so that network operators can also implement the best energy-saving strategies on the segment. Sleep modes are already being adopted in SCBSs to reduce energy consumption during off-peak periods [15].

The challenges mentioned above are the main drivers for the contributions of this research and the developed algorithms, simulations and experiments given in the following chapters.

1.4 Thesis Aim and Objectives

The aim of this research is to investigate the key issues that can enable low-cost street-to-rooftop backhaul connectivity in outdoor urban environments using mmW technologies under NLOS conditions. The aims of the research are addressed through the following objective:

1. The first objective is to carry out a comprehensive review of recent state-of-the-art research on SCB requirements, emerging enabling technologies and proposed solutions. A number of technologies that can be harnessed to develop a low-cost high-capacity NLOS SCB solution are identified. The limitations of existing solutions are also identified, and ways to address the limitations in this research are suggested.

2. The second objective is to design a novel SCB architecture, termed the cognitive NLOS SCB (CNSCB) system, based on massive MIMO, mmW, cognitive radio and NLOS propagation by diffraction. The proposed architecture makes use of diffraction points to guide the mmW pencil-beam RF signals from one SCB radio device to another, using location information available in databases and artificial intelligence algorithms based on cognitive intelligence. The aims of the architecture are to reduce backhaul costs by implementing Point-to-Multipoint

(PtMP) configuration using massive MIMO, provide up to 1Gbps data rates using mmW frequency bands and use carefully planned diffraction points to enable NLOS street-to-rooftop backhaul connectivity.

3. The third objective is to develop learning, configuration and optimisation algorithms to enable the radio devices to intelligently select reliable transmission paths under NLOS conditions. The aim is to use device intelligence to create multiple NLOS paths that can alternatively be used as possible backhaul paths, hence improve link reliability.

4. The fourth objective is to develop a model which incorporates circuit power and trasnmitted traffic in analyzing and comparing the energy efficiency of the proposed SCB architecture. In the proposed analysis, energy consumption due to circuit power and transmitted traffic is considered. The is aim to determine the energy efficiency of the backhaul solution by taking into account the energy consumed during transmission of data from the user device up to the backhaul aggregation site.

1.5 Research Methodology

An investigation into the SCB requirements for outdoor small cells is first carried out to determine the performance requirements of prospective architectures. Emerging enabling technologies that can be used in developing these architectures are identified and key limitations noted.

The proposed CNSCB system involves operations at different layers from the application layer to the physical layer. Deriving a stringent optimal mathematical solution to evaluate its performance is therefore difficult. In this thesis, advanced approaches and proposed novel algorithms, together with mathematical models are used for each of the investigated topics. The performance of each proposed

architecture is evaluated and compared with those in existing literature. The limited interactions among the proposed backhaul systems also result in increased difficulty in numerically modelling the system and evaluating its performance. This has motivated the use of the MATLAB simulation tool to evaluate the performance of the proposed algorithms.

In order to gain a better understanding of the behaviour of mmW signals under NLOS conditions, with diffraction at specific locations as the mode of propagations, a numerical analysis of the diffraction loss, based on the single knife edge diffraction model is carried out. Experimental work to determine the feasibility of using prototype radio devices operated at 17GHz and 60Ghz spectrum bands in a typical outdoor urban environment is carried out. The aim of the experiments is to test the proposed concept of using the SKED model to enable NLOS street to rooftop backhaul connectivity. Using received signal strength and data rate, delay, jitter and packet loss as QoS metrics, the performance of the radio devices is evaluated.

The ultimate goal is to explore the different technologies to achieve an intelligent, high capacity NLOS SCB solution capable of evolving to 5G systems.

1.6 Thesis Scope and Limitations

Outdoor small cell deployments will vary significantly depending on the requirements of individual network operators. As a result, when considering backhaul solutions for small cells, there will be no one size fits all. Heterogeneous backhaul deployments are therefore being proposed in literature [16]. Where SCBS are deployed in close proximity to existing wired connection, this will be the preferred choice. Furthermore, for SCBS located where LoS to an aggregation site is available, LoS connectivity will be used. Sub-6GHz solutions are also being proposed in isolated locations where connectivity, rather than capacity is the basic required. This work is limited to

developing a street-to-rooftop NLOS solution to SCBSs installed in locations with no existing wired or wireless connectivity, and LoS conditions do not exist.

Cognitive radio technology (CRT) has been used in managing spectrum utilization in networks with limited wireless resource, with the cognitive engine (CE) being the source of intelligence of the radio devices [17]. It is assumed in this work that there is a single network operator in the deployment area, spectrum resources are abundantly available at mmW frequency bands. The application of CRT is, therefore, limited to using algorithms based on the concepts of the CE to enable learning, reasoning, and optimization in the SCB radio devices. Knowledge representation is a key building block in the CE. The development of a database of the information used in the learning, reasoning, and optimization is assumed to be available in a logically centralized or distributed network database provided by the network operator.

Systems operated at mmW frequency bands are considered as distance limited due to the high atmospheric absorption and signal blockage and are not adversely affected by interference due to the narrow beam-width. Interference is therefore not considered in determine the performance of the proposed system. However, under ultra-dense network deployment scenarios, where interference may not be ignored, interference mitigation techniques may be required, but are outside the scope of this work.

SON concepts are a key requirement in 5G networks. The definition and development of the concept through cognitive technologies is central to this work. A database is one of the key components of a SON-based system, and is required in the solution proposed in this research for storage of geo-location information of radio devices and diffraction points. It is also required for storage of link performance parameters and the implemented algorithms. However, the development of such a database is outside the scope of this work and information used in the learning, reasoning and

optimization algorithms is assumed to be available in a logically distributed network database.

1.7 Research Novel Contributions

This thesis addresses the problem of providing backhaul connectivity to outdoor urban small cells. Several procedures to address the problem are considered, with a special focus on diffraction loss analysis and evaluation at mmW frequency bands, link establishment and optimisation algorithms and energy efficiency analysis and evaluation model. The novel contributions of the research are summarised below.

1.7.1 Contribution to body of knowledge

Emerging state-of-the-art technologies being proposed for 5G transport networks are reviewed. Existing state-of-the-art SCB architectures are also studied and their main contributions and limitations summarised. A review of the ongoing activities in the definition and standardization 5G requirements, which is still ongoing, is carried out, with a focus on backhaul for small cells.

1.7.2 Novel NLOS backhaul architecture

In this thesis, the CNSCB system, a novel SCB architecture for enabling NLOS street-to-rooftop backhaul connectivity in outdoor urban environments is proposed. Employing automatic antenna steering technology, a NLOS SCB link is established by carefully pointing an RF beam to a diffraction point, which guides the beam to the receiving radio device. Device intelligence, based on cognitive technology, enables the creation of multiple-paths between radio devices to improve link reliability. A link-monitoring algorithm allows the radio devices to perform self-healing through early detection of mal-performance of a link and switching to a predetermined

alternative path. The architecture makes use of the flexibility and cost-effectiveness of the PtMP architecture by employing massive MIMO technology. The architecture allows the autonomous addition and removal of backhaul links by using activation and deactivation algorithms implemented using reinforcement algorithms. The wide mmW spectrum bands allows the system to increase of decrease link capacity through adjustment of the operating bandwidth. Compared to existing solutions, the CNSCB system is cost-effective, flexible, scalable and easy to deploy.

1.7.3 Framework for analysing diffraction loss at mmW frequencies

Using mmW frequencies in urban environments has always been considered a challenge due to propagation loss and signal blockage. NLOS connectivity is accomplished in this research by taking advantage of the signal blockage phenomenon, and using diffraction points to redirect signals towards a radio device. Analysing and quantifying the amount of diffraction loss helps in determining the usability of a diffraction point for a backhaul link, and is one of the novel contributions of this research. Results of the numerical analysis show that the diffraction loss suffered by mmW signals falls within standard ITU values for wireless systems. Insight into the best possible positions of diffraction points relative to the LoS path, and the location of radio devices is also provided.

The feasibility of using the proposed architecture in a typical outdoor urban environment is evaluated through experimental work done with prototype 17GHz and 60GHz radio devices. The results of the experimental work show that the architecture is feasible for establishing NLOS backhaul links that meet current SCB QoS requirements. Work on the proposed architecture and experimental work culminated in the publication of two conference papers [19, 20]

1.7.4 Novel algorithms for link establishment, configuration and coverage optimisation

Throughout the work, a number of algorithms are developed. An algorithm for autonomous establishment of multiple-path NLOS links is proposed. The algorithm is designed to minimize human intervention in the configuration and establishment of the backhaul links, hence reduce link set-up time. An algorithm for evaluating and ranking links according to their performance characteristics is developed and simulated using MATLAB. The algorithm determines the performance of a link based on the signal strength obtained reinforcement learning algorithm for implementing artificial intelligence in the backhaul radio devices based on cognitive radio, a technology previously used for managing spectrum utilization in wireless networks.

1.7.5 Energy efficiency analysis and evaluation framework

A model for accurately analysing and evaluating the energy efficiency of the proposed system, which incorporates energy consumption by equipment and energy consumed in the encoding and decoding data on the user devices, SCBS and backhaul radio devices is proposed.

1.7.6 Research Outputs

The research described in this thesis has generated ideas that have resulted in the following research outputs.

Journal Papers:

1. B. Malila, O. Falowo, N. Ventura, *Intelligent NLOS Backhaul for 5G Small Cells*, pp1-1, IEEE Communication letters, Vol. PP, Issue: 99.

Conference Publications:

1. B. Malila, O. Falowo, N. Ventura, *Design of a Cognitive Small Cell Backhaul System for Non-Line-of-Sight Deployment in Urban Canyons*, SATNAC, 2014.

2. B. Malila, O. Falowo, N. Ventura, *Small Cell backhaul network design using Genetic Algorithm*, SATNAC, 2015.

3. B. Malila, O. Falowo, N. Ventura, *Millimeter wave small cell backhaul: An analysis of diffraction loss in NLOS links in urban canyons*, pp1-5, IEEE Africon, 2015.

4. B. Malila, O. Falowo, N. Ventura, *Analysis of diffraction loss in NLOS small cell backhaul links deployed in urban canyons*, pp.1-6, IEEE Eurocon, 2015.

5. B. Malila, O. Falowo, N. Ventura, *Performance analysis of NLOS small cell backhaul using 17GHz point-to-point prototype radio*, pp1-6, IEEE MELECON, 2016.

6. B. Malila, O. Falowo, N. Ventura, *Energy Efficiency Analysis for Outdoor Wireless Small Cell Backhaul*, pp.1-6, IEEE WCNC, 2017.

7. B. Malila, O. Falowo, N. Ventura, *Optimising NLOS Backhaul Coverage For 5G Small Cells Using Genetic Algorithm*, SATNAC 2017, accepted, to appear in the proceedings of SATNAC2017.

8. B. Malila, O. Falowo, N. Ventura, *Routing Multiple Description Video Over NLOS Small Cell Backhaul*, accepted, to appear in the proceedings of IEEE Africon 2017.

1.8 Thesis outline

This thesis addresses the challenges identified earlier of how to backhaul outdoor small cell networks in outdoor urban environments using wireless systems operated at mmW frequencies. The work presented is organized into seven chapters. The first chapter introduces the viewpoints, motivations and thesis contributions. The goal of the research is stated in accordance with the requirements for backhauling densely deployed small cell networks in outdoor urban environments.

Each chapter starts with an introduction which highlights the main contribution and chapter overview. A section on related work is also included on the research topic covered in the chapter. The challenge addressed and technical solution provided are analysed. In the analyses chapters, a system model is used to evaluate the solution or concept. A brief summary is given at the end of each chapter.

Fig. 1.4 shows a system diagram of the organisation of chapters 4 to 6, in which the proposed models and algorithms that can be implemented in the proposed architecture are presented. NLOS backhaul coverage is the most critical capability of the CNSB system. Four sections in Chapter 4 are dedicated to presenting the schemes proposed to adress this problem. The models and algorithms for the support of NLOS operation and SCBS location coverage models and algorithms are presented. The ideas are separated into four sections. The first section deals with the single knife edge

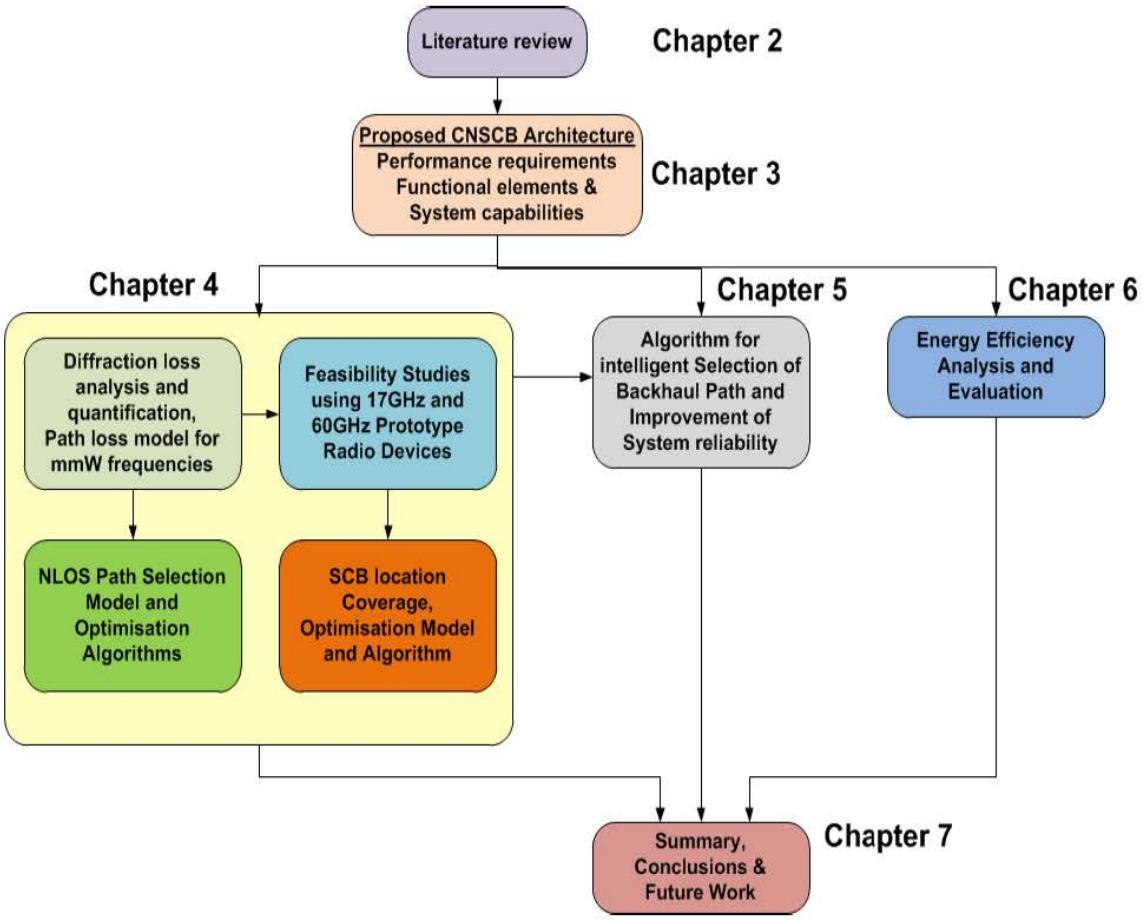

Figure 1.4: System diagram of models and algorithms for supporting the CNSCB architecture

diffraction model, which is used in analysing and quantifying the amount of diffraction loss suffered on a link, and hence determine usability of the links. Diffraction loss is one of the parameters used in the proposed propagation model to determine the path loss on the NLOS links. The feasibility of the proposed architecture is evaluated through experiments carried out using prototype SCB radio devices operating in frequency division duplexing (FDD) mode at 17GHz and 60GHz. Details of the experiments and results obtained are given in the second section. Details of models and algorithms for enabling the creation of NLOS street-to-rooftop backhaul links are given in the third section. The last section presents a model and algorithm for

selection of an optimal number of diffraction points that be used for covering specific SCBS location.

Chapter 2: Explains the major challenges associated with backhauling outdoor urban small cell networks. The SCB performance requirements as defined by the NGMN and those being developed for 5G backhaul solutions are explained. Key enabling technologies are identified. A review of recent ongoing research into backhaul solutions for outdoor small cells is given, and their limitations identified. A brief discussion on how the identified limitations are addressed in this research is given. The chapter concludes with a summary of the key points addressed therein.

Chapter 3: In this chapter, a novel NLOS SCB architecture, termed the cognitive NLOS SCB system designed to enable intelligent link creation under non-line-of-sight conditions using preselected diffraction points is presented. Its functional components are presented and the system operation explained. A mapping of the system capabilities to the current and future SCB performance requirements is presented, highlighting how the system addresses these requirements. The chapter concludes with a discussion of the key points and a summary of the issues presented in the chapter.

Chapter 4: Examines how the proposed architecture harnesses the identified technologies to create street-to-rooftop NLOS backhaul paths. Due to the limited knowledge on the behavior of mmW signals when impacting a diffracting object, an analysis and quantification of the diffraction loss at mmW frequencies is first studied using the single knife edge diffraction model, which best represents the rooftop to street scenario for the SCBS to aggregation site links. Comprehensive numerical results are presented. The feasibility of using the proposed model in a real-world

scenario is studied using 17GHz and 60GHz prototype SCB radio devices in a typical outdoor urban canyon environment. Results of the propagation measurements and network level QoS performance evaluation are presented.

A novel algorithm for the creation, performance evaluation and ranking of multiple-path backhaul links to ensure reliable NLOS backhaul links is developed. Simulation results are presented. Finally, a new application of the concept of the maximal coverage location problem (MCLP) in solving the illumination of the SCBS locates is proposed. An optimization algorithm designed to ensure that each SCBS location is covered by a certain number of diffraction points developed. Simulation results showing that a SCBS location can be covered under NLOS conditions by the required minimum number of diffraction points are presented.

Chapter 5: This chapter presents the key feature of the CNSCB system which differentiates it from existing solutions. A novel reinforcement learning algorithm developed around the conept of cognitive intelligence that enables to the backhaul radio devices to autonomously determine if a wireless channel performance characteristic are within those defined for the backhaul link is developed. The algorithm performs the self-healing aspect of the SON concept on the CNSCB system. Simulation results are presented and show that the algorithms enables the radio devices to make autonomous decisions to maintain consistently reliable NLOS backhaul connectivity. A conference paper on the proposed model and developed algorithm was positively reviewed at he IEEE VTC 2017 (Sydney), but unfortunately could not be presented to allow publication due to financial constraints. However, the work was revised, improved and submitted to the IEEE Comm Letters and is still under review (Indicated in research contributions under journals above).

Chapter 6: Highlights the limitations in existing energy efficiency evaluation models for mobile backhaul networks, specifically the SCB segment, and proposes a model for analysing and evaluating the energy efficiency of the CNSCB system. The model defines a new way of evaluating the energy consumed on the user to aggregation site segment of the mobile network, which includes the SCB segment. The energy efficiency is determined using a recently developed model for evaluating the energy efficiency of mobile networks. Results of numerical analysis show that the proposed PtMP architecture is more energy efficient that PtP SCB architectures. Furthermore, the energy efficiency of both configurations is shown to decease with increase in the number of backhaul links and backhaul traffic.

Chapter 7: Summarises the thesis, presents major conclusions and discussions on the current limitations of the proposed solutions and possible areas areas of future research.

Chapter 2

Background and Literature Review

2.1 Introduction

Chapter 1 introduced this research by highlighting the need for deploying small cell networks to address the increasing demand for mobile broadband wireless connectivity. Backhauling the traffic from outdoor urban small cell networks was identified as one of the major challenges in fully realising the benefits of small cell networks. This chapter reviews the small cell backhaul requirements, emerging small cell bakhaul technologies and recent state-of-the-art architectures and solutions. Limitations of the architectures and solutions are identified.

The rest of the chapter is organised as follows. Section 2.2 provides a background to the SCB problem, outlining the performance requirements, challenges related to meeting the requirements and key enabling technologies. Section 2.3 reviews literature related to recently proposed SCB architectures and solutions. The work is categorised into in-band backhaul solutions, strategic node-placement solutions and SON-based solutions. The review describes the contributions and limitations of

the proposed solutions. The final section summarises the chapter, concluding with a short description of how this thesis addresses the identified solutions.

2.2 Background

This section identifies the backhaul requirements for small cell networks and highlights those that present the major challenges to address in outdoor urban environments. A number of technologies envisioned to be key in addressing these challenges are presented.

2.2.1 Small cell backhaul requirements and challenges

This section summarises the SCB requirements, as defined by the next generation mobile network (NGMN) alliance and some of the key players in the ongoing requirements definitions for 5G transport networks. The major problems viewed as stumbling blocks in meeting these requirements are discussed. Before the requirements and challenges are discussed, an overview of the backhaul systems in heterogeneous network deployments is given.

2.2.1.1 Backhauling heterogeneous access networks

The deployment of mobile networks has been characterised by installation of base stations on roof tops or masts to maximise network coverage. Microwave links are used to connect the base stations to aggregation sites where high speed fibre optic cable is used to transport the traffic to core networks. Several hops of microwave links can be used to connect base stations located hundreds of kilometres from the core network. One of the requirements of microwave links is clear line-of-sight (LoS). In urban areas fibre optic cable are used due to the reduced distances to the core networks. However, where it has been been feasible to use fibre, roof mounted microwave links are used.

The emergence of heterogeneous access network deployments has introduced a new dynamic in the way mobile network traffic is transported to core networks. For example, cloud radio access network (C-RAN) architectures require more complex last mile architectures referred to as fronthaul and midhaul [21]. Existing wired connectivity is expected to be used for backhauling indoor small cell networks. While it has been possible for network operators to easily adapt existing backhaul solutions to most HetNet access technologies, doing the same for outdoor small cell networks has proved to be a challenge, especially in urban canyon environments. Unlike in the case of macro base stations, small cell base stations (SCBS) will be installed in locations with no existing telecommunications infrastructure and mounted 3-6m above ground [22]. Using existing microwave solutions will result in low capacity backhaul links which could prove to be a capacity bottleneck. Using existing roof mounted aggregation sites will reduce operational costs, however, clear the frequency bands used in existing microwave solutions, i.e. 10-24GHz, require clear LoS for proper operation. Installation of wired technologies will slow down the roll out of small cell networks, as well increase capital costs of small cell deployments.

A typical deployment of mobile transport networks is illustrated in Fig. 2.1. Aggregation sites provide termination points for several backhaul links. Traffic from both MBSs and SCBSs uses aggregation sites located on top of masts or rooftops. In cases where direct wired connectivity to the core network is available, this is used as backhaul. Recently, in-band backhauling, where small cell backhaul links share the same resources as user equipment on the MBS over the X2 interface, has been proposed [23]. This research focuses on developing a solution for backhauling outdoor urban SCBSs installed in locations with no access to existing connectivity to aggregation sites and LoS microwave is not feasible due to signal blockage.

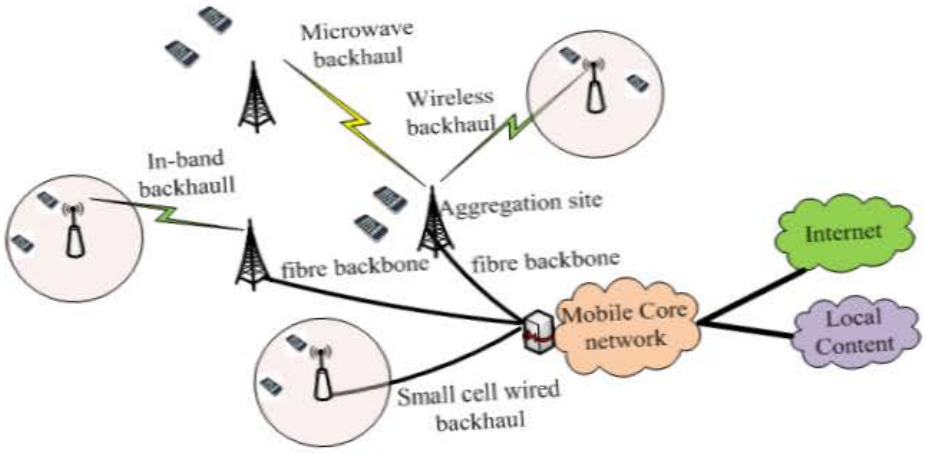

Figure 2.1: Backhaul architecture for heterogeneous access networks

As a result of the capacity and LoS limitations of existing wireless backhaul technologies, there has been increased interest in the use of 30-90GHz spectrum bands, commonly referred to as millimeter wave (mmW) technologies, for cellular networks. To this end, extensive feasibility studies on the propagation characteristics of mmW frequencies in urban environments have been carried out [8, 9, 24]. Results of the feasibility studies show that mmW technologies have the capability to provide Gbps backhaul capacity. Another observation from the results is the availability of multipath propagation due to diffraction and reflection, which can enable NLOS operation. Results of the studies provide a basis for the development of NLOS propagation models for mmW frequencies and their application in access and backhaul networks. However, a number of challenges associated with mmW technologies exist and need to be addressed before suitable SCB solutions can be realized. This research proposes the use of diffraction points to direct mmW signals between backhaul radio devices mounted at street level and roof level, to achieve non-line-of-sight (NLOS) connectivity.

2.2.1.2 Backhaul requirements for outdoor urban small cells

In addressing the SCB problem, two perspectives have been considered. The first is the initial requirements definitions carried out by the next generation mobile network (NGMN) alliance [5]. The second is the 5G transport requirements definitions currently under development by various organizations in industry and standardization bodies [25].

The NGMN, in consultation with a number of mobile network operators, outlined the SCB requirements from the operators' view [5]. Based on their findings, the SCF provides a technical review of the requirements in UDN small cell deployments, aligning them to the deployment use cases for small cells: capacity hot-spot, "peppered" capacity for QoE enhancement, outdoor not-spot, and indoor not-spot [4]. This research study focuses on the first three scenarios for outdoor small cell deployment.

According to NGMN, the issues that need to be considered when developing SCB solutions include capacity, coverage, cost, physical design, latency, synchronization, reliability, security, and availability [5]. Solutions to some of the requirements are being addressed on the macro cell backhaul segment and can be adapted for the SCB. However, capacity, coverage, cost and physical design are regarded as the most challenging for SCB systems [26, 27]. A detailed explanation of these requirements and challenges associated with meeting them is also given.

Standardization of 5G systems is currently ongoing. However, the general direction of the main goals of 5G is emerging as a result of efforts by several international research groups [21]. According to the wireless communication enablers for the twenty-twenty information society (METIS), emerging requirements for the 5G access network include 1000x increase in capacity, up to 100x more connected devices, data

rates in the order of Gbps, latency below millisecond ranges, lower cost and higher energy efficiency compared to today's networks [28, 29]. These requirements have a direct impact on the design and implementation of SCB networks.

While there is no one solution that will address these requirements, the backhaul could capitalize on the diversity in the QoS requirements of 5G services and heterogeneous backhaul solutions could be adopted. For example, tactile communications require milliseconds of latency, compared to minutes for smart metering applications. Furthermore, smart metering requires long battery life of up to ten years, whereas, for video conferencing, latency and throughput are more crucial. A detailed description of 5G services and application performance requirements is given in [30]. The diversity in the applications requires that 5G backhaul systems be scalable and flexible. In addition to this, 5G transport networks also need to be dynamic and adaptable, in response to real-time changes in network traffic and wireless channel conditions [31].

From both the NGMN and 5G perspectives, operator implementations of SCB systems will depend on the reason for deployment. Due to the diversity of services in 5G systems flexibility, scalability, adaptability, and dynamicity will be critical in addressing the backhaul requirements. Furthermore, the variability in SCB requirements will also depend on the reason for deploying the small cells, i.e. "peppered hotspot" for QoE enhancement, capacity hotspot and not-spot [4]. This research study focuses on capacity, coverage, cost, and energy efficiency. The following section gives a detailed description of the challenges addressed in this research.

2.2.1.3 Challenges in backhauling outdoor urban small cells

Backhaul requirements definition provides a guideline for product vendors, researchers, and network operators in developing suitable backhaul solutions. While some of the requirements can be met by adapting solutions that have been developed for the

macro cell backhaul, capacity, coverage, costs and energy efficiency are especially challenging in outdoor urban environments. The following sections describe how these factors affect the SCB segment.

SCB coverage: Backhaul coverage is defined as the ability to provide backhaul connectivity to a specific SCBS site, which meets the QoS performance requirements defined for the particular backhaul link [22]. The critical network QoS performance parameters include data rate, packet loss, and latency. In wireless networks, the achievable data rate is directly related to the system bandwidth and signal-to-interference ratio (SINR). Higher frequency bands with wider channel bandwidth have higher channel capacity, hence achievable data rates. Packet loss is negatively affected by link availability and outage. Link outage and unavailability result in packet loss and this directly impact user QoE due to dropped packets. Packet loss is a major problem in wireless systems operated above 6GHz especially in urban environments [4, 32].

Adding cognitive intelligence in radio devices and wireless networks is one of the goals of 5G, designed to prevent failure, hence outage and packet loss. This is achieved by proactively anticipating link outages and taking mitigating measures using one of the key aspects of self-organising networks (SON), i.e. self-healing. Software-defined networking (SDN) is an emerging technology that is expected to play a key role in improving SCB resilience, flexibility, and scalability [26]. However, its application in ultra-dense network (UDN) deployments is limited by the increase in exchanged control information, which can cripple the network capacity. On the other hand, implementation of cognitive intelligence in the backhaul radio devices such as learning and decision-making minimizes the amount of control information carried on the transport networks. One of the objectives of this research is to develop algorithms that can be implemented in SCB radio devices to minimize the control information exchanged over the backhaul links.

SCB capacity: For wireless backhaul systems, link capacity depends on the system bandwidth, SINR and the modulation scheme used. Existing microwave solutions have narrow channel bandwidths, making it practically impossible to meet the SCB requirements. While high modulation indices results in high data rates, they are associated with high bit error rates and increased system complexity. Achieving high SINR ratios can also be a challenge in UDN deployments. The use of mmW technologies therefore provides a cost-effective way of achieving high data rates, and are discussed in more detail below.

Dimensioning backhaul capacity in UDN deployments is a complex issue. The backhaul links must support peak traffic requirements, have the scalability to cover future requirements and respond to statistical traffic variations in real-time [21]. The target mean backhaul throughput for 5G small cells is 100Mbps-1Gbps, and the peak data rate is estimated to range from 10 to 50Gbps [33]. While mmW technologies will enable the achievement of high data rates, the dynamics in the access network traffic, coupled with the need to reduce energy consumption, require the use of artificial intelligence (AI) in the networks in order to achieve optimal operation. Some of the SON techniques that can be used are proposed and implemented in this research.

SCB costs: The backhaul in mobile networks has always taken a significant portion of the total network costs [35]. Operators aim to bring down the cost of the SCB segment to 10% that of the macrocell backhaul [26]. However, this must be achieved without compromising network QoS or user QoE. The main costs on wireless backhaul are due to equipment, energy consumption, spectrum, planning, implementation, and management.

UDN deployment increases network complexity due to increased requirement for planning, implementation and management costs. SON has been adopted on the access network to reduce costs associated with these factors [36]. It is also one of

the key technologies expected to help address the complexities associated with UDN deployment in 5G [37].

Another aspect that impacts the cost of backhaul is the decision to make use of PtMP or PtP configuration, with the former having been proved in legacy networks to be more cost effective. PtMP NLOS operation using mmW technologies for 5G SCB solutions is one of the configurations most desired by network operators. Use of massive MIMO at mmW frequencies is the subject of ongoing research [38, 39]. This research, builds on these research results to develop a cost-effective and scalable SCB system.

SCB energy efficiency: Energy consumption in the telecommunication sector is currently estimated to be 12% of global consumption, contributing 1% to global carbon emissions. Furthermore, energy costs are estimated to constitute 50% of mobile operators' operational costs [40]. While the energy consumption in macrocell backhaul systems is estimated to be less than 5% of the total network energy consumption, the value is expected to reach 50% with the creation of UDN deployments [40].

High data rates and the delivery of real-time applications are some of the key contributors to increased energy consumption [41]. Reducing overall network carbon footprint is one of the objectives of 5G towards green communications [41]. This is a complex task since, as is the case in reducing network costs, it must be achieved without compromising network QoS and user QoE. Use of SON techniques such as multi-objective optimization is key in achieving trade-offs between energy efficiency and network performance [40]. As previously explained, use of sleep modes is one of the techniques being proposed for reducing energy consumption in densely deployed SCBS. This can also be used to achieve the same in SCB systems. The work on

energy efficiency in this research is limited to analysing and evaluating the energy efficiency to two possible deployment configurations of the proposed SCB solution.

The following section describes how massive MIMO, mmW, NLOS operation, cognitive radio technology (CRT) and SON technologies can help bridge the gap between SCB requirements, challenges, and required solutions.

2.2.2 Key enabling technologies for SCB solutions

Massive MIMO and mmW technologies have been identified as some of the key technologies in cost-effectively addressing capacity challenges in 5G SCB networks [42–44]. NLOS operation will enable wireless street-to-rooftop SCB connectivity at mmW frequencies [8, 9]. Low-cost devices based on advanced CMOS technologies, license-exempt or partially licensed spectrum bands and SON capabilities achieved through CRT, are expected to reduce capital and operational expenses [45]. The following section provides, in more detail, how these technologies can be harnessed to realize 5G SCB solutions.

2.2.2.1 mmW technology for Gbps capacity

mmW technologies have not been used for cellular communications due to high propagation losses, which limit achievable link distance to less than a kilometre [26]. However, the evolution of access networks to small cells with radii of 10-200m has made the use of mmW more attractive, making the issue of distance not a challenge anymore. Furthermore, the short hop links achievable using mmW frequencies provide natural isolation between links, hence improved SINR and better spectral efficiency through higher frequency re-use. The high penetration loss of building materials also provides natural isolation between indoor and outdoor mmW communications [46].

Details on the propagation characteristics of mmW radio signals is given in appendix A.1

mmW has therefore become a technology of interest for 5G backhaul due to the wide operating bandwidth, which ranges from 250MHz to 5GHz per channel and translates to Gbps channel capacities [47, 48]. This enables implementation of high capacity links without the need for complex implementations on the radio modules [49]. Efforts to promote the adoption of mmW have culminated in the implementation of several standards. IEEE802.11ay is one of the most recently formed group, which defining a target of 20Gbps data rates using mmW radios [21, 43]. To date, Qualcomm and Samsung are the only vendors that have announced the availability of products promising Gbps data rates at 60GHz and 28GHz prototype respectively [50, 51].

Recent results of extensive propagation studies at New York University Wireless, at mmW frequencies, are summarized in [8]. Results of the studies have demonstrated that use of compact, high gain directional antennas with narrow beam width can be used to mitigate the problems of atmospheric absorption. However, the resultant narrow beam width from the use of high-gain antennas increases the need for more accurate antenna alignment [9, 52]. This increases the complexity associated with the deployment of backhaul radio devices. Automatic antenna steering technologies are recommended to mitigate this challenge.

Another challenge that prevented the adoption of mmW technologies for commercial purposes is previous techniques used for building radio devices at mmW frequencies, which resulted in costly, bulky and low volume multi-chip hybrid assemblies. This resulted in large, expensive radio devices, which would not have been suitable for UDN deployments due to the requirement of low-cost small form-factor devices. The emergence of CMOS system-on-chip, digitally assisted phased array systems and wide-band wafer-scale integration for multi-band sensing technologies is reversing

this [45, 53]. In addition to this, CMOS technology and modern CMOS processes continue to scale into nanometre dimensions, enabling the development of low-cost small form factor mmW transceivers [53]. These developments have contributed significantly in bringing down the cost and size of mmW radio devices.

The authors in [21], observe that the relatively low-cost of mmW technology, accompanied by the challenges related to its propagation are the major driving forces for the increasing research interest in the technologies, NLOS propagation being a major challenge. Even though recent feasibility studies confirm the possibility of using mmW frequencies for NLOS communications, practical solutions still need to be developed. Furthermore, techniques for establishing NLOS links are still an interesting research area and is the focus of this research.

2.2.2.2 Massive MIMO for cost and energy efficiency

Massive MIMO technology promises to address the capacity and cost challenges in 5G systems through increased network capacity per unit area [14]. This is achieved by equipping base stations with a large number of antennas, which are operated coherently and adaptively to serve several end-point radio devices. The antennas focus transmitted signals into smaller regions, resulting in increased throughput and higher energy efficiency [14]. The technology enables the deployment of PtMP wireless solutions which are more cost-effective than PtP configurations [54].

Inheriting the advantages of microwave massive MIMO, mmW massive MIMO is based on flexible beamforming, spatial multiplexing, and diversity. This results in improved reliability and flexibility in wireless systems [55]. Furthermore, properly designed massive MIMO at mmW frequencies results in narrow beam backhaul links that are scalable and have limited interference [54]. Some of the challenges associated with mmW massive MIMO include the increased difficulty in channel estimation due

to a large number of antennas at the base station and the need to feedback channel state information at the receiver since precoding and combining is required in the uplink and downlink respectively [55]. The SCB solution proposed in this research study combines the advantages of these technologies to enable a high capacity low-cost PtMP SCB architecture.

2.2.2.3 NLOS propagation by diffraction for SCB coverage

NLOS propagation is key in enabling the deployment of street-to-rooftop SCB links in outdoor urban areas since signals are prone to obstruction by buildings and other structures. However, achieving NLOS operation at frequencies above 6GHz is a challenge due to poor propagation characteristics of signals at these frequencies. This is the reason why microwave backhaul systems for macro-cells are based on LoS rooftop-to-rooftop links. Strategies that have been used to realize NLOS backhaul solutions for small scale deployments in legacy systems include the use of passive reflectors, repeaters and daisy chaining. These strategies will not be cost-effective in UDN deployments. NLOS propagation by diffraction at mmW frequencies in urban environments has therefore been the subject of recent propagation studies [8]. The presence of the signals is attributed mainly due to signal diffraction by roof edges and corners of buildings; and reflection by the glass and metallic building materials.

Other propagation studies at 60GHz carried out in [24], show signals diffracted from vehicles and lamp-post to be stronger than those from building edges. However, this research focuses on signals diffracted from diffraction points located on roof edges with predetermined location coordinates. The location information aids the radio devices in determining the exact antenna pointing direction towards a diffraction point. This avoids depending on random signals in determining suitable NLOS propagation paths. Furthermore, in this research the SKED model is used in determining suitability of

diffraction points as signal anchor points and may be difficult to use the model on locations other than roof edges.

2.2.2.4 Cognitive technology for device intelligence

Device intelligence has been identified as one of the key enablers in 5G [41]. One way that has been used to realize intelligence in radio devices is through CRT [56]. The cognitive engine (CE), the main source of artificial intelligence (AI) in cognitive radios, enables self-awareness, learning, and decision-making. The main feature which differentiates the CR from traditional, sensing and adaptive radios, is the learning capability. Learning enables a CR device to increasingly acquire knowledge of the operating environment and improve its performance with time. A functional model of a CE consists of a knowledge base, reasoning engine and learning engine [57].

Knowledge representation is the description and expression of the knowledge in a data structure or database that a computer can handle. For wireless systems, the contents of a database include minimum data rate, system bandwidth, records of bit error rate (BER), geographical location information etc. Machine reasoning refers to the use of acquired knowledge to deduce factual conclusions based on current facts in the knowledge base. The learning process involves identification of new knowledge that results in improved system performance. A detailed description of these concepts is given in [58]. In this research the knowledge database is assumed to be available in the radio device or in a remote network database. The development of reasoning and learning algorithms to enable intelligence in the radio devices is part of this research. The algorithms are developed using the concepts of reinforcement learning (RL) and genetic algorithm (GA)

The GA is a metaheuristic search and optimization technique based on the theory of evolution in which the best species are permitted to reproduce and be part of the next

generation. GA is inspired by the process of evolution which is based on inheritance, selection, and crossover or recombination in which species with the strongest genes are allowed to reproduce faster. The theory of GA was formalized by Holland based on Darwin's theory of evolution [59]. Unlike other heuristic methods, the GA has popularly been used in CR due to its ability to optimize more than one objective function [60]. GA also be used in CR to effect the learning processes due to its capability to evolve the link performance parameters to required values [61]. For these reasons, the GA is used in this research study in the design, learning, and optimization algorithms of the proposed SCB solution. A detailed description of the GA elements and processes is given in appendix A.2.

2.2.2.5 SON for dynamic, flexible and scalable SCB

The purpose of cognitive intelligence in radio devices is to enable SON capabilities. This is achieved through the learning and reasoning algorithms implemented in the CE. The standardization of SON has been driven by 3GPP in the 3GPP technical specifications from release 8 to reduce total cost of ownership in LTE networks [36]. The importance of SON in 5G networks is also illustrated by the inclusion of SON standards in 5G specifications [62]. SON functionalities are categorized into self-configuration, self-optimization and self-healing functions.

Self-configuration is a collection of algorithms designed to minimize human intervention in the installation and activation of network devices, thus enabling "plug and play" features. This results in reduced installation costs and faster rollouts. According to studies carried out by Ericsson, the introduction of SON in networks has been proved to reduce the cost of network maintenance by 90% and increase rollouts by 40% [63]. Self-optimization algorithms are aimed at maintaining network QoS with minimal intervention from the network operator. The requirement for NLOS operation at mmW frequencies for outdoor urban small cells is an additional complexity which

requires the use of the self-optimization functionality of SON and is used in this research study in the development of the proposed SCB solution. Self-healing is a collection of learning algorithms designed to detect problems and take mitigation measures to minimize or avoid the impact on overall network performance, and is used in this research to harness in developing the cognitive NLOS SCB solution proposed in this research.

The following section reviews literature on the most recently proposed SCB architectures and solutions. The main contributions and limitations in reviewed articles are summarised. A brief summary of how these issues are addressed in this thesis is given.

2.3 Related Work

With 5G rollouts expected to commence in 2020, there is an increased urgency in the research community to develop high capacity, intelligent backhaul connectivity. Extensive reviews on the SCB problem have been carried out recently [21, 26, 27, 43, 64]. The topics related to backhauling outdoor urban small cells cover very broad research areas and the topics tend to overlap. This makes categorising them challenging. The breadth and depth of issues also makes developing solutions equally challenging [21], This is further complicated by the diversity of services, applications and traffic patterns served by small cells. Different SCBS deployment scenarios and different architectures for base station and backhaul radio integration introduce even more diversity in possible backhaul solutions [5]. 5G backhaul requirements such as energy efficiency, dynamicity and flexibility also need to be incorporated into any proposed solution [62].

This research has focused on solutions and architectures that have been proposed to address the street-to-rooftop backhaul connectivity using mmW technologies.

This is because solving the problem of ensuring connectivity between SCBS's and roof-mounted aggregation sites will pave the way for developing techniques to address other problems in backhaul networks such as energy efficiency, intelligent traffic routing and optimization of the expected myriad of network parameters expected in 5G. The following section reviews the most recently state-of-the-art solutions and their limitations.

A number of solutions and technologies are currently being proposed for backhauling small cell networks [21, 26]. However, the literature identified in this research focuses on those that address the problem in outdoor urban environments. The identified SCB solutions have been classified into in-band backhauling, strategic node placement and those that based on SON techniques.

2.3.1 In-band SCB solutions

In-band backhauling is a technique for providing backahaul connectivity to SCBSs using the same wireless channels used for providing access to end user mobile devices. Resource allocation is divided into those for the user devices and those for connecting the SCBS's. In-band backhauling is implemented in two-tier long-term evolution (LTE) HetNets, where small cells overlay macro base station, for capacity enhancement. The same base station antennas are used for both backhaul and access. Radio resources are scheduled such that backhaul traffic uses the same frequency as access traffic. Fig 2.2 illustrates a simple comparison between out-of-band (a) and in-band (b) wireless backhauling of SCBSs. In the case of out-of-band backhauling (a), the user equipment (UE) and SCBS use different frequency bands for F_1 and F_2 respectively for downlink transmissions. Whereas in the case on in-band backhaulling, the UE and SCBS use the same frequency band F_1 for downlink transmissions.

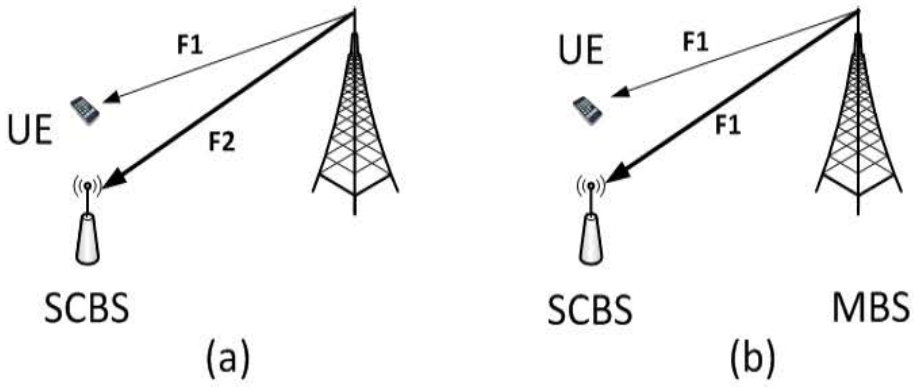

Figure 2.2: Simple comparison of out-of-band (a) and (b) in-band wireless SCB

The benefits of in-band backhaul architectures include the use of existing LTE features such as the PtMP architecture, ability to quickly deploy new features on the backhaul segment, dynamic joint access and backhaul optimization aimed at improving user experience and improvements in overall network operation efficiency.

Some of the limitations of in-band backhauling include co-channel interference between the access and backhaul links, and reduced access network capacity, especially in the legacy systems due to resource sharing. Advances in interference coordination schemes are expected to address the issues related to co-channel interference [21, 35]. However, these schemes come with increased costs and system complexity. According to recent studies, advances in massive MIMO and mmW technologies will enable high capacity in-band backhaul solutions [65]. The advantages of using in-band backhauling and some techniques to minimize interference between the access and backhaul links in systems based on massive MIMO and mmW are also summarized in [66]. In view of these developments, research into in-band backhauling in 5G systems is gathering pace.

Coldrey et al., proposed a NLOS in-band backhaul solution for two-tier LTE-based HetNets [67]. The proposed system architecture is shown in Fig. 2.3. The hub and client are collocated with the MBS and SCBS respectively. They provide IP-based

backhaul to the SCBS. The LTE radio interface and UE features are implemented on the client while eNB features are implemented on the MBS. High gain steerable antennas are used to direct the antennas to the best signal. Simulation results for 6GHz and 28GHz systems in PtP and PtMP configuration show the highest data rates for the 28GHz PtP system.

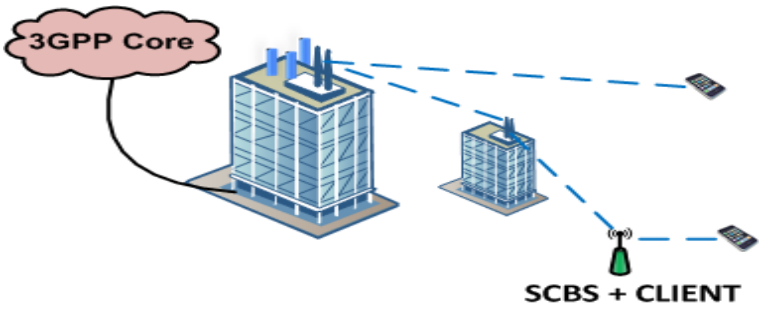

Figure 2.3: LTE-based in-band backhaul architecture with backhaul client in SCBS [67]

The advantage of the solution is the use of LTE features on the backhaul that can be upgraded to 5G features such as massive MIMO, advanced beam forming and low latency. The drawback of the solution is that, while areas of strong rooftop-to-street level signals are available, the areas where they are detected may not be the exact locations required by network operators for SCBS deployment. Deployment locations for SCBS will based on the density of the users, sources of access network traffic or coverage limitations of macro base stations. While the authors recommend the use of high-gain steerable antennas to detect signals, knowledge of the exact deployment location of a SCBS is critical in directing the signal to that location. In this research, the use of diffraction points to redirect signals to a SCBS location is proposed. The proposed solution makes use of knowledge of the exact location coordinates of SCBS and diffraction points. The radio antennas are therefore pointed towards a diffraction point and automatic antenna steering used to refine the search for the signal. This

is expected to improve system set-up time as well ensuring that SCB coverage is provided in the exact required locations.

Taori and Sridharan propose a wireless in-band backhaul that uses the X2 interface in a PtMP configuration system at 28GHz [66]. The PtMP functionality is achieved by dynamically steering antenna beams of the antenna array system at the MBS to different SCBSs at different time slots. A conservative path loss model proposed in [47] is used to achieve NLOS operation. Fig. 2.4. illustrates the proposed solution. A drawback of the solution is the assumption of LoS connectivity, Like in [67], the issue of NLOS operation is not properly addressed, which will be a challenge in urban canyon.

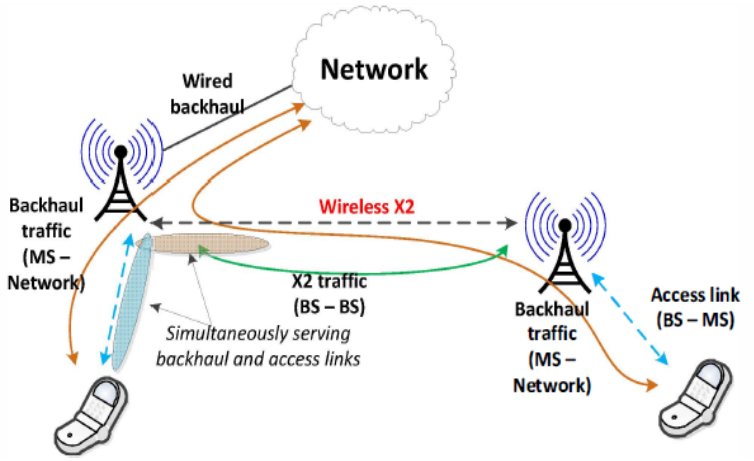

Figure 2.4: In-band backhauling with UE traffic over X2 wireless interface [66]

As highlighted in the introduction to this section, interference between backhaul and access links is a problem in in-band backhauling. A number of backhaul solutions that address the problem of co-channel interference between between the backhaul and access links were identified. The authors propose three Strategies to mitigate interference between the backhaul and access links are proposed in [23, 38]. While the proposed techniques are quite novel, the main drawback of the solutions is that the problem of NLOS operation is not addressed. A hybrid deployment of in-band and

out-of-band backhaul solution using massive MIMO is presented in [68]. The authors propose techniques to mitigate co-tier and cross-tier interference on the downlink. The issue of NLOS operation is also not discussed. However, the authors indicate that a path loss exponent (PLE) of 3 is used in the propagation model. This value of PLE is, according to [8] associated with near-LoS links. However, this might not be suitable for NLOS operation using mmW frequency bands because of the possibility that the signal can be completely blocked. Similarly, [65, 69] propose an adaptive full duplex in-band SCB system and assume a path loss exponent of 3 for the outdoor urban SCB in their simulations,as illustrated in Fig. 2.5. A major drawback of the solution is the assumption of LoS operation, which is not feasible in outdoor urban deployments.

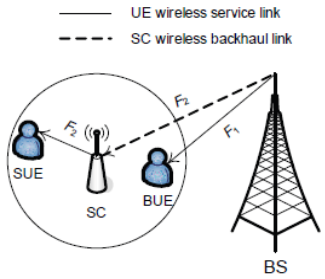

Figure 2.5: In-band backhaul with assumed LoS backhaul connectivity [68]

2.3.2 Strategic node-placement based solutions

In strategic node-placement-based backhaul solutions, the radio devices are strategically placed such that there is LoS connectivity between the street-level and roof-mounted device and an intermediate radio device installed on top of a building located between the street-level and aggregation level backhaul locations. This is illustrated in Fig. 2.6. Four backhaul radio devices are used in total. However, in some proposed strategies less than four devices are used as will be shown in some of the the reviewed cases. In addition to addressing the NLOS coverage problem, the architectures

to some extent, also address issues related to backhaul flexibility, scalability, and cost-effectiveness.

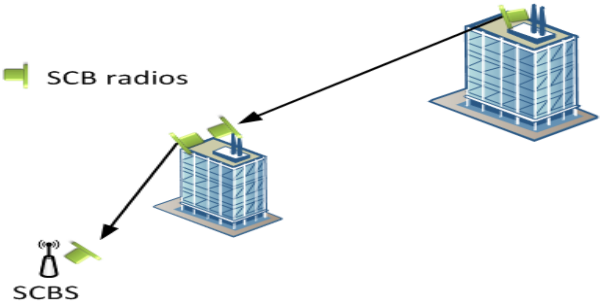

Figure 2.6: Simple comparison of out-of-band (a) and (b) in-band wireless SCB

Shi, proposes a Type-A relay, which can be illustrated by considering an architectural split of the 3GPP Type 1 relay's UE and eNB modules into two geographically separate entities [70]. An architecture of the system is shown in Fig. 2.7. The main advantage of the system is that it is based on LTE standards, making it possible to implement some of the LTE features such as SON. The use of an addition node to facilitate LoS operation between the two end nodes of a backhaul link at 5.8GHz and 28GHz is proposed in [71]. The SCB radio node, termed the aggregator node (AN), is placed on lower buildings in such a way that it has clear visibility of both the aggregation and the street level backhaul radios.

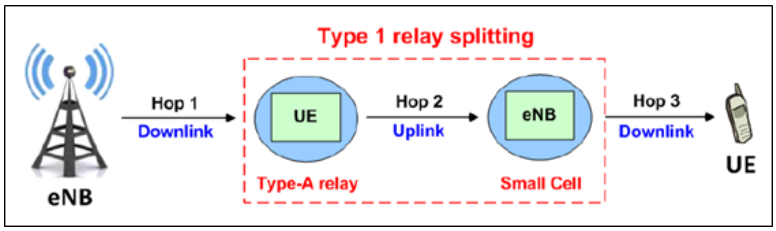

Figure 2.7: LTE-based backhaul with strategically placed Type-A relay [70]

In [72], Bojic proposes the use of separate frequency for street-to-street and street-to-rooftop backhaul links . 60GHz radios are proposed to provide short-hop street-to-street backhaul links and 70/80GHz radios are used for longer rooftop-to-rooftop

backhaul links. Like in [73], 60GHz repeater links are proposed to address the NLOS problem, which may not be cost effective in UDN deployments.

Villar et al., propose a PtMP system operated in the Q-band i.e. 40.5GHz - 43.5GHz, capable of providing 3GHz operating bandwidth, hence Gbps capacity [73]. An architecture of the system is illustrated in Fig. 2.8. The advantages of the proposed architecture include high link capacity and better spectral efficiency through PtMP. However, the proposed use of daisy-chaining around buildings to ensure NLOS operation is not cost effective in UDN deployments due to an increase in the number of deployed network devices.

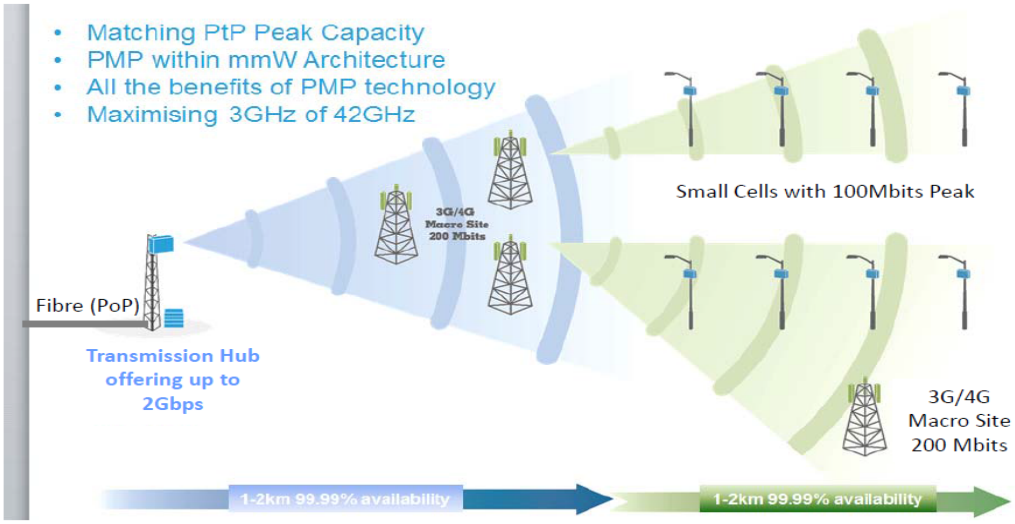

Figure 2.8: Layered backhaul architecture for small cell [73]

Zolotukhin et al. and Sayenko et al., also propose optimal placement of backhaul radio devices to ensure NLOS operation [74, 75]. The results obtained show the that the relay nodes need to be placed close to the hub location and that the deployment of SCBS is not only dependent on enhancing capacity at the MBS cell edge, but also on the operator's need to provide coverage in macro base station coverage holes. Even though the studies considered the sub-6GHz spectrum band, the node placement

strategy can be adapted to higher frequencies as suggested by Sayenko et al., in the concluding remarks of their article [75].

While the node-placement strategies ensure backhaul coverage of small cell sites, deployment of additional radio devices creates an additional site hence operational costs in site rentals, energy, and planning. Another limitation of the solutions is that in UDN deployments, manual deployment of additional equipment results in installation, configuration and network management costs. Increasing the number of deployed devices per backhaul link also increases network complexity. In this research the proposed maximum number of installed backhaul devices installed per link is two. Diffraction points located between the street and aggregation backhaul sites, with the assistance of antenna steering technology installed in the radio devices, is used to direct signals to the radio devices.

2.3.3 SON-based solutions

The in-band backhauling and strategic node-placement backhaul solutions discussed above focus on dealing with problems arising from ensuring reliable wireless connectivity on the backhaul segment. For 5G systems, attention must also be paid to the network's ability to adapt to variations in small cell network traffic and network and applications QoS requirements. Furthermore, NLOS operation at mmW frequencies adds to the network parameters that must be configured and optimized. Moreover, in UDN deployments, the classic always-on strategy will need to change to "turn on when needed", if energy saving targets on the networks are to be achieved [37]. The definition of different energy saving modes for radio devices, i.e. off, standby, hot-standby, sleep and hibernation impact the topology of the network and parameters such as energy efficiency, latency, signaling overheads and flexibility to return to normal operational state [37].

Given these challenges, incorporating SON capabilities with end-to-end network intelligence will exploit the cognition of application context, the state of the access network and that of the SCB wireless channel. In line with this thinking, a number of researchers have proposed to use SON techniques to address the network complexity and management costs associated with backhauling outdoor small cells.

Lakhani proposes the use of cognitive network intelligence to improve NLOS operation in an area in which the SCBS can be served by a primary SCB system or a cognitive backhaul system [76]. An architecture of the proposed system is shown in Fig. 2.9. The hub radios provide connectivity to the core network and are located on rooftops. The concept of SCB NLOS operation based on the single knife edge diffraction model (SKED) [9] is proposed. The street backhaul radio node detects deteriorating performance on the backhaul link, proactively notifies the primary SCB radio hub and request connection to the cognitive SCB radio hub. The primary hub grants permission if there are spectrum holes on the cognitive network. Otherwise, the request is declined.

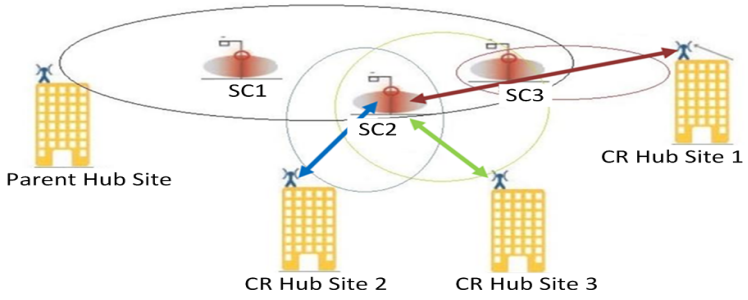

Figure 2.9: Cognitive small cell backhaul system with CR Hub sites providing connectivity when parent hub site is not available [76]

The proposed architecture provides a cost-effective way to provide resilience under NLOS conditions. The solution also provides insight on the use of CRT in achieving SON capabilities in SCB networks. However, the proposed operating frequency of 10-20GHz presents limitations in capacity, which is a problem for network operators

currently using the 6GHz to 23GHz solutions. Furthermore, the possibility of signal blockage even when spectrum holes are available is not considered. Enabling NLOS operation is one of the main objectives of this research. In addition to this, CRT is used to improve link reliability by using the secondary network when the primary links fail. However in this research the cognitive intelligence is used achieve the same by selecting the best propagation path without the use of additional equipment.

A self-organizing wireless mesh network (SWMN) backhaul solution based on PtP mmW links is proposed in [33]. Fig. 2.10 shows the function components of the backhaul radio devices. The solution features full SON capabilities designed to reduce operational costs. Issues of flexibility, scalability and network dynamicity in the event of changes in network traffic and topology are also addressed. Furthermore, the solution incorporates energy saving features. However, the issue of link establishment under NLOS conditions is not addressed. In outdoor urban street-to-rooftop backhaul links, LoS blockage is not always a temporary event, rather it can also be a permanent feature.

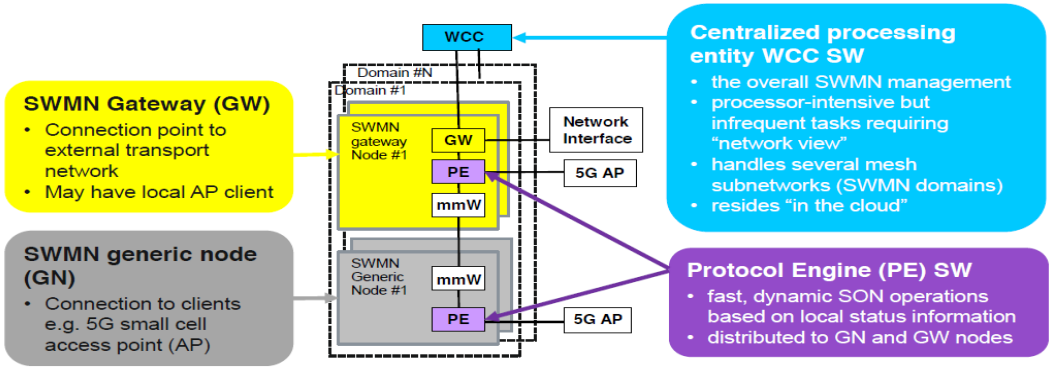

Figure 2.10: Architecture of self-organising wireless mesh backhaul system [33]

Algorithms that automate the deployment of wireless nodes in UDN deployment scenarios are critical in reducing operational costs and also give devices the intelligence required for autonomous operation. To this end, Karamad et al. propose an algorithm for optimal placement of SCB hub locations and optimal antenna orientation in an

urban environment under NLOS conditions [34]. The signal at the street location is assumed to be received via multiple paths due to multipath propagation. While the algorithm is proved to be more efficient than other existing algorithms, the deployment of new hub locations is not cost effective. Furthermore, use of existing hub locations is preferred in order to achieve cost savings. While adjustments in antenna orientation can result in improved link performance, there is a limit to which the orientation can be varied. Link establishment can, therefore, be a challenge under the circumstances.

2.3.4 Discussion

The literature presented above have attempted to address the problem of backhauling outdoor small cells. The limitations of in-band backhauling solutions include interference between backhaul and access links, the need for trade-offs between access and backhaul capacity and the inability to address the NLOS problem at higher frequencies. Strategic node-placement solutions suffer from increase deployment and operation costs. The proposed SON-based solutions do not properly address the NLOS problem as well. Save for the solutions proposed in [33, 34], the solutions reviewed do not address the issue of scalable network capacity. This is critical if the solutions are to be adapted to the emerging 5G systems where high capacity is a critical requirement. The solution proposed in this research provides a holistic approach to addressing the SCB problem by considering low cost implementation of NLOS links, scalable network capacity through the use massive MIMO technologies and using artificial intelligence to implement SON techniques in dealing with large-scale node deployments. Device intelligence is also used in improving link reliability under NLOS conditions.

2.4 Chapter Summary

The SCB problem arises due to the deployment of small cell networks at street level, in outdoor locations with no existing communications infrastructure. This chapter outlined the small cell backhaul requirements as defined by the next generation network mobile (NGMN) alliance and those being defined for 5G transport systems. Those that are particularly challenging to address include ensuring high capacity, reliable and flexible backhaul links under NLOS conditions. In addition to this, the solutions must be cost effective and energy efficient. A number of technologies that can be harnessed to address these challenges have been identified, and they include mmW for Gbps capacity, massive MIMO cost effective PtMP architectures, SON for managing network complexities and reducing management related costs and cognitive technology for adding intelligence to radio devices.

A survey of recent literature proposed to address the SCB problem for outdoor urban small cells is presented. The literature was been categorised into in-band backhauling, strategic node-placement and SON-based solutions. A review of in-band backhaul solutions can potentially reduce time-to-deployment and capital and operational costs. However, some of the drawbacks include interference between access and backhaul links, whose mitigation techniques can increase network complexity. There is also a limit to the achievable backhaul capacity. Furthermore, since in-band backhauling uses access network spectrum bands, the problem of NLOS operation at higher frequencies is not addressed. Strategic node-placements solutions provide a simple way of getting around the signal blockage problem in urban environments. However, under dense network deployment scenarios, the deployment of devices can be time consuming expensive and increase network complexity. In addition to this, increasing the number of devices could reduce the energy efficiency of the backhaul segment. SON in the backhaul is an emerging concept. As such, only two articles covering

SON outdoor SCB solutions were identified. The articles focus on the use of SON to manage network complexity and increasing network scalability, flexibility and dynamicity. However, in all cases, the issue of NLOS connectivity is not properly addressed, even though the solutions propose the use mmW frequency bands.

This research proposes to addresses the limitations identified in the reviewed literature, focusing particularly on enabling high capacity NLOS backhaul links in outdoor urban canyon environments. The proposed backhaul architecture is based on propagation by diffraction. Predefined diffraction points, with the aid on automatic antenna steering technology signals between the street-mounted and roof-mounted backhaul radio devices. Using intelligence installed in the radio devices, the radio devices can autonomously set up multiple backhaul links and identify best performance links that can be used. The proposed use of massive MIMO reduces operational costs due to PtMP operation capability and reduced number of deployed devices. Energy efficiency is an added benefit that comes from reduced number of deployed devices. Algorithms for implementing sleep modes in radio devices are not part of the developed algorithms for the CNSCB system proposed in this research, however, an analysis of the energy efficiency of the system is given in Chapter 6. Network management costs are also reduced through self-configuration, self optimisation and self-healing, i.e. SON, achievable through addition of intelligence in the radio devices. Details of the proposed backhaul architecture, system and capabilities are given in Chapter 3.

Chapter 3

Proposed Cognitive NLOS Small Cell Backhaul (CNSCB) System

Developing small cell backhaul (SCB) architectures that fully address the current and future QoS performance and backhaul connectivity requirements of small cell networks in outdoor urban environments under NLOS conditions is a challenging task. Millimeter wave (mmW) technologies are being proposed to provide backhaul links capable of delivering data rates in the Gbps ranges. However, mmW radio signals suffer from signal blockage in outdoor urban environments. Ensuring non-line-of-sight (NLOS) backhaul connectivity is one of the major limitations of existing solutions.

To this end, the chapter presents a novel wireless backhaul system capable of providing reliable street-to-rooftop backhaul connectivity for outdoor small cell networks. Termed the cognitive NLOS SCB (CNSCB) system, the architecture is based on mmW frequency bands to achieve Gbps data rates. Propagation by diffraction using pre-defined diffraction points, with location coordinates stored in a local or network database, is considered to mitigate signal blockage. Automatic antenna steering technology is assumed in the solution, to allow the radio antennas to be steered towards the required diffraction points locations. Massive MIMO technology is

proposed to achieve the cost-effective point-to-multipoint (PtMP) architecture, that is very much desired by network operators to minimise capaital and operational expenses under dense deployment scenarios. The novelty of the architecture is the ability to use cognitive intelligence, implemented using learning and optimisation algorithms installed in the cognitive engine (CE) of the radio devices, to autonomously create multiple-path SCB links, and optimise NLOS coverage of SCBS locations.

The design of the CNSCB architecture is guided by the current backhaul requirements defined by the next generation mobile network (NGMN) alliance, and those being proposed for the future 5G transport networks. The requirements considered in the proposed architecture are NLOS coverage at mmW frequencies, ease of deployment, cost-effectiveness and system reliability. Energy awareness is one of the key requirements in 5G transport networks. Implementation of sleep modes is being proposed in access networks recommended under low-traffic conditions, and the same is expected to adopted on the backhaul segment. The development of the required algorithms is out of the scope o the scope of this work. However, a scheme for analysing and evaluating the energy efficiency of the proposed architecture is developed.

A detailed description of the proposed architecture, including the functional components and system operation is first presented. A description of how the proposed architecture addresses the limitations of existing solutions and emerging 5G backhaul capacity, coverage and reliability requirements is given is finally given.

3.1 Introduction

Small cell networks are emerging technologies expected to enable ubiquitous access network coverage and high user data rates. However, it is critical to ensure that the traffic is cost-effectively and reliably transported to core networks. Backhaul

architectures that incorporate device intelligence are key in addressing the NLOS backhaul problem identified in this research. The key components of a cognitive radio are the cognitive engine, which consists of learning and optimisation algorithms, and a database, which stores the environmental, network and performance measurement information. The learning and optimisation algorithms provide the radios with the intelligence required to perform self-configuration, self-optimisation and self-healing capabilities, which is necessary to manage system complexity and minimise human intervention during installation and operation.

Incorporation of the cognitive engine in the CNSCB architecture is designed to allow the radio devices to autonomously attach to the network, identify suitable diffraction points, evaluate and rank the performance of each NLOS path, establish connectivity and be able to switch to an alternative path in the event of mal-performance of the primary path.

3.2 Related Work

Apart from failing to properly addressing signal blockage at super-6GHz frequency bands, the solutions reviewed in sections 2.3.1 and 2.3.2 do not incorporate SON capabilities required in 5G systems to address system complexities that result from ultra-dense network deployments, and to reduce installation and management costs. The solutions in section 2.3.3 incorporate intelligence in the architectures through SON capabilities to address these challenges. However, they also fail to properly address the requirement for NLOS operation in urban environments. This section identifies three architectures whose limitations have been carefully considered in the design of the CNSCB system proposed in this chapter.

Wainio and Seppanen proposed a self-optimising mmW architecture in which the backhaul nodes are interconnected as a mesh network with PtP links [33]. The

solution has SON capabilities enabling autonomous network configuration and traffic engineering with minimal Operations, Administration and Maintenance (OAM) intervention. Other features include the capability by radio devices to selection a node with which to establish connection, and automated resilience scheme to minimize the impact of signal outage due to rain, snow and human and vehicular traffic. A major drawback of the solution is that the problem LoS blockage by building at mmW frequency bands is not addressed. PtP LoS links are assumed, whose application in built-up areas would be limited. Incorporating NLOS operation capability in such an architecture can address the SCB coverage problem. The objective of the CNSCB architecture is, therefore, to incorporate SON capabilities, as well as achieve NLOS backhaul coverage at mmW spectrum bands.

Villar et al. propose a hierarchical PtMP architecture operated in the 40.5 GHz to 43.5 GHz frequency band [73]. The architecture achieves the Gbps data rates and low-cost requirements of 5G SCB architecture. A remote network management system (NMS) is proposed for managing the radio devices. Simulation results obtained show that the proposed PtMP star architecture does not meet the LoS constraints. Daisy chaining using relays is proposed to achieve the required segment coverage and expected Gbps capacity. The successful use of the NMS to remotely manage the radio nodes depends on the availability of connections to nodes. This is because backhaul connections are the only form of connectivity to the radios. The concept of self-configuration proposed in the CNSCB addresses this problem by allowing the radio devices to autonomously establish the backhaul links, self-optimize and self-heal. NLOS operation is also addressed by use of diffraction points.

Lakhani et al. propose the use of cognitive intelligence to address the NLOS backhaul coverage problem in outdoor urban environments [76]. In the proposed architecture it is assumed that the aggregation site would be located in a location

where it can provide coverage to a given number of SCBSs. However this will not be feasible if existing aggregation sites are to be used. Furthermore, SCBS deployment locations will be determined by network operator's requirements for providing access connectivity. While the use of a secondary cognitive radio network to provide alternative connectivity in the even of failure of primary backhaul links, it is not clear if the secondary aggregation site backhaul radios would have been planned with the need to provide NLOS links to the SCBS. The CNSCB system addresses the SCBS location coverage problem by selecting diffraction points that are strategically located to ensure NLOS connectivity between the street and aggregation site radio.

The main idea behind the CNSCB system is to provide NLOS backhaul coverage to locations required by network operators to deploy SCBSs. The main question to be answered is how backhaul radio devices can autonomously create NLOS backhaul links based on propagation by diffraction, by using device intelligence realised using learning and rasoning algorithms implemented in the cognitive engine of the radio devices. Some of the SON capabilities achieved in [33], for example, also used in the CNSCB architecture for autonomous link establishment, while the single knife edge diffraction model used in [76] is also used in the proposed architecture.

3.3 System Design Considerations

The main objectives of the CNSCB system are two-fold. Firstly, to enable NLOS backhaul connectivity to SCBSs deployed by network operators in locations with no existing connectivity to core networks and no direct LoS connectivity to existing aggregation sites located on rooftops. The backhaul links must be able to provide minimum data rates of 180Mbps, as well as scale to Gbps capacity requirements of 5G systems. NLOS connectivity is based on propagation by diffraction and is achieved by use of radio signals diffracted on the roof-edges of buildings.

The second objective is to minimize the need for detailed network planning and design normally associated with wireless backhaul systems. This is achieved by automating the network build-up and link establishment process. The key capability of the CNSCB system is device intelligence, inbuilt in the cognitive engine of the backhaul radio devices. The cognitive engine allows the complexities associated with the establishment of NLOS links to be hidden from the network operations. The in-built algorithms make it possible for the backhaul radio devices to connect to the network, establish the NLOS links, establish optimal operation configuration and take corrective measures to minimize the impact of link or node failure. The cognitive engine, therefore, gives the CNSCB system the SON capabilities required to minimize backhaul costs and maintain high network performance, hence user QoE.

The following subsections summarise the key small cell backhaul requirements considered in the design of the CNSCB architecture.

3.3.1 Scaling link capacity to Gbps

The CNSCB architecture must meet the NGMN and 5G SCB minimum capacity requirements of 180Mbps, as well as scale to the 5G minimum requirements of 1Gbps. The proposed in-band backhaul solutions fall far short of the capacity and scalability into Gbps ranges. Strategic node placement solutions do not address these issues as well. SON solutions implemented in mmW frequency bands could match the capacity requirements. However the issue of scalability to 1Gbps is not addressed. The use of mmW technologies on the CNSCB will enable Gbps link capacities without the need for complex implementations on the radio interface. Capacity scalability can be achieved by varying the assigned bandwidth per channel.

3.3.2 Increasing backhaul connection density

The requirements for dense deployment of backhaul connectivity in 5G follows the expected increase in not only small cell networks, but also D2D, M2M and IoT systems that will require backhaul connectivity to core networks. The proposed in-band solutions can result in higher connection densities. However, the use of sub-6GHz frequency bands will limit the scalability of the solutions. A major limitation of strategic node-placement solutions is the inability to scale to large numbers of backhaul links since the implementation and operational costs would increase.

The CNSCB must therefore be able to provide large numbers of backhaul links per unit area. Dense deployment of backhaul links will be possible in the CNSCB due to the use of high gain antennas on the mmW, which results in narrow beam-width signals and short-hop links caused by high attenuation of signals at mmW frequencies. The use of massive MIMO will enable PtMP configuration, with large numbers of antenna arrays installed at the aggregation sites. Assigning each antenna array to a SCBS location will enable scalable connections, giving rise to a large number of backhaul links per unit area.

3.3.3 Providing NLOS coverage at mmW frequencies

While the 5G requirements do not explicitly define the need for backhaul coverage, the need for high reliability can be interpreted as the ability to ensure coverage as well. The coverage requirement for "*exotic*" deployment locations at street level required defined by the NGMN would also include the need for coverage even under NLOS conditions. This is one of the basic requirements for providing backhaul connectivity to outdoor small cells. In-band backhaul solutions do not address this requirement as sub-6GHz capable of NLOS operation are assumed. For solutions proposed in the mmW bands, the problem is not properly addressed. Strategic node-placement

solutions address this problem by using additional backhaul radio nodes, which, as explained in chapter 2, leads to increased operational costs. The reviewed SON solutions do not address the coverage problem.

The proposed CNSCB system must therefore be able to address the NLOS coverage requirement by making use of diffraction points to create visibility between the aggregation and street level SCB radio locations. This will differentiate the CNSCB system from all the reviewed solutions, except for the one proposed in [76]. However, the authors do not provide further explain how system reliability can be achieved. The CNSCB must be able to use cognitive intelligence algorithms implemented in the radio devices to improve the reliability of the NLOS backhaul link. Details of how the coverage problem is addressed in this research are given in Chapter 4.

3.3.4 Ease of backhaul link deployment

Ease of deployment is a requirement of the NGMN for small cell backhaul links due to the expected large numbers of backhaul links. In-band backhaul solutions could achieve this since there would be no need for frequency planning in an existing access network. Only the small cell site would require planning. Strategic node-placement solutions present the most challenge in ease of deployment due to the need to plan for three installation sites, i.e. the two end radio sites and the intermediate site. SON solutions can meet this requirement due to the use of intelligence in the network implementation.

The proposed incorporation of SON capabilities in the CNSCB must enable the radio devices to address the requirement for ease of deployment, using self-configuration capability to attach to the network with minimal human intervention. Self-optimization also eases the deployment process since the intelligent radio devices are able to fine tune themselves to the optimal performance requirements of the network.

Furthermore, the radio devices, through self-optimization, are able to optimize the number of possible NLOS paths between the backhaul radio devices through a selection and ranking process.

3.3.5 Dynamic response to variations in access network traffic

High mobility is a requirement for access networks which gives rise to a high number of handovers, hence fluctuations on the access network traffic per base station. These fluctuations are transferable to the backhaul segment. The CNSCB system must be able to to dynamically respond to these fluctuations through the device intelligence. The state of the backhaul links can be monitored in real time, allowing the system to make decisions regarding the traffic that can be allowed onto the backhaul from the SCBSs. Details of algorithms proposed in this research to address the service-awareness on the backhaul are given in Chapter 5.

3.3.6 System reliability

5G defines high reliability for transport networks. Consequently, the NGMN/SCF requires SCB system to have protection against system failures, which can be a result of equipment failure or wireless link mal-performance. Both the in-band and strategic node-placement solutions do not address the issues of system reliability. SON solutions make use of the SON capabilities to improve overall system performance. However, since the issue of NLOS connectivity is not addressed, system reliability is seriously compromised without reliable connectivity.

The CNSCB system must be able to minimize the effects of system failures by early detection, with a focus on the wireless link connectivity performance. This can be achieved by implementing self-healing SON capability through cognitive learning and

reasoning algorithms to ensure reliable NLOS backhaul connectivity. Details of how these algorithms improve system reliability are given in Chapter 5.

3.3.7 System energy efficiency

The NGMN/SCF requires that the backhaul systems be energy-aware due to a large number of backhaul links and high traffic volumes. Although energy efficiency on the backhaul is currently a hot research topic, the development of algorithms for energy management on the backhaul is out of the scope of this research. However, it is assumed that those developed for implementation in SCBSs can be adapted for use in the backhaul radio devices. All the reviewed solutions do not address the energy efficiency requirement either. In this research, work on energy efficiency is limited to the analysis and evalaution of the energy efficiency of two possible network configuration of the CNSCB system i.e. PtP and PtMP.

3.3.8 Interference and propagation loss

For the CNSCB system, the effects of interference are considered to be negligible due to the use of mmW frequencies, which results in narrow beam width as explained in Chapter 2. The effects of diffraction loss are therefore considered to be more predominant, and the CNSCB system is designed to address the impact of diffraction loss on the performance of the backhaul links. The system is also designed to address the effects of variations due to changes in weather conditions such as rain or snow, since these negatively impact signal strength, and temporary signal blockage by humans and vehicular traffic.

3.4 Proposed System Architecture

This section describes the CNSCB network architecture, functional components and system operation. Fig. 3.1 shows an architecture of the proposed CNSCB system. A backhaul link consists of two radio devices, a street backhaul radio (SBR) collocated with a SCBS, and an aggregation backhaul radio (ABR) collocated with aggregation equipment such as routers or switches at rooftop level. The SBR is connected to the SCBS using Ethernet cable. The ABR is connected to a router or switch and

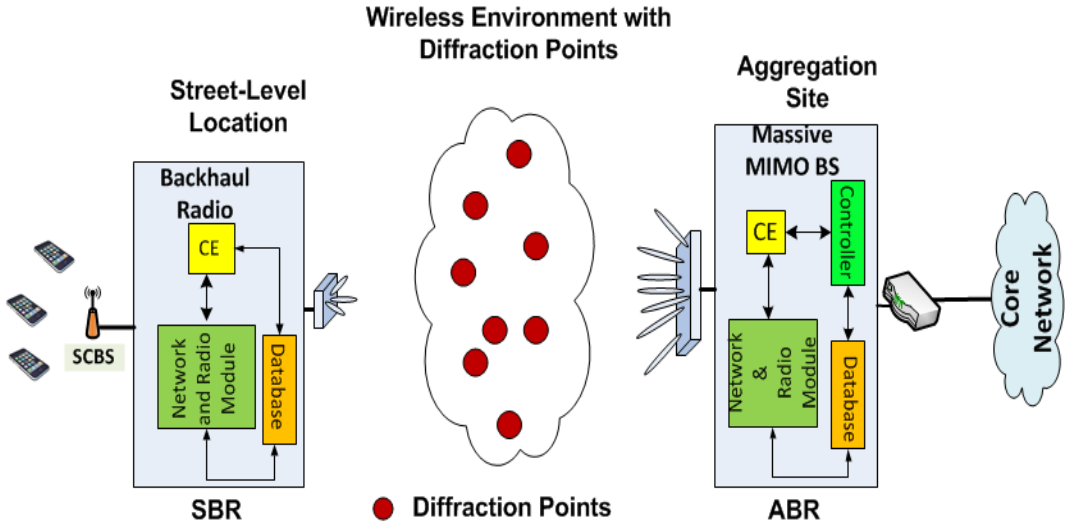

Figure 3.1: CNSCB system architecture

provides interconnection between the backhaul link and core networks via high-speed fiber optic cabling. It is assumed that there is no direct LoS connectivity between the SBR and the ABR.

The backhaul radio devices consist of a cognitive engine, a local database, a network module and a radio module. In addition to this, the aggregation site radio in the PtMP architecture has a control module. Details of the functions of the elements are given below.

The wireless channel consists of a set of diffraction points with predefined location coordinates. The diffraction points act as anchor points for the radio signals and are assumed to have full visibility of both radio devices, providing the backhaul connectivity. The signal path, therefore, consists of a line-of-sight link between the street backhaul radio and a diffraction point, and another line-of-sight link between the diffraction point and the aggregation site radio. The radio antennas are assumed to have automatic antenna steering technology, enabling them to be simultaneously pointed to a diffraction point to create the end-to-end NLOS SCB link. The antenna steering to the required diffraction point is aided by the location coordinate points in the databases.

3.4.1 Functional components

The CNSCB system consists of two types of backhaul nodes: the nodes with a single radio module for single wireless link connection, and the massive MIMO nodes with several radio modules for multiple wireless links emanating from the node. The nodes with single radio modules are used in the SBR and ABR nodes in the PtP configuration and the SBR in the PtMP configuration. The massive MIMO nodes are used as the ABR in the PtMP configuration. The architecture of the radio nodes is based on the DoD-LTS architecture [57]. Single or multiple antennas can be implemented on the street backhaul radios. The key components of both the street radio and massive MIMO radio are the cognitive engine module, a knowledge database, radio module and network module. In addition to these components, the ABR has a controller module, whiose function is to coordinate the assignment of resources to the SBRs. This research focuses on the algorithms that can be implemented in the cognitive engine to achieve the SON capabilities. Figs. 3.2 and 3.3 show the simplified architectures of the street level and aggregation site backhaul radio devices respectively.

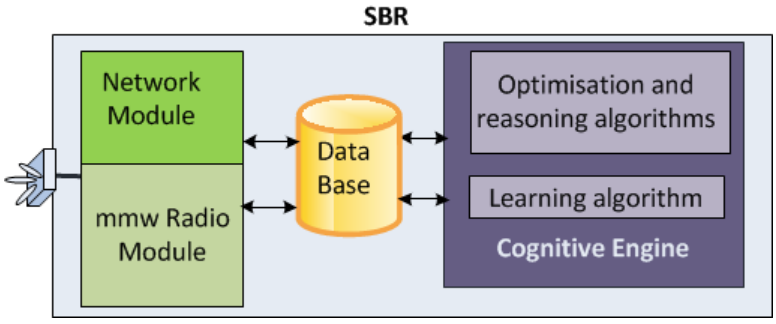

Figure 3.2: Architecture of CNSCB street-level radio node

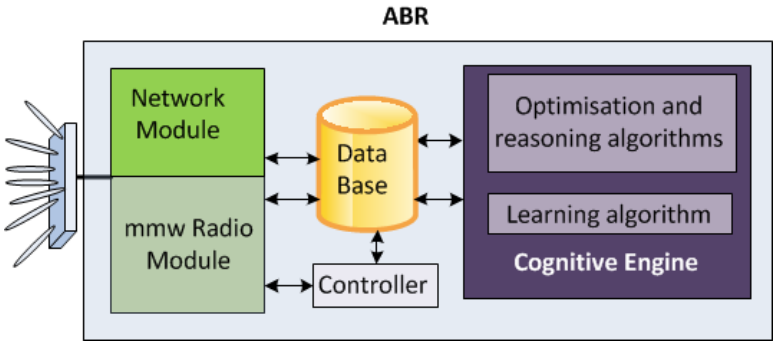

Figure 3.3: Architecture for CNSCB aggregation site node consisting of massive MIMO system

The massive MIMO system consists of a large number of antenna modules that are implemented to achieve the massive MIMO capability. The radio modules of the system are assumed to have beam switching capabilities as in [77–79]. In addition to the components of the nodes with a single radio module, the system has a control module.The module enables the radios to activate or deactivate links as new SBRs are added or removed from the network respectively.

3.4.1.1 Cognitive engine

The novelty of the CNSCB radio nodes lies in the algorithms implemented in the cognitive engine which form the basis of the intelligence of the backhaul radio devices. It consists of learning and reasoning algorithms based on reinforcement learning and GA respectively. The learning algorithms give the radio devices the capability to

gather information about their operating environments, as well as the performance parameters predefined by the network operator. The reasoning algorithm is used in the assessment of the quality of the backhaul link in comparison to the predefined performance criteria. They also assist in fine tuning the internal parameters of the radio devices in order to meet the performance requirements during the optimization processes.

3.4.1.2 Radio module

The radio module consists of the antenna elements and implementation of modulation schemes. The antennas are assumed to have automatic antenna steering mechanisms for directing the beam towards the desired diffraction point. The antennas are also assumed to have beam steering capabilities, which is required to mitigate signal degradation due to other effects such as pole swaying [80]. Beam steering lenses have been developed and implemented for TDD access and backhaul systems [79, 81] and are assumed to be implemented in the CNSCB system radio nodes. The radio module provides link state information to the cognitive engine learning and reasoning modules. The latter then determines whether remedial action is required or not. For example, in the event of deteriorating link conditions, the reasoning engine decides the remedial action that must be taken. The required action can be switching to a different diffraction path that provides better performance. Another possible action would be switching to a lower modulation and coding scheme.

3.4.1.3 Database

The database, stores the location information of radio devices and diffraction points, temporary information about link performance, and results of the cognitive engine's learning, reasoning, and optimization processes. The location information of the radios and diffraction points is a key input in the establishment of links between the

radio devices. The use of distributed databases has the advantage of reducing control traffic carried on the backhaul networks. This is important in UDN deployments because of the large number of backhaul devices that can be deployed. The performance details of the paths are stored in a permanent network database in the core network. The information is uploaded at initial network set-up and at any other time whenever there are permanent changes to the location of diffraction points, such as addition or removal of a building.

3.4.1.4 Network module

The network module enables the radio devices to attach to the network and contains authentication, network address and other information required to establish connectivity with other devices and the core network.

3.4.1.5 Controller module

The control module in the PtMP architecture can be a dedicated network entity or it can reside in the core network. In this research, a dedicated module is proposed to minimize control traffic over the backhaul links. Its main task is to maintain an optimal topology, through addition or removal of SBR devices or enforcing sleep/active modes on the network. The controller is able to optimize the topology dynamically based on the environmental, traffic or network conditions, gathered through the cognitive engine learning module. Although it is a critical component of the CNSCB, its development is left for future work.

3.4.2 Network model

Fig. 3.4 illustrates how multiple backhaul paths are created between a street backhaul radio device and a massive MIMO base stations on the CNSCB system. A backhaul link is established by simultaneously pointing the radio antennas to the

same diffraction point. Possible multiple paths between the backhaul radio devices are created by alternately pointing the radio antennas to different diffraction points. The number of possible paths depends on the number of available diffraction points between radio devices. Establishment of a backhaul connection depends on whether the resultant radio link meets the performance requirements predefined by the network operator, i.e. latency, throughput, packet loss and received signal strength at the radio device. A communication loop is a set-up between the two radio devices, allowing

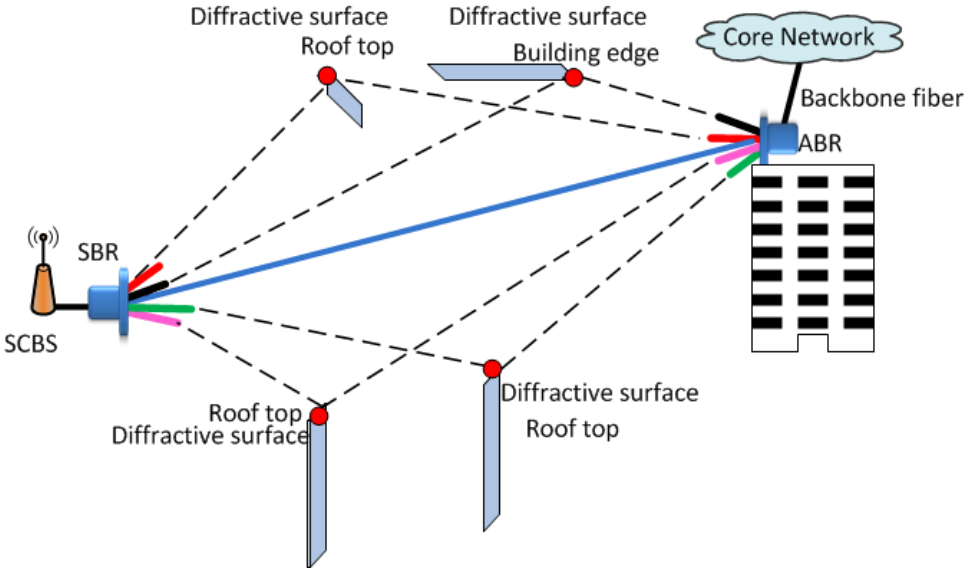

Figure 3.4: Network Model

the devices to perform network level tests. Values of the measured performance parameters such as throughput, delay, and packet loss are compared with those stored in the database. Details of links with parameters falling within the predefined ranges of values are stored in the database. The process is repeated until the maximum number of possible paths is reached. The list of possible paths is rearranged in order of performance, starting with the best performing link. The link performance information is uploaded into the network database, while details of only five links are stored in the radio database. Only information for the five links is stored on the radio device in order to save memory space and also avoid slowing down the processes of

the radio devices. The link in the first position, i.e. the best performing link, is used for setting up the backhaul link. Connection to the SCBS (for the SBR) and the switch or router (for the ABR) is then established. A signal to indicate the presence of the link is sent to the core network or SCBS, triggering the placement of data on the backhaul link.

3.4.3 Network Topology

Fig. 3.5 illustrates the two possible network topologies of the system, i.e. PtP or PtMP. PtP connectivity is established using two single radio devices at each end of the backhaul link. It is used when a SCBS location is isolated and providing a massive MIMO base station is not economically viable. In the PtMP configuration,

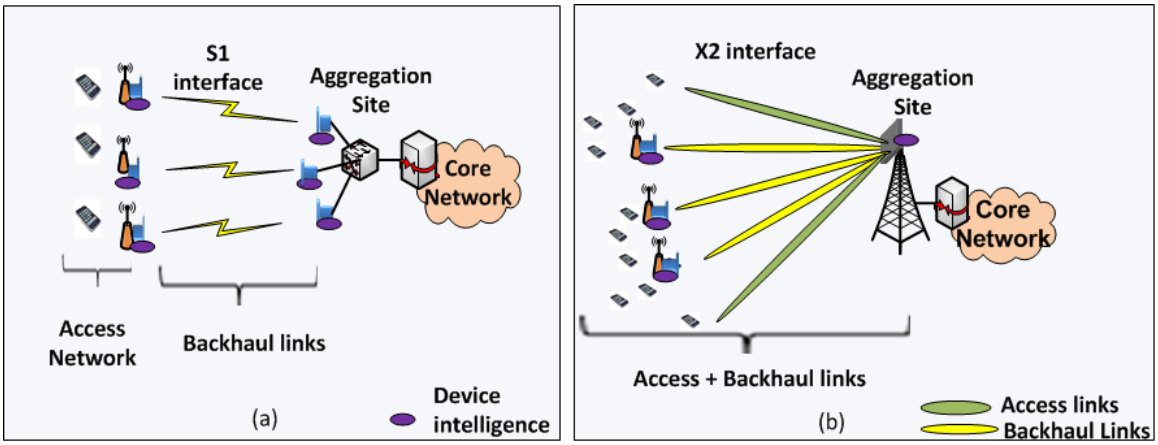

Figure 3.5: Network topologies

the ABR is implemented using a massive MIMO system and a single radio device at the SCBS location. The PtMP configuration addresses the requirement for cost effective implementation of large numbers of backhaul links and for increasing per unit area backhaul coverage. NLOS operation is possible in both configurations and is achieved through diffraction points.

3.5 System Operation

The CNSCB is a sub-network of the mobile transport system capable of providing intelligent, high capacity NLOS Ethernet backhaul connectivity to small cell networks.

The system concept is based on the use of intelligence algorithms implemented in the cognitive engine to gather link performance information and geolocation of diffraction points to establish NLOS connectivity between backhaul radio devices. Wireless channel performance information includes received signal strength, latency, throughput and packet loss ratio.

3.5.1 Link Setup

The operation of the CNSCB system involves three phases: (1) installation of radio devices, (2) establishment of the NLOS link and (3) link performance optimization. Fig. 3.6 illustrates the procedure for connection set up from device power up to the point when the system is ready for data transmission. The procedure is explanied the following sections.

3.5.2 Device installation and network attachment

The physical installation involves mounting the radio device to a lamppost, side of building etc., and pointing the antenna in the general direction of the peer radio. After powering up, the radio device uses the minimal configuration to connect to the network. The SBR can connect to the network using WiFi connection or a UE interface. The ABR attaches to the network via the Ethernet connection to the switch or router.

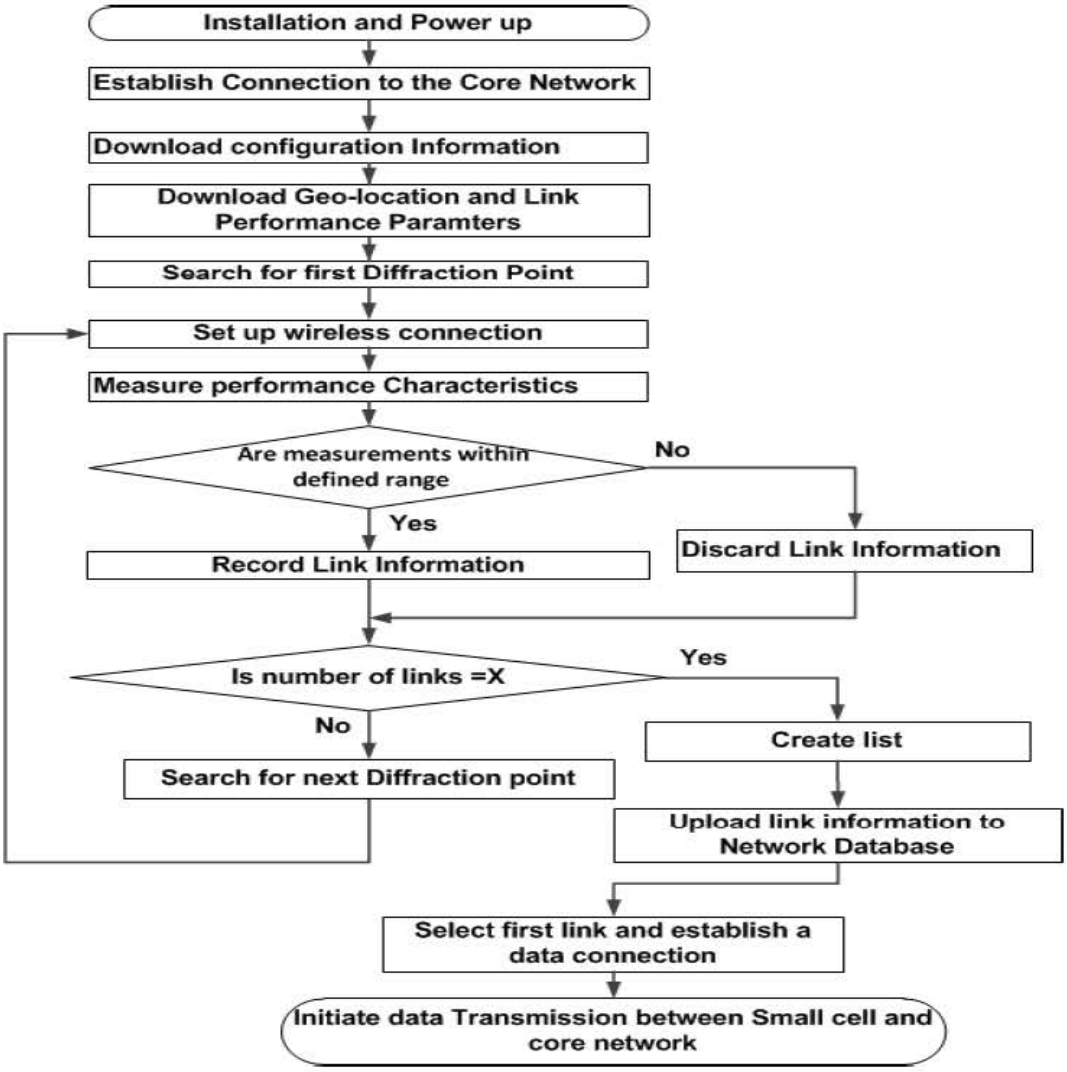

Figure 3.6: Procedure for backhaul link set up

3.5.3 Obtaining network and environmental information

After attaching to the network, the radios must obtain information or knowledge about the network and operating environment from the network database. The information downloaded includes the full configuration details specific to the mobile operator's network such as operating frequency, location information about peer backhaul radio device, SCBS to connect to and possible diffraction points. It is assumed that a network database with coordinates of the diffraction points, backhaul

network exists. Development of such databases is out of the scope of this research and is left for future work. The information obtained is used in the decision-making process, deciding which peer radio to connect to, the diffraction points to use and whether to establish a link or not using the identified radio and diffraction point.

3.5.4 Establishing multiple-links

To make initial connection set up, the antennas of peer radios are simultaneously pointed to the same diffraction point and the radios sense the received signal strength. If it is above a predefined threshold, a wireless connection is established, otherwise, the radio antennas are automatically pointed to the next nearest diffraction point. When a signal above the threshold is detected, the antennas are locked to the diffraction and the link establishment process is started.

3.5.5 System self-healing

The radio devices constantly monitor the performance of the primary link, a self-healing aspect of the CNSCB. In the event of the link performance falling below the predefined performance requirements, the radio recalls the next best link, tests for conformance to the initial performance parameter values, and establishes a connection. Should it fail, the process is repeated until a suitable link is identified. System performance is improved through the use of existing information to correct a mal-performance of the system.

During periods of low traffic levels, the radios re-scan the environment for possible new and better-performing diffraction points and store the information in a network database for long-term use by the system. The process of obtaining knowledge is the learning process of the radio devices.

The cognitive cycle is closely related to the SON processes, i.e. self-configuration, self-optimization and self-healing. The self-configuration and initial set-up process is the process of obtaining knowledge from the operating environment, i.e. the learning process. The self-healing process is initiated when the radios detect deterioration in the performance of the link. The reasoning part of the cognitive process is when the radio devices decide to establish a new connection based on the information obtained about the performance of the network. The reasoning and learning processes of the cognitive process result in the self-optimization processes when the radio devices constantly compare the current operating state of the link and take mitigating measures to restore the link to the correct performance status.

3.5.6 Self-optimization

The optimization processes involve the determination of optimal performance parameters of the radio devices under various wireless channel conditions and temporary signal blockage. The process also involves the determination of the optimal number of paths that can be used by a set of radio devices forming a backhaul link. The quality of the link is used to determine the suitability of a diffraction point to be used as a backhaul link. Points with excessive diffraction loss would result in poor link quality and are removed from a list of possible connection points through an optimization process. The locations of diffraction points that result in backhaul links with an optimal performance above a given threshold are stored in the database and can be used alternatively in the event of deterioration in the performance of the primary link.

In addition to the algorithms used in the establishment of NLOS link in the CNSCB system, energy awareness capabilities can be incorporated into the CNSCB system, making it possible to implement sleep modes using the inbuilt device intelligence.

Device intelligence also enables topology changes in response to changes in access network traffic levels to optimize energy utilization. Implementation of sleep modes on access networks is part of ongoing research and the same solutions can be adopted for use on the CNSCB system. This can be achieved through joint design and optimization of the access and backhaul networks. The development of these algorithms is outside the scope of this research.

3.6 Mapping standard performance requirements to system capabilities

The developed CNSCB system is optimised for backhauling 5G outdoor urban small cells as shown in Fig. 3.7. The architectural design aims to address the limitations identified in existing literature, to achieve backhaul performance levels defined by the NGMN alliance and those being developed for 5G transport systems. The use of mmW frequency bands tackles the requirements for Gbps capacity and low latency requirements. In addition to this, the expected light-licensing will bring down the cost of spectrum, hence cost per transmitted bit. The short transmission ranges allow high frequency reuse, hence increased spectrum efficiency.

Massive MIMO technology allows implementation of the PtMP configuration, so much desired by network operators due to its cost-effectiveness. NLOS operation is the ket capability of the CNSCB system since since using mmW technologies in urban areas results in high signal blockage. A major objective of the CNSCB system is to minimize human intervention in network and link planning and implementation. This is achieved by flexibility in using potential diffraction points and autonomous link establishment and optimization. The key enabling element is the cognitive engine that resides in the backhaul radios. Link reliability and protection against failures and anomalies is achieved through the self-healing process, which is implemented using

learning and reasoning algorithms of the cognitive engine. Due to the increasing contribution to global warming by telecommunication networks, the CNSCB must be energy aware and energy efficient. This can be achieved by implementing sleep modes in the radio devices during periods of low traffic volumes. Implementation of sleep modes is not considered in this research and is left for future work.

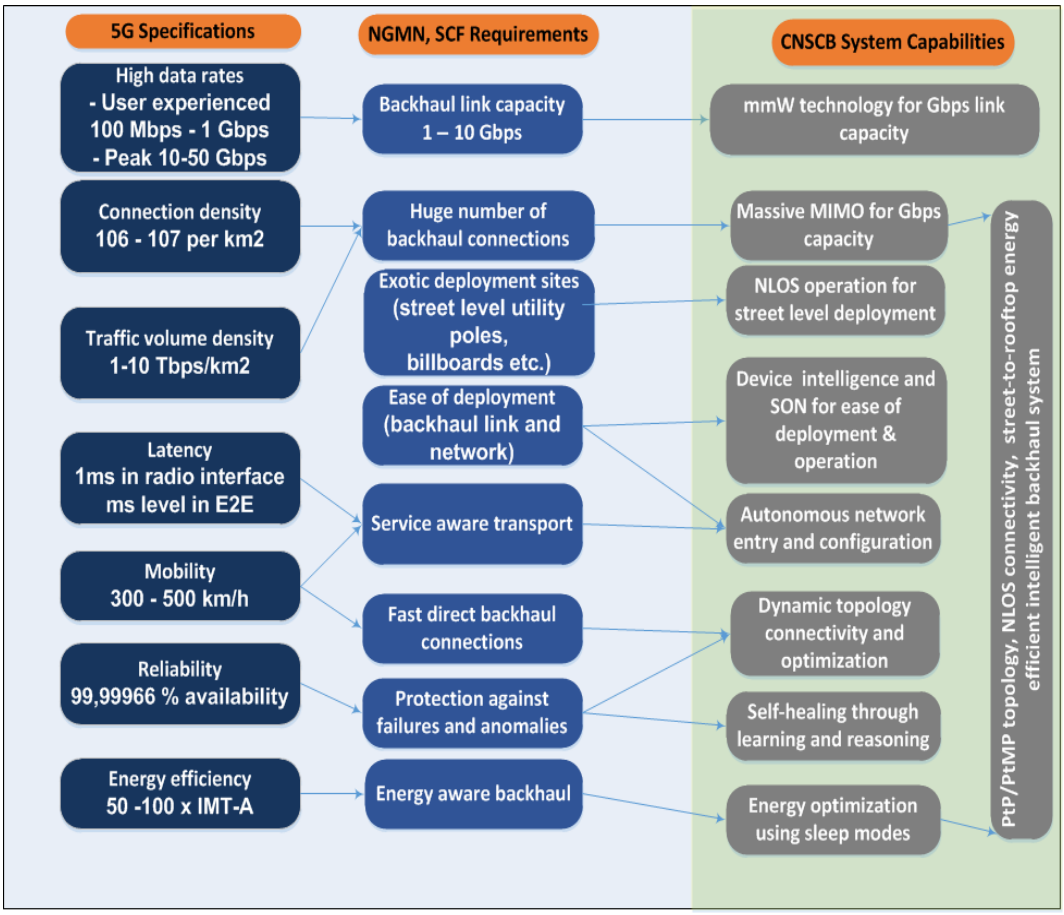

Figure 3.7: Mapping 5G and NGMN requirements to CNSCB system capabilities: Deducted from [33]

3.7 Discussion

The design of outdoor urban SCB backhaul architectures that holistically address the the coverage and capacity requirements, among other issues, is a challenge since Gbps data rates achievable with mmW technologies require that the NLOS problem be addressed due to signal absorption and blockage. The proposed CNSCB architecture uses device intelligence to create multiple-path NLOS paths that can alternately be used by a pair of backhaul radio devices. The radio devices measure the radio and network performance parameters on a path, compare with values stored in a local or network database. If the measured values are within the minimum allowable threshold, e.g. signal strength; or maximum allowable values, e.g. allowable delay, then then details of the link which include coordinates of the diffraction point used are stored in the radio or network database. Using in-built algorithms, a radio device can select the best path and establish connectivity. A key feature of the proposed architecture is the ability to provide NLOS backhaul connectivity at specific locations where it is required. This is critical for network operators, whose small cell deployment will be guided by the need to provide broadband access where it is required. This capability differentiates the CNSCB solution from existing NLOS solutions, where illuminated locations are identified and network operators expected to deploy SCBSs in those locations - the challenge being that there might be no requirement for access in those locations.

An algorithm that can be implemented in the radio devices to ensure system reliability under NLOS conditions are presented in Chapter 5. The system model, based on reinforcement learning is presented. The developed algorithm and simulation results are presented.

While energy efficiency optimization algorithms are not developed in this thesis to address the energy efficiency and awareness requirement of the SCB segment, it is

assumed that some of the solutions being developed for use in SCBS devices can be adopted and implemented in the backhaul radio devices. However, a model to analyse and evaluate the energy efficiency of the CNSCB system is presented in chapter 6.

3.8 Practical application areas of the proposed system

The proposed CNSCB system is aimed at addressing the backhaul capacity and coverage problems in outdoor urban environments. A number of application areas for the proposed system exist. Backhauling small cell base stations densely deployed in outdoor urban environments. In this case, intelligent backhaul systems can minimize the deployment cost due to automation. Furthermore, the building roof edges can be used as diffraction points for directing radio signals between the street-level and roof-level locations. The proposed system can also find application in remote locations where it may not be cost-effective to deploy macro bases stations. Typical examples are clinics in rural areas where mobile applications can be used for delivering healthcare services. In such scenarios, the proposed intelligent backhaul system can be implemented with reduced costs compared to tradition backhaul systems without intelligent capabilities. Carefully selected infrastructures can be used as diffraction points.

3.9 Chapter Summary

This Chapter reviewed on some of the SCB architectures that have been proposed of the literature. One of the major drawbacks identified in the literature is the inability to clearly address the NLOS connectivity problem, while one solution assumes LoS operation, which will not be the case in outdoor urban environments. However, the concepts of SON and use of cognitive intelligence, automate the management and configuration of the systems, also proposed in this research, are some of the strengths of the proposed architectures.

A novel NLOS backhaul architecture is proposed, which mainly uses device intelligence to enable creation of NLOS backhaul connectivity in locations where its required by network operators. The key component of the backhaul radio devices is the proposed algorithms that can be implemented cognitive engine of the radio devices. A description of how multiple-paths per backhaul link can be created using several diffraction points is given. A mapping of the 5G transport specifications to the SCB requirements as defined by the NGMN and SCF and the CNSCB capabilities is provided. Chapter 4 provides a detailed description of the proposed models, and link establishment and location coverage optimisation algorithms.

Chapter 4

NLOS Backhaul Coverage for Outdoor Small Cells

5G systems are expected to be highly reliable, with the ability to self-protect against failures and malfunctions. The deployment of SCBSs at street level in urban areas makes providing backhaul connectivity that meets these requirements using systems operated at mmW frequency bands a problem due to signal blockage. The problem addressed in this chapter is how to reliably use mmW technologies to connect street-mounted SCBSs to the core network using existing roof-mounted backhaul aggregation sites, with no line-of-sight between the two locations. The CNSCB architecture presented in chapter 3 was designed to address NLOS SCB connectivity by using device intelligence to assist in the autonomous creation and performance optimization of NLOS links using diffraction points located on the edges of roofs.

The effects of diffraction loss on mmW radio signals are first studied to determine their suitability to meet the minimum signal strength requirements of the NLOS links, and results of numerical analysis presented. The suitability of the proposed NLOS model to create NLOS links in a practical deployment scenario is studied through experimental work using prototype SCB radio devices. NLOS models suitable for use

at mmW frequencies, algorithms for autonomous creation of NLOS links and SCBS location coverage optimisation are developed. Simulation results are presented and discussed.

4.1 Introduction

Providing NLOS SCB connectivity at mmW frequencies will enable networks operators to provide high capacity backhaul connectivity to outdoor urban small cell networks without the need for complex implementations on the radio modules. However, if the problem of signal blockage is not addressed, it will be practically impossible to achieve reliable connectivity. The single knife edge diffraction (SKED) geometry is used in this research to model street-to-rooftop backhaul links, using diffraction points located on roof edges, and visible to both SCBS and aggregation site locations as intermediate signal anchor points. This way, the blockage of the mmW radio signals is mitigated. However, because of the pencil-size beam of the mmW radio signals, which result from the use of high gain antennas, automatic antenna steering capabilities would be required in the radio devices to focus the radio beams to the diffraction points. Furthermore, the expected large numbers of deployed backhaul links will demand the use of self-configuration, self-optimization and self-healing algorithms to reduce operational costs by minimizing human intervention in the network operation. To this end, the use of cognitive intelligence, implemented through artificial intelligence algorithms, are developed and their performance evaluated through simulations in this chapter.

The main theme of this chapter is to harness the high capacity of mmW technologies, the SKED geometry and artificial intelligence algorithms to ensure reliable NLOS backhaul connections to outdoor small cells in outdoor urban environments. The main contribution of the proposed scheme with respect to existing literature is the analysis of mmW diffraction loss, and novel algorithms for multiple-path selection

and SCBS location coverage optimisation. From the reviewed work, To the best of our knowledge, there is no other solution that takes all these techniques and models at one time, to holistically address the SCB problem in outdoor urban areas.

The chapter is divided into four sections, covering an introduction, related work, proposed model (where applicable), developed algorithms, simulation results and a discussion. The chapter concludes with a summary.

4.2 Diffraction Loss Analysis and Evaluation at mmW frequencies

This section presents results of analysis of diffraction at mmW frequencies. A review of the related work is first given. This is followed by presentation of the proposed propagation model for street to rooftop NLOS backhaul links, the problem formulation and concludes with a presentation of the results.

4.2.1 Related work

Propagation models for mmW systems operated in outdoor urban environments have not been fully studied. Most of the propagation studies have focused on frequencies below 30GHz, the operating frequencies of most commercial communication systems [82–85]. The limitations of the proposed propagation models in capturing propagation characteristics of millimetre wave frequencies, such as signal blockage in outdoor urban environments and high atmospheric absorption, have necessitated the development of new propagation models for the frequencies such as the one developed in [8], and is shown in equation (4.1). In this model, propagation loss in outdoor environments, including loss due to diffraction, is generalized and presented as loss due to "*urban clutter*" represented as $X_\sigma(dB)$ in equation (4.1).

$$PL(dB) = PL_{d0}(dB) + 10log_{10}\frac{d}{d_0}(dB) + X_\sigma(dB) \tag{4.1}$$

where X_σ is the zero mean Gaussian random variable which caters for clutter in urban environments, d is the distance between the radio device and d_0 is the nearside antenna distance, PL_{d0} is the close in free space path loss in dB, which is a function of the signal wavelength, λ and is given by:

$$PL(d_0) = 10log_{10}(\frac{4\pi d_0}{\lambda})^2 \tag{4.2}$$

The model takes into account signal blockage by vegetation, vehicles, humans and buildings. However, in the case of the CNSCB system, the effects of these blockages are expected to be minimal on the street-to-diffraction point segment due to the orientation of the antenna towards the rooftops and all suitable diffractions are assumed to have clear LoS with the aggregation sight since most urban scatters are usually up to ten meters above ground. Furthermore, it is assumed that the radio antennas are equipped with automatic antenna steering technology for steering the radio beams to the exact location of a diffraction point. Diffraction loss is therefore the main source of propagation loss on the link. It is therefore necessary to quantify this loss in order to evaluate the performance of the radio links.

4.2.2 Propagation model for mmW street-to-rooftop NLOS backhaul links

The propagation model defined in equation (4.1) does not take into account the effects of interference from radio signals from other systems due to the narrow signal beam-width which is a result of the use of high gain antennas. Furthermore, diffraction loss is therefore expected to have more impact on the signal loss than X_σ. In order to capture the effects of diffraction loss on the NLOS backhaul paths, we propose a model which incorporates the actual calculated value of diffraction loss. The propagation model in equation (4.1) is therefore modified and rewritten as follows:

$$PL(dB) = PL_{d0}(dB) + 10log_{10}\frac{d}{d_0}(dB) + X_\sigma(dB) + J_{(v)}(dB) \tag{4.3}$$

where $J_{(v)}$ is the diffraction loss. This equation in the subsequent sections for determining the path loss on the diffraction paths.

The SKED model, developed by the ITU-R [86] provides a method for determining the diffraction loss on an object represented as a single knife edge. The Deygout and Walfisch-Bertoni models were developed to predict the propagation loss in outdoor urban environments due to sharp edges, with the latter specifically developed for street-to-rooftop wireless links and are also frequency independent [85, 87]. The Walfisch-Bertoni model, in conjunction with the SKED model are therefore used in this research.

4.2.3 Problem formulation

The CNSCB system depends heavily, on propagation by diffraction for establishing street-to-rooftop backhaul links. The performance of a link depends on the diffraction loss suffered on the path. The geometry of the SKED model is shown in Fig. 4.1. This geometry is similar to the street-to-rooftop topology of the NLOS backhaul paths. In the figure, h, d_1 and d_2 represent the distance of a diffraction point from the LoS path, the distance of a transmitter, (T_x) from a diffraction point D and the distance of receiver (R_x) from the same diffraction point, respectively. The SKED model is

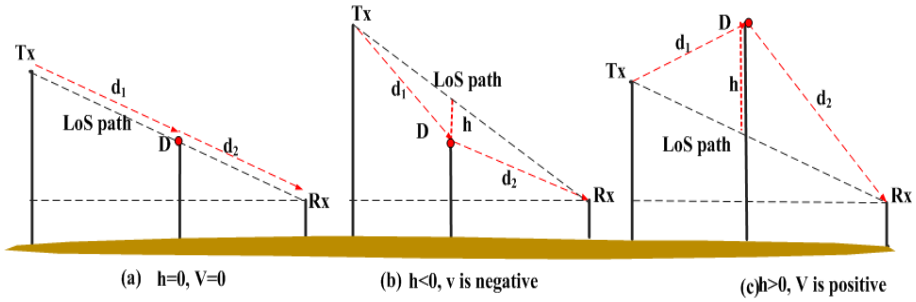

Figure 4.1: Single knife edge geometry for SKED model

used as the basis for analysing the performance of the CNSCB system. The model is used to predict the energy loss at a selected point when a radio signal impinges

on an obstructing object. It also provides insight into the order of magnitude of the diffraction loss when the diffracting object is treated as a knife edge. The diffraction loss depends on h, d_1, d_2 and λ, the wavelength of the operating frequency of the system. As the signal impinges on a diffracting object and leaves the surface, it experiences a change in direction from that of the original path. The phase difference between the two paths, ϕ, is also a function of h, d_1, d_2 and λ. The relationship between the parameters can be represented as [86]:

$$\phi = \frac{\pi}{2}V^2 \tag{4.4}$$

where V is the Fresnel-Kirchoff diffraction parameter given by:

$$V = h\sqrt{\frac{2(d_1 + d_2)}{\lambda d_1 d_2}} \tag{4.5}$$

Equation (4.5) holds for h $\ll$ d1, h $\ll$d2 , and h $\gg \lambda$. When the value of $h = 0$, i.e. when the bore-sight of the signal touches the diffracting point, $V = 0$. This is illustrated in Fig 4.1 (a). In this case, all the electrical energy of the signal is lost due to diffraction. When h $\ll 0$, i.e. the line of sight is above the diffracting edge, as shown in Fig 4.1 (b), V is negative and the energy loss due to diffraction is relatively low. When h $\gg 0$, as shown in Fig. 4.1 (c), the line of sight path is below the diffracting edge, the diffraction loss is positive and increases with increase in h.

Fresnel zones can also be used to describe diffraction loss as a function of the difference in length between the line- of sight path and that followed by the diffracted signal. Assuming non-overlapping Fresnel zones, the relationship between the radius of the n^{th} Fresnel zone and the SKED model diffraction loss parameters can be represented as follows [86]:

$$r_n = \sqrt{\frac{n\lambda d_1 d_2}{d_1 + d_2}} \tag{4.6}$$

where r_n is the radius of the n^{th} Fresnel zone. For a circle of radius r_n, the excess path length is given by $\lambda/2$, λ, $3\lambda/2$, etc. for $n = 1, 2, 3, \ldots$. The radius r_n depends on the values of d_1 and d_2, and is maximum when $d_1 = d_2$. The diffraction loss is

considered minimal if the obstructing object does not block the first Fresnel zone. If 55% of the 1st Fresnel zone is clear of the diffraction point, further clearance does not have significant impact on the diffraction loss.

The diffraction loss of objects that are modelled as single knife edges can be estimated using the classical Fresnel solution shown in equation (4.7), where *F(v)* is the complex Fresnel integral [88]. The diffraction loss $J_{(v)}$for $V > -7$ can be approximated using equation (4.8) [89]. The propagation model for predicting the path loss, including diffraction loss, can therefore be rewritten as shown in equation (4.9).

$$F_{(v)} = \frac{(1+j)}{2} \int_{v}^{\infty} exp(\frac{-j\pi t^2}{2}) dt \tag{4.7}$$

$$J_{(v)} = (\sqrt{(v-0.1)^2+1} + v - 0.1) \tag{4.8}$$

$$PL_{dB} = PL_{(do)} + 10log_{10}(\frac{d}{d_o}) + X_{\sigma(dB)} + J_{(v)}dB \tag{4.9}$$

4.2.4 Simulations results

This section presents results of numerical simulations carried out to determine effects of single knife edge diffracting surfaces on radio signals at various millimetre wave frequencies. The model is implemented in MATLAB. The aim of the simulations was to determine the diffraction loss at a given diffraction point along a NLOS path. Equation (4.9) is used in calculating the diffraction loss, and equation (4.5) is used to determine the values of V. The values of diffraction loss obtained in the analysis can be used as input to the learning and optimisation algorithms of the radios' cognitive engine. Typical values of d_1 and d_2 for SCB links are used in determining the diffraction loss. The values of r_n and λ for radio signals in the 30GHz to 90GHz frequency bands, which are expected to be used in 5G wireless systems, are used.

4.2.4.1 Variation of diffraction loss with distance of diffraction point from LoS path

Potential diffracting edges in a backhaul coverage area can be located at various distances h, above or below the LoS path. In this analysis, h is varied vertically between +0.18m and -0.18m. The value is the radius of the first Fresnel zone for the 70GHz frequency band determined using equation (4.8). The values of d_1, d_2 and λ were fixed at 40m, 160m and 0.0043m respectively. The latter is the wavelength of a signal at 70GHz. Fig. 4.2 illustrates the variation of the diffraction loss, J_v, with h. The results show that the diffraction loss is lower below the diffraction point and increases for points above the line of sight path. The results show that the impact of

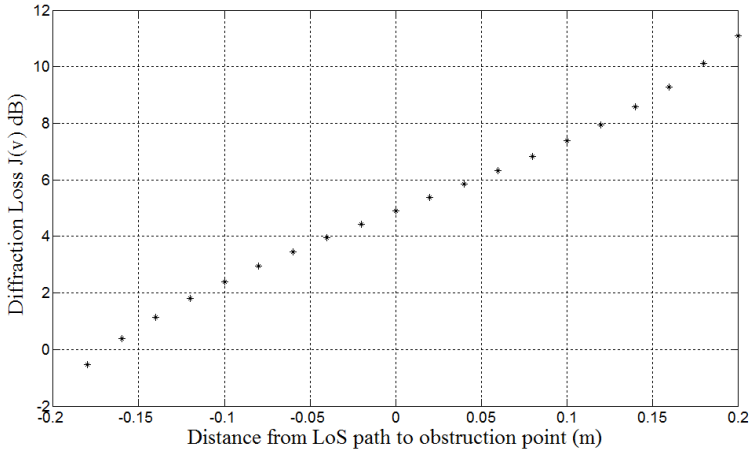

Figure 4.2: Variation of diffraction loss with depth of diffraction point from the line of sight path

diffraction on points below the line of sight path is less than on those above. It can therefore be concluded that when selecting diffraction points in the initial network planning stages, points below the line of sight path must be given preference.

4.2.4.2 Variation of diffraction loss with distance between transmitter and diffraction point

In this simulation, the distance between between a diffracting point and transmitter is varied. The transmitter to receiver distance is fixed at 200m, a typical distance for street-to-rooftop SCB links. The values of wavelength were calculated using the standard relationship between frequency and wavelength, which given by:

$$\lambda = \frac{v}{f} \tag{4.10}$$

where the value of v is the default velocity of light in a vacuum, i.e. 300,000Km/s, f is the frequency of the signal. Fig. 4.3 illustrates the variation of diffraction loss with d_1 for different frequency bands. It can be observed from the that the diffraction

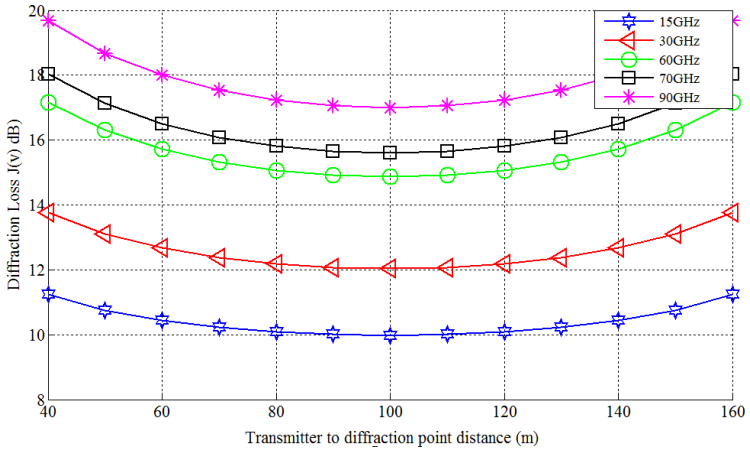

Figure 4.3: Variation of diffraction loss with transmitter to diffraction point distance for different frequency bands

loss increases rapidly when the distance between the transmitter and the diffraction point decreases. This is due to antenna near-side effects, which describe the loss in signal strength close to a transmitting antenna due to self-interference. For outdoor environments this distance is 100m-1000km and up to 1m for indoor environments. According to the Fig. 4.3, the diffraction loss starts increasing for points less than 50m towards the radio device. The location of the points when the diffraction loss

starts to increase are illustrated in Fig. 4.4. The diffraction loss can be considered to be considered constant between the points **a** and **b**, and **c** and **d** If the street backhaul radio is transmitting, diffraction points nearer to the radio than point a can cause high diffraction loss. The increase in diffraction loss closer to the antennas can be due to interference between the received signal and those scattered on impact. At the transmitter side, the loss can also be due to self-interference at the antenna due to the transmitted signal interfering with signals from nearby scatterers. It can be concluded that diffraction points beyond certain distances towards the backhaul radio devices result in high diffraction loss and must be avoided. In this case, from Fig. 4.3, this can be distances less than 60m.

In the graph, lower frequencies are observed to be less susceptible to diffraction loss. The minimum diffraction loss for the frequency bands above 6GHz i.e. 15GHz-60GHz is approximately 15dB compared to that of sub-6GHz systems which 10dB. This can be explained by the larger radius of the Fresnel zones and wavelength at lower frequency bands, which allows more signals to travel round the obstruction points. For all the frequency bands, minimum diffraction loss occurs for points in the middle of the transmission-reception path.

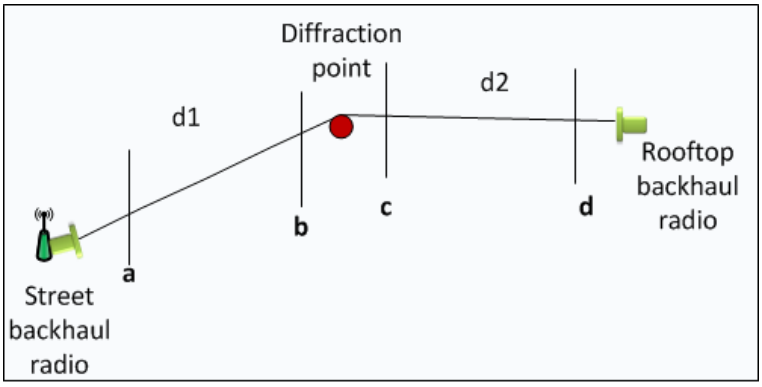

Figure 4.4: Antenna near-side distances

4.2.4.3 Variation of diffraction loss with wavelength

In this section, effects of diffraction loss for frequency bands between 30Ghz and 100GHz is studied. Wavelength, a characteristic of frequency used in the SKED model, is used in the study. The values of d_1, d_2 and h were fixed at 40m, 160m and 0.18m respectively. The distance between the transmitter and reciever is assumed to be 200m. This analysis is important since allocation of mmW spectrum bands for SCB links is expected to vary from country to country.

The results obtained in Fig. 4.5 show a decrease in diffraction loss with increasing wavelength. This illustrates the susceptibility of the frequencies to diffraction loss at higher frequencies. Similar to the previous case, the smaller wavelengths associated with high frequencies show high diffraction loss values compared to lower frequencies. However, even though the lower frequencies are less susceptible to diffraction loss, they have smaller channel bandwidth, which results in smaller channel capacity. A trade-off between acceptable diffraction loss and required channel capacity may therefore be necessary during implementations.

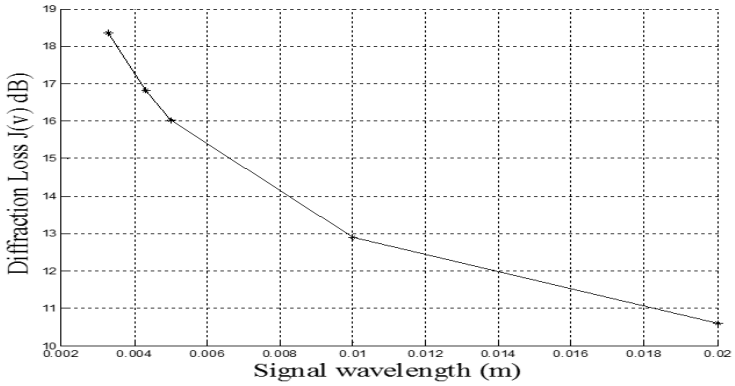

Figure 4.5: Variation of diffraction loss with wavelength

4.2.4.4 Variation of diffraction loss with phase difference between LoS and diffraction paths

The values of the phase difference, ϕ, are varied between 0^o and 12^o both in azimuth and elevation. The maximum value that can be used in radio devices is defined by the ITU to be 12^o [90]. The relationship between the phase difference and the Fresnel-Kirchhoff diffraction parameters is as given in equations (4.4) and (4.5). In this case, V was obtained using fixed values of h, d_1, d_2 and λ of 0.18m, 40m, 160m and 0.0043m respectively. The variation of the diffraction loss with ϕ is shown in Fig. 4.6. The results obtained show that diffraction loss increases as the angle between

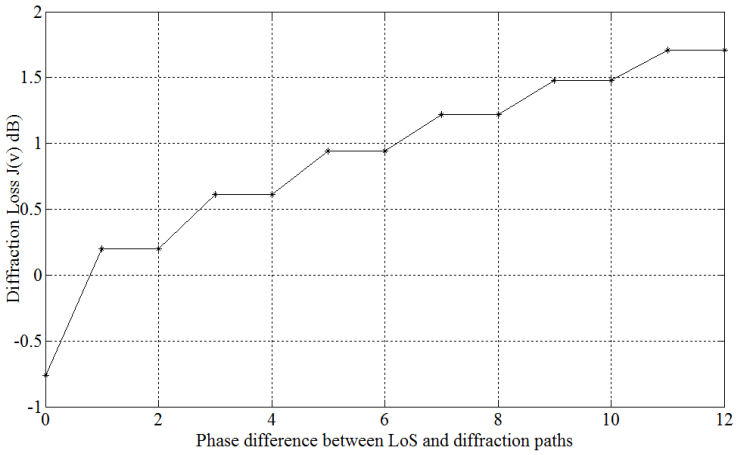

Figure 4.6: Variation of diffraction loss with phase difference between LoS and diffraction paths.

the LoS path and diffraction path increases. It can therefore be concluded that using propagation paths closer to the LoS path results in better performing links due to the reduced diffraction loss.

4.2.4.5 Variation of diffraction loss with transmitter to receiver distance

The length of SCB links is expected to vary from about 100m to 1000m. In this analysis, an operating frequency of 70GHz with a λ value of 0.0043m was used. The

value of h is fixed at 0.18m. Values of diffraction loss were determined for transmitter to receiver distances of 200m, 400m, 600m and 800m. The transmitter to obstruction distance d_1 was varied from 5m to 195m for the 200m link, 5m to 380m for the 400m link, 5m to 595m for the 600m link and 5m to 795m for the 800m link.

Fig. 4.7 illustrates the variation of diffraction loss with the transmitter to receiver distances for the 70GHz frequency band with wavelength 0.0043m. The diffraction loss is observed to increases exponentially closer to the transmitter and receiver, and is constant for a short distance for the short-hop links and constant for longer for the longer links. The increase in diffraction loss closer to the transceivers is due to the antenna nearside effect on the transmitter and receiver, which results in high power loss at distances closer to the antenna. The results show that longer links are less susceptible to diffraction loss than shorter links. It can therefore be concluded that for links shorter than 100m, the diffraction loss would be excessive. The use of aggregation sites close to SBR locations must therefore be avoided.

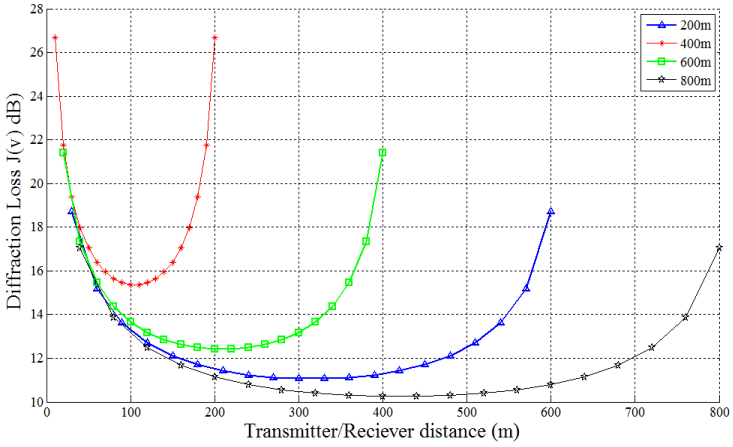

Figure 4.7: Variation of diffraction loss with transmitter to receiver distances

4.2.5 Discussion

Diffraction loss at mmW frequencies has been quantified using the Fresnel-Kirchoff integral, with parameters determined using the SKED model. A pathloss model that takes into account the actual diffraction loss on a backhaul path was proposed and is critical in determining the performance of the backhaul links. Results of the diffraction analysis show that diffraction loss increases with: (1) increase in operating frequency, (2) at diffraction points closer to radio locations, (3) at points above LoS path and (4) with increase in angle between LoS path and diffraction path. A trade-off is therefore required between achievable link capacity and acceptable diffraction loss, hence link QoS.

At the planning stage, using points above LoS path and closer to the radio locations must be be avoided. The phase difference can therefore be used as a guideline for estimating the values of h for particular diffraction points, when values of d_1 and d_2 are known. It also provides discrete values of ϕ which can be used as input to a cognitive radio in the self-configuration and optimization processes. The results obtained are similar to those obtained in [84] with values of h around 100m. The following section describes experimental work carried out to validate the proposed NLOS operation in typical practical deployment scenario

4.3 Feasibility Studies Using Prototype Radio Devices Operated Above 6GHz

As of December 2016, only Samsung and Qualcomm had announced a 60GHz chip-set and 28GHz prototype for small cell backhauling radio devices respectively [50, 51]. Because of the limited availability of fully operational radios, most evaluations of street-to-rooftop backhaul links at frequencies were measurement campaigns done

using channel sounders. To validate the NLOS concept proposed in this research, feasibility studies were therefore carried out using prototype radio devices operated at 17GHz and 60GHz. The purpose of the experiments was two-fold. First, it was important to demonstrate that the proposed concept of NLOS links using frequency bands above 6GHz can be realised in real life situations. Second, it was also necessary to determine the ease with which the links can be established, given the narrow beam-width of radio signals at these frequencies. Furthermore, results of the experimental tests provide insight into the performance of the radio devices in outdoor urban canyon environments using roof edges as diffraction points.

4.3.1 Related Work

The development of backhaul radio devices for outdoor small cells is still in its infancy. More real life experiments are are therefore required, since wireless systems operated above 10GHz provide high capacity links without the need for complex enhancements on the radio modules. Most experimental work on non-line-sight rooftop to street level small cell backhaul connectivity has been on propagation studies aimed at testing the feasibility on non-line-of-sight operation at frequencies above 10GHz using channel sounders as signal generators. Hansryd et al., Bennai and Coldrey et al., performed propagation measurements at 24GHz, 28GHz, 60GHz and 70/90GHz frequency bands [9, 18, 91]. In most of the experiments, measurements of the signal strength showed the presence of strong signals that can be used for backhaul connectivity in most potential small cell locations. The presence of the signals was attributed to the multipath-rich scattering environment of the urban areas considered. The results show that it is feasible to establish high capacity links under non-line-of-sight conditions, dispelling the myth that communications under such conditions are only possible when there is line-of-sight between the radio devices.

However, ensuring coverage of a specific SCBS location is not properly addressed since area coverage is used in the measurements.

Okvist et al., present results of propagation measurements using prototype radio access devices operated at 15GHz [92]. While the experiments were used to determine coverage on the access segment, the same scenario can also be used to determine the performance of a back link between two backhaul radio devices. Signal strength was used as the performance evaluation parameter. The results obtained show that outdoor coverage was limited to areas that are in line-of-sight with the test points. However, the test points were mounted 8.5m and 12.5m above ground on the sides of buildings, while the other radio devices was installed 2.9m above ground. The limited outdoor coverage could be a results of signal blockage by buildings and other urban infrastructures. The outdoor coverage could be improved by installing the radio devices at roof tops, and carefully pointing the antennas to specific potential locations of small cell base station locations, where the other backhaul radio would be collocated. This can be achieved automatic antenna steering technology

4.3.2 Test Environment

The experiments were carried out at the upper campus of the University of Cape Town, a typical area where street-to-rooftop links would be required to backhaul small cell base stations deployed to provide ubiquitous broadband connectivity from the existing indoor IEEE 802.11 hotspots to outdoor 5G operator managed small cells broadband mobile access, and improve QoE for the students and staff population of over twenty-five thousand during a full semester session. The rows of buildings on the campus area are similar to those in most city centres.

Fig. 4.8 shows an aerial view of the upper campus obtained using Google Earth. A location at the top of Menzies building provides a suitable location for an aggregation

site which can be used to connect SCBS's to core networks via high-speed fiber links. The location is currently used as an aggregation site for backhaul links for indoor and outdoor IEEE 802.11 hotspot access points on the campus. Since the IEEE 802.11 backhaul links are operated at 5GHz, NLOS connectivity is easily achieved. However, in the case of SCB links operated above 6GHz, NLOS connectivity would require techniques proposed in this research if street-to-rooftop backhaul links need to be established.

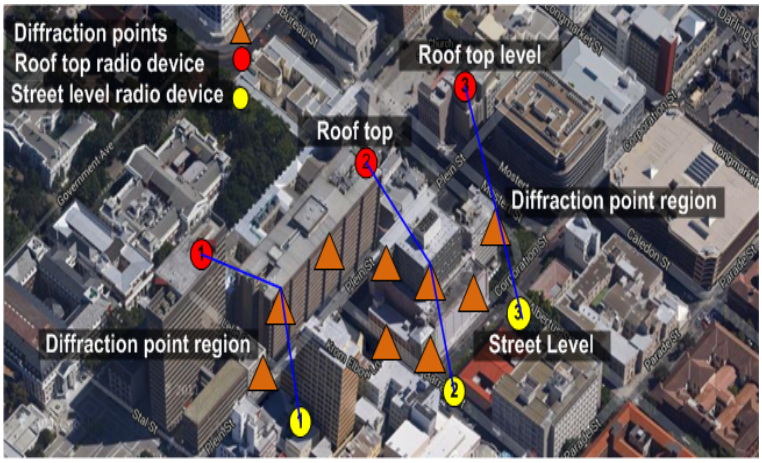

Figure 4.8: Test environment: An aerial view of University of Cape Town with marked node points. (Courtsey: Google Earth)

4.3.3 Feasibility studies using 17GHz radios

The frequencies around 17GHz do not form part of the mmW frequency bands. However, the increasing demand for spectrum in existing commercial bands is prompting the development of equipment in new spectrum bands. The adjustable channel bandwidth, variable modulation and small form factor with integrated antenna in this radio product makes it suitable for use as SCB radio [4].

4.3.3.1 Radio specifications and equipment set up

Table 4.1 shows specifications of the radio devices. A description of the equipment used in the experiments is presented in Table 4.2. The equipment set up at each test location is as shown in Fig. 4.9. The radio devices were mounted on a tripod stand. At each test instance, the antennas of the rooftop and street level radio devices were simultaneously point to the same diffraction point. A telescope was used for fine alignment of the antennas to the diffraction points. Fig. 4.9 (a) shows the set up at the street level. The equipment set up at the aggregation site located on the roof of Menzies Building is as shown in Fig. 4.9 (b). The radio device and laptop were powered from a 12V DC battery. A DC-AC inverter was used to convert the DC voltage to AC required to power the test equipment. The radio was connected to the inverter using power over Ethernet (PoE) cable. The use of the battery and inverter shows the possibility of using solar energy to power radio devices, thus reducing the power tapped from the main grid, hence network carbon footprint.

Table 4.1: 17GHz Radio specifications

Description	**Value**
Carrier Frequency High band	17.225GHz
Carrier Frequency Low band	17.125GHz
Transmit/Receive Intermediate Frequency (IF)	1.2GHz
Transmit/Receive Local Oscillator (LO) Frequency	18.225GHz/16.025GHz
Maximum Transmit Level	-4dBm to -10dBm
Transmit/Receive Antenna Gain	33.6dBi
Receiver Noise Figure	3-4dB
Channel Bandwidth (software adjustable)	14MHz to 56MHz
Modulation (Hitless Automatic Adaptive Coding and Modulation-HAACM)	QPSK to 1024QAM
Throughput (Full Duplex)	400Mbps
Receiver Sensitivity	-57.4 to -82.3 depending on modulation scheme
Mass	6Kg
Dimensions	315x256x130mm

Table 4.2: Experimental equipment

Equipment	Description	Qty
Backhaul radio devices	17GHz FDD with integrated antenna, power over Ethernet interface, Gigabit Ethernet interface, test point for received signal strength	2
Laptop	Gigabit Ethernet interface for providing a web interface for configuring the radios and recording results of link quality tests.	2
12V DC battery	Supplied with inverter for supplying AC power to the laptop and radio devices	2
Telescope	Mounted on each radio and used for accurately pointing the antenna to an identified diffraction point.	2
Laser Distance measuring tool	For determining the distance of the radio devices relative to the ground and the distance between the radio devices and the diffractions	1
Tripod stand (1.5m)	For mounting the radio devices with adjustable brackets for vertical and horizontal antenna alignment	2

Figure 4.9: Equipment set-up: (a) SBR device at street level, (b) ABR device at rooftop level

The aggregation bakhaul radio (ABR) was mounted at the rooftop location on top of Menzies building. The street backhaul radio (SBR) was installed on the ground level about 30m below the roof level with a line-of-sight distance of about 200m. The location of the radio device was strategically selected to be below the shadow region

of possible diffraction points. The radio could be moved to several positions in the signal shadow region below the diffraction point.

The location set up was such that rooftop edges existed between the ABR and the SBR. Potential diffraction points were manually identified. To establish a path, the ABR was pointed towards a diffraction point using the telescope. Brackets mounted on the tripod stand were used to finely adjust the antenna pointing towards a diffraction point. The distance measuring tool, which is equipped with UV light was used to determine the distance between the ABR and the diffraction point. The SBR located in the shadow area of the transmitted signal was first moved manually with the antenna pointed towards the general direction of the diffraction point. Using the brackets mounted on the tripod stands, the radio antenna was finely adjusted horizontally and vertically until the strongest signal was detected. The antenna position was locked and the distance between the radio antenna and the diffraction point measured. The strength of the detected signal was recorded. The distances between the transmitter, ABR and the receiver, SBR, were recorded as d_1 and d_2 respectively. The measurement procedure was repeated for different locations and diffraction points as shown in Fig. 4.10. Two test areas and several radio locations were considered. Locations marked $DP_{(1-2)}$ are diffraction points and those marked $TP_{(2-11)}$ are the locations of the SBR. TP_1 was the fixed location of the ABR. Results of the propagation measurements and link quality tests were recorded for each test point of the SBR. Test area 1, with test points $TP_{(2-6)}$ was located closer to the aggregation radio site (TP1) while test area 2, with $TP_{(7-11)}$ was located further away from the aggregation site. The values of the distances and received signal strength for each link are given and discussed in the next section. The radio performance metrics were obtained from an on-board web interface radio devices developed by the manufacturer, via the laptop.

Figure 4.10: Node deployment

Fig. 4.11 shows network model with the radio locations, diffraction points, and propagation paths. The location of the ABR is fixed, but that of the SBR is moved in search of the best signal. The signal strength at several SBR locations was measured. The SBR was fixed at the location presenting the highest signal strength. Ten test points with potential for good signal were identified (TP2 to TP11). The distance d_1 represents the distance from the ABR to the diffraction point. Distances $d_{2,1}$ to $d_{2,11}$ represent the second leg of the transmission path between the diffraction point and the SBR.

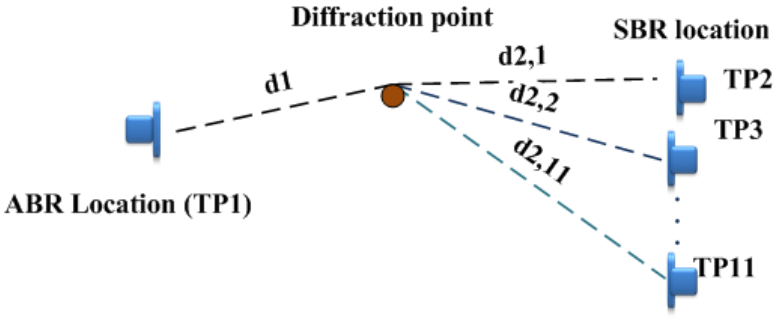

Figure 4.11: Network model

4.3.3.2 Results of propagation measurements

This section presents results of the radio propagation measurements. Preliminary measurements were taken under LoS conditions to determine the optimal performance of the radio under the best propagation conditions. The best signal obtained under these conditions was -32dBm. This value was obtained with modulation, transmit power and channel bandwidth set to 64QAM, -5dBm and 40MHz respectively. With the ABR focused on diffraction point DP1, results of the signal strength for the various test points are shown in Table 4.3. The best link had a received signal strength of -36dBm, with a link length of 78m. However, it can be observed that the longest link of 166m, had a signal strength of -39dBm. This shows that interference due to reflections tends to play a key role in the strength of the signal due to reflections from nearby scatters.

Table 4.3: Results of radio propagation measurements

Link	d_1**(m)**	d_2**(m)**	**Link length(m)**	**RSSI (dBm)**
TP1-TP2	33	34	67	-82
TP1-TP3	33	40	74	-63
TP1-TP4	33	46	79	-57
TP1-TP5	33	59	92	-47
TP1-TP6	33	45	78	-36
TP1-TP7	118	31	149	-63
TP1-TP8	118	33	151	-51
TP1-TP9	118	38	156	-45
TP1-TP10	118	42	160	-38
TP1-TP11	118	48	166	-39

For the single knife edge diffraction (SKED) model, the diffraction loss at a point depends on the variables h, λ, d_1 and d_2. : In these tests, λ, h and the distance between the ABR and the diffraction point were fixed since the operating frequency and location of diffraction point and ABR are fixed. Diffraction loss is therefore determined by the values of the NLOS path segment between the diffraction point and the SBR. Only the distance from the diffraction point to the SBR, d_2 was varied. The

difference in diffraction loss is therefore attributed to the distance between the SBR and diffraction point. Other causes of signal power loss could be due to scattering in the test area. Self-interference is also another problem associated with FDD operation in wireless devices. This could also be another cause of the weakening of the received signal strength.

Results obtained when ABR was pointed towards diffraction point DP2 are also shown in Table 4.3. The link lengths varied from 149m to 160m. Like in the above test scenario, the distance between the diffraction point and the ABR was fixed. The distance from the diffraction point to the test positions TP7 to TP11 varied as the radio was moved in search of a good link quality. The strongest signal strength of -38dBm was obtained on the 166m link with the SBR on test point 10. The strong signal obtained could be attributed to the increased distance between the diffraction point and the SBR. While an increase in distance results in increased free space path loss, self interference could have more severe effects on the received signal, especially in FDD mode. As shown in the results of the numerical analysis of diffraction loss in the previous section, short hop links are more prone to higher diffraction loss due to the antenna near-side effects. Another challenge that would affect the radio performance is self-interference since the radios are operating in FDD mode. The results show that most of the links in test area 2 have better RSSI values, i.e. stronger signal strength than those in area 1 which indicates that the shorter hop links were more prone to diffraction loss than the longer links in test area 2. The same observation was also recorded in [8, 18], where short-hop rooftop to street level links tend to be more prone to diffraction loss than longer links. Another reason for the low signal strength in test area 1 could be a result of too many reflections since the area was surrounded by metal door frames and window frames, which was not the case in test area 2. It can be concluded from the results that test points test points 6, 11 and 10 represent the best possible locations for installation of SBR backhaul radio devices.

4.3.3.3 Results of link quality tests

In addition to the radio propagation measurements, link quality tests were also conducted to determine the capability of the established non-line-of-sight links to meet the minimum QoS requirements for the small cell backhaul segment defined by the next generation mobile network (NGMN) alliance and 5G backhaul networks. Values of the four QoS metrics used for packet-based networks, i.e. data rate, delay, jitter and packet loss were obtained. The recommended values for these parameters are shown in Table 4.4 [5, 21]. The performance requirements of the services offered on small cell networks are expected to vary due to the large number of applications expected, e.g. gaming, video streaming and voice. The limits on the requirements take these variations into account.

Table 4.4: QoS performance requirements for the small cell backhaul segment [5, 21]

Parameter	NGMN requirement	5G requirement
One way delay	1-60ms, >60ms potentially acceptable depending on application	<1ms
Data rate	>180Mbps	>1Gbps
Jitter	<20ms	<1ms
Packet loss	<0.1%	<0.1%

The QoS values for the established links were obtained using iPerf, a network performance measuring tool that was developed for measuring transmission control control (TCP) and user datagram protocol (UDP) bandwidth performance, and is freely available on-line. Insight into the performance of a communication link is obtained by entering the iPerf commands on a computer connected to the transmitting or receiving device. After entering the necessary commands, iPerf automatically generates data between two devices configured in client and server mode. The connection set up is shown in Fig. 4.12. The software was downloaded and installed on the two laptops that were connected to the radio devices. The laptops were

configured to operate in client-server mode. An Ethernet cable was used to connect the laptops to the radio devices, which have an Ethernet interface. The data was transmitted over each of the established backhaul links over the several diffraction points. Table 4.5 shows results of the link quality tests for the links discussed in the

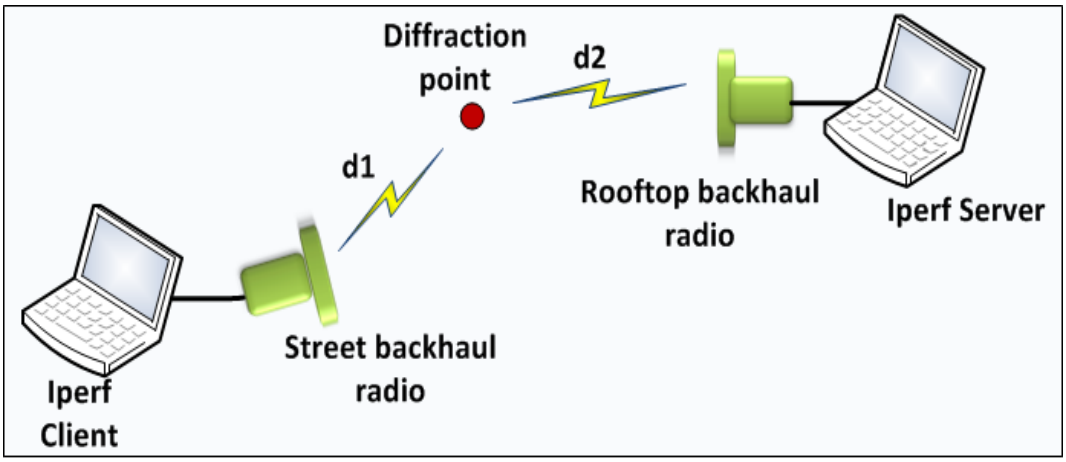

Figure 4.12: Set up for measuring link throughput, packet loss, jitter and delay

previous sections. The tests were aimed at determining the achievable throughput, the link delay, jitter and packet loss ratio for each established link. In all cases, the radio web interfaces indicated the link status as up, i.e. the connection between the two radios was established.

The results obtained show that the average round trip delay for all measurements varied between 0ms and 1ms. The lack of values between 0 and 1 might be attributed to the lack of granularity in the Iperf measurement results. The maximum allowable delay for on the small cell backhaul segment varies from 1-60ms depending on the application as shown in Table 7.4. While the delay is within the acceptable limits and radio link indicating link availability status, values of jitter and packet loss ratio did not meet the minimum performance requirements, hence making the identified link unusable. For example, jitter values greater than the upper bound of 20ms were

Table 4.5: Results of link quality tests

Test Point	**QoS Metric**				
	Round trip delay (ms)	**Jitter (ms)**	**Packet loss %**	**Thru/put (Mbps)**	**Capacity (Mbps)**
2	1	1246	95	192	384
3	1	438.9	92	100	160
4	0	33	95	190	192
5	0	3.9	0.02	20	44
6	1	0.425	0.10	180	192
7	0	3.47	61	100	150
8	0	3.9	47	182	194
9	1	34.9	90	10	49
10	0	5	0.08	198	260
11	1	0.72	0	180	200

obtained for links on test positions 2, 3, 4 and 9. The rest of the values obtained fall below the upper bound value.

The maximum allowable packet loss ratio and is defined as:

$$packet\ loss\ ratio\ =\ \frac{packets\ sent - packets\ received}{packets\ sent}$$

For the SCB segment, the upper bound value for the packet loss ratio is 0.1%. The experimental values obtained varied from 0% to 95%. From Table 7.5 the upper bound is 0.1%. This is the same value defined by the International Telecommunication Union (ITU) for voice service, assuming that high-quality voice codecs are used on the voice applications.

The available bandwidth values varied from 10Mbps to 192Mbps on both the uplink and downlink. Two of the links, i.e. TP5 and TP9 had throughput of less than 50% of the channel capacity. Of interest is the difference between the available link capacity recorded on the radios and the throughput achieved by Iperf. At each instant, the radios determine the available link capacity depending on the propagation characteristics. The system throughput is observed to be lower than this value in all cases. This could be because of errors happening at the high layers. While high

throughput was recorded, it was also observed that the other performance metrics were below the minimum or maximum allowable values, and thus could render the links unusable. This is due to the bursty nature of IP traffic, and the unstable nature of wireless links. For example, if a large number of packets are transmitted at the time when the received signal strength is low, this results in large packet loss ratio. However the system may record a high throughput. The overall performance of the link therefore depends on the values of all the QoS parameters.

Fig. 4.13 shows a representation of the overall performance of the non-line-of-sight backhaul system including radio and QoS performance characteristics. The RSSI

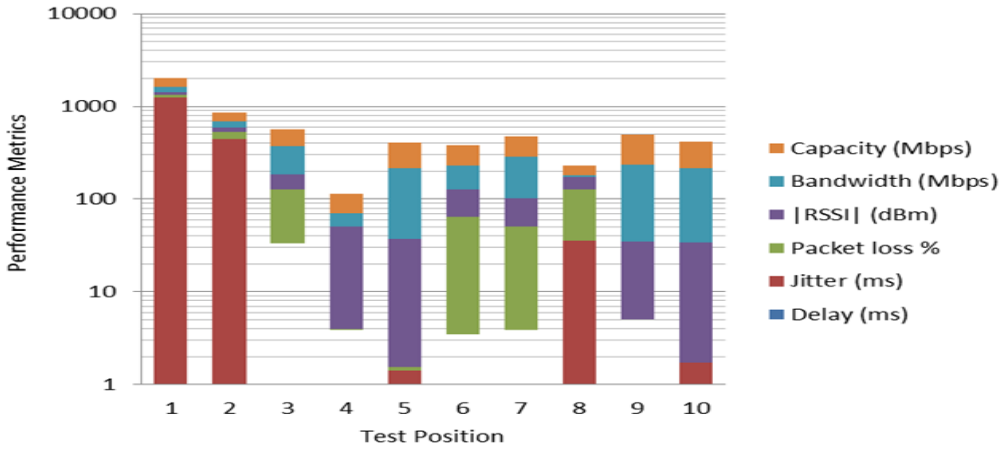

Figure 4.13: Radio link characteristics and QoS values

values are represented as magnitude for clarity, with the highest value being the weakest signal strength. A logarithmic scale of 10 is used to represent the data due to the large variation in the range of values. Jitter, received signal strength, and packet loss present the highest variations for all the test positions. The delay for short-hop links such as those expected in small cell backhaul links, i.e. up to 2000m, is minimal due to the short distances. Most of the delay can be attributed to processing delay in the radio devices. For the SCB system, the tests have shown the insignificant effect of delay on the various test positions even for the links with low signal strength, as

long as connection is established between the two radio links. Jitter and packet loss present the worst variations, with jitter varying from 0.72ms to 1246ms and packet loss ratio from 0% to 0.95%.

As shown in the Table 4.5, the average round trip delay for all measurements varied between 0ms and 1ms. The maximum allowable network delay for applications on IP networks is 2ms. While the delay is within the acceptable limits and radio link indicating link availability status, values of jitter and packet loss ratio did not meet the minimum performance requirements, hence making the identified link unusable. For example, jitter values of 1246ms and 438.9ms were obtained for links on test positions 2 and 3. All the links had jitter values above the maximum required value of 0.1ms. This could be attributed to the high packet loss recorded, snice those links with high packet loss values recorded the highest jitter values.

4.3.3.4 Performance analysis

With no other systems currently deployed at 17GHz in the test area, and given the short distances between the radio devices, the loss in signal strength can be attributed to the diffraction loss due to the obstructions along the propagation path. The channel capacity for a link is given by Shannon's law. Since the channel bandwidth B is fixed, the signal to ratio (SNR) therefore predominantly causes the decrease in the detected signal strength. With no other systems operating at 17GHz in the area, the most probable source of interference is likely to be inter-symbol-interference (ISI) arising due to multipath propagation. This interference power is likely to cause high error rates and hence a decrease in data rate.

4.3.4 Feasibility Studies Using 60GHz Prototype Radio Devices

Unlike the above scenario, the 60GHz frequency band is one of the mmW frequency bands being proposed for 5G access and short-hop backhaul links. The aim of this experiment was to determine the ease with which the radio could be set up and backhaul connectivity established, given the narrow beam width of the of the resultant radio signal at 60GHz. The two segments of the proposed non-line-of-sight architecture are expected to have line-of-sight between the diffraction point and the radio devices. In addition to testing the ease with which the antenna pointing can be established, the experiment also provided information on the ease with which the line-of-sight link segments can be established. Furthermore, the signal propagation characteristics of the 60GHz short-hop links were also studied.

4.3.4.1 Radio specifications and operation

Table 4.6 shows the specifications of the 60GHz radio used in the experiments. The specifications fall within those outlined by the Small Cell Forum for mmW backhaul devices.

Table 4.6: 60GHz Radio specifications

Description	**Value**
Carrier Frequency High/Low Band	62-63GHz/59-60GHz
RF Bandwidth Null-to-Null	750MHz
Transmit/Receive IF frequency	8-9.1GHz
Transmit/Receive LO Frequency	16.3-18.3GHz
Transmit Power	-7dBm
Receive noise figure	8dB
Receive sensitivity	-72dBm
Transmit/Receive antenna	38dBi with Dielectric Lens
Beam width	2^o
Mass	5kg
Dimensions	297x272x250mm

The radio signal is produced as follows. An integrated frequency synthesizer is used to create a low phase noise Local Oscillator (LO) signal between 16.3GHz and 18.3 GHz. This is divided by two and split into quadrature components. The quadrature components are used to modulate differential baseband signals onto 8GHz to 9.1GHz sliding Intermediate Frequency (IF). The filtered signal is amplified with 17 dB of variable gain. This signal is then mixed with three times the LO frequency, up converting it to an RF signal between 57GHz and 64 GHz. The step size of the synthesizer is equal to 540MHz when used with a 308.5714MHz reference crystal. This is compatible with IEEE channels in the ISM band. When used with a 285.714MHz reference crystal this equates to 500MHz steps. The lower mixing product at 40GHz to 46GHz is attenuated by integrated notch filters. Using two RF amplifiers to provide gain, up to -12dBm differential output is achieved.

4.3.4.2 Equipment set up and experimental procedure

The equipment set-up was the same as those for the 17GHz radios. However, connection to the laptops was made via a USB port since the Ethernet interface is not yet developed. The Putty terminal emulator was installed on the laptops and used for running the radio software via the USB connection.

The experiment was set up on a balcony between two building blocks as shown in Fig. 4.14. The laser distance measuring tool described earlier, was used as a pointer for aligning the antennas towards each other, and for measuring the distance between the two radios. The received signal power was recorded on the laptop via the USB connection. The distance between the radios was varied between 2m and 46m. Values of received signal strength indication (RSSI) were obtained for six test intervals.

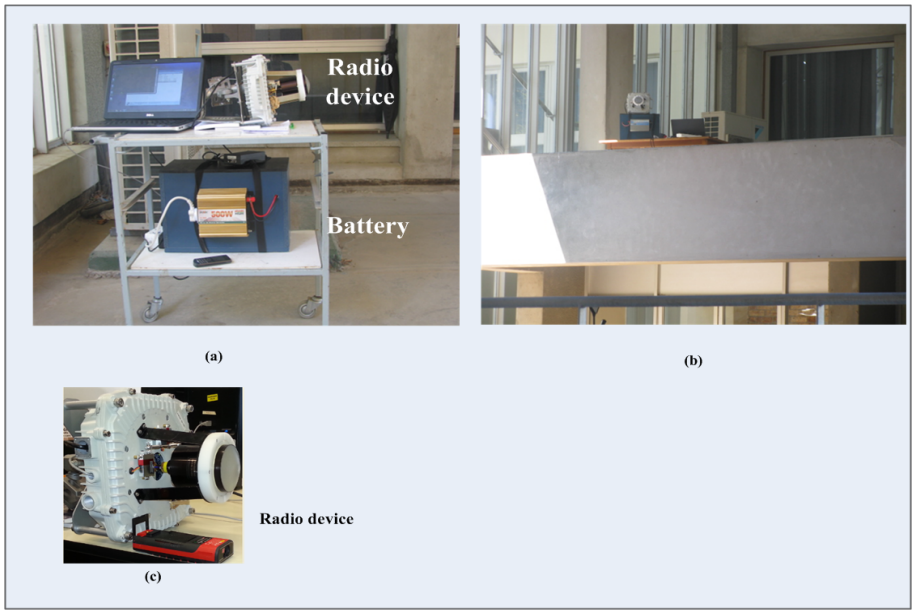

Figure 4.14: Equipment set up for 60GHz tests

4.3.4.3 Results of propagation measurements

The information in Table 4.7 shows the received signal strength values obtained for different transmitter/receiver distances. One radio was to transmit and receive at 62.5GHz and 59.5GHz respectively, while the other radio was set to transmit and receive at 59.5GHz and 62.5GHz respectively. The best signal strength was observed when the radios were aligned bore-sight to bore sight. A significant amount of time was spent manually aligning the antennas for maximum signal strength.

Table 4.7: Link RSSI values

TX/Rx distance (m)	**Uplink freq. (GHz)**	**RSSI (dBm)**	**Downlink freq. (GHz)**	**RSSI (dBm)**
2.06	62.5	-48	59.5	-38
8.17	62.5	-44	59.5	-34
20.77	62.5	-48	59.5	-40
29.45	62.5	-51	59.5	-43
44.85	62.5	-55	59.5	-46
46.9	62.5	-59	59.5	-49

Fig. 4.15 illustrates the variation of the signal strength with distance between the two radios. The signal strength at 2.06m is the same as that obtained at 20.77m. The same trend is observed for the downlink channel. This could be a result of reflections on the signal path causing interference and hence reduction in signal strength. As the distance increased, an average decrement of about 0.9dB/m was observed for both the uplink and the downlink. Of note also is the significant difference between the uplink and downlink signal strength. This shows the significant effects of atmospheric attenuation on the signal at 62.5GHz and 59.5GHz, with the higher band experiencing higher attenuation. Another explanation to this difference could be the difference in the transmit and receive powers in the radios. The differences in the signal strength results in reduced interference between the two transmit and receive channels. This has the effect of increasing spectral efficiency and throughput due to reduced interference. The results show that teh developed radio products can be used for short-hop backhaul links between diffraction points and SBRs and ABRs. However, antenna alignment at the proved to be time-consuming, but this could be resolved by using automatic antenna steering algorithms.

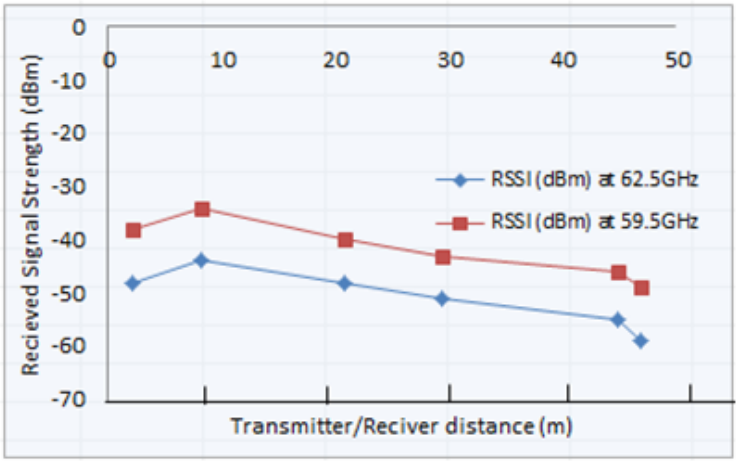

Figure 4.15: Variation of received signal strength with distance at 60GHz

4.3.5 Discussion

The results of the 17GHz radio devices suggest that it is possible to establish NLOS connectivity in a typical urban canyon environment. The results obtained show that by selecting an appropriate diffraction point, a specific location can radio strong enough to enable connectivity. Further tests at network level also revealed that the links can meet the QoS requirements of a typical SCB link. However, the need for carefully pointing the antennas towards the diffraction points was observed.

The experiments using the 60GHz radio devices were aimed at evaluating the performance of short-hop links at this frequency band, and the ease with which LoS connectivity can be achieved. This is because the topological design of the CNSCB system assumes LoS connectivity between a diffraction point and the SBR and ABR devices. The signals observed on the links were above the acceptable threshold for a distance of up to 46m. However, the signal strength observed on the 62.5GHz band was found to be 10dB lower than that observed on the 59.95 frequency band. This shows the sensitivity to atmospheric absorption of the frequencies around the 60GHz operating band. This results in the quality of the link on the uplink performing better than that on the downlink, but on the same radio devices.

4.4 NLOS Multiple-path Selection and Optimization

The key characteristic of the CNSCB system is the ability to improve system reliability by switching transmission paths in the event of deterioration in the performance of a link that is currently in use. This section presents an algorithm for creating the multiple paths and determining the radio performance characteristic of each link at initial network. A brief review of related work is first given, followed by the system model. The problem is formulated then simulation results presented.

Work related to the provision of NLOS backhaul connections in outdoor urban environments. An algorithm that can be implemented in the cognitive engine of the backhaul radio devices is given.

4.4.1 Related Work

A number of solutions addressing the SCB coverage problem have been proposed in literature. A solution leveraging 3.5GHz for NLOS and 60GHz LoS technologies is proposed in [93]. The achievable average peak throughout obtained was 700Mbps and 98.72Mbps for the LoS and NLOS backhaul links respectively. While this exceeds the current backhaul capacity requirements defined by the NGMN alliance, it may not scale to 1Gbps requirements for 5G backhaul. Furthermore, 3.5GHz spectrum bands have capacity limitations due to the small cahnnel bandwidth. The LoS operation proposed for the 60GHz system will have limited application in outdoor urban environments under NLOS conditions. The idea of strategically deploying SCBS to locations with existing fibre proposed in [94] is cost-effective. However, small cell deployment is likely to be in locations where wireless access is required, and not necessarily where there is network presence. Furthermore, the process of planning and deploying wired small cell backhaul can be time-consuming. The strategic placement of radio nodes between SCBS locations and aggrgegation sites is proposed in [70, 71]. In both cases, the use of additional radio devices can result in increased equipment, installation and energy costs.

4.4.2 System model

Each path between a street backhaul radio and aggregation site radio can be modelled using the single knife edge diffraction geometry. A simplified representation of the geometry for a single backhaul path is shown in Fig. 4.16. S and D are the backhaul

radio source and destination nodes respectively. The points marked A are nearside antenna distances, beyond which the diffraction loss increases exponentially, as shown in the results of the diffraction loss analysis. The parameters d_1, d_2 and h are the SKED model parameters as defined in the previous section. The direction of the signal is assumed to be from the source to the destination and only one direction is considered for simplicity.

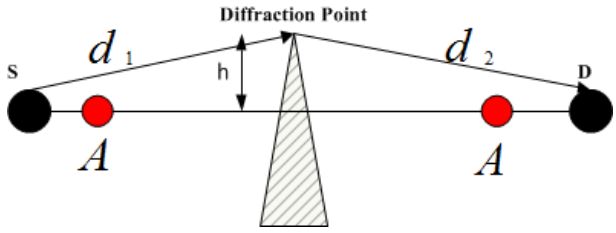

Figure 4.16: Geometry of the single knife edge diffraction model

4.4.3 Path Selection Algorithm

Fig. 4.17 illustrates the proposed path selection algorithm for the CNSCB system. The algorithm forms part of the reasoning algorithms of the radios' cognitive engine. The path selection algorithm starts with determination of the model parameters. The values of $h_{(i)}$, $d_{(i1)}$ and $d_{(i2)}$ are as defined earlier and can be obtained from the radio database based on the location information of preselected diffraction points, or can be randomly generated as will be described in the following section, and proposed in this research. $J_v(i)$ is the diffraction loss for a particular diffraction path where the diffraction point i is used. $J_v(max)$ is the predetermined tolerable diffraction loss on a link and is used as the threshold for determining a suitable value of the diffraction loss on a link. M is the total number of possible paths for each set of radios forming a backhaul link.

Based on the results of the diffraction loss analysis, the algorithm will accept points with values of $d_{(1)}$ greater than the antenna nearside distance. The diffraction loss is

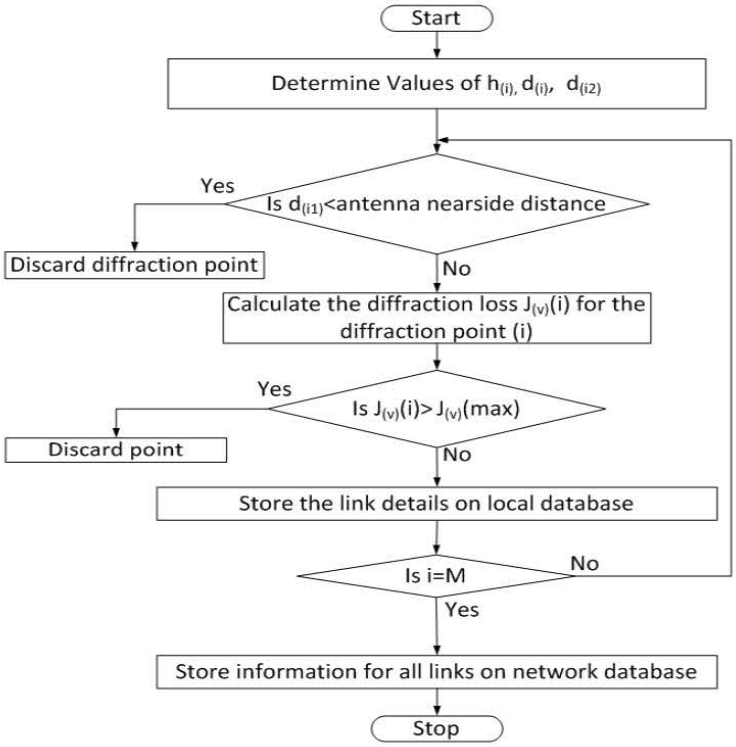

Figure 4.17: Path selection algorithm

then calculated using the SKED model parameters, i.e. $h_{(i)}$, $d_{(i1)}$ and $d_{(i2)}$, randomly generated using a genetic algorithm. The value of the wavelength required in the calculation of the diffraction loss, is supplied by the network operator and can be obtained from the network database. The wavelength and operating frequency are obtain at the initial stages when the radio devices attach to the network. If the calculated diffraction loss is greater than the predefined value, the point is discarded, otherwise details of the diffraction point are stored in the local database of the radio device. The process is repeated until all the diffraction points in the database have been assessed.

The decision to make use of a diffraction point depends on the diffraction loss on the path. The energy loss on a diffraction point is observed through the strength of the signal received by a radio device. A high received signal strength indicates low

diffraction loss and a weak signal strength indicates high diffraction loss. Losses due to atmospheric absorption are assumed to be minimal due to the use of high gain antennas on the radio devices and short distances associated with densely deployed small cells. Once the number of predefined links is reached, the information about all the links including the calculated diffraction loss is uploaded to the network database which assumed to be located in the core network or in the cloud.

4.4.4 Problem Formulation

The single knife edge diffraction model parameters can be represented as a vector of variables p=$\{\lambda,\ d_{i1},\ d_{i2},\ h_i\}$, we formulate the NLOS network design problem as a multi-objective optimization problem whose aim is to minimize diffraction loss on a backhaul path. Diffraction loss is re-modelled as a function of of the vector p, of the single knife edge diffraction model parameters and given in the objective function as:

$$J_{(v)} = min \sum_{i=1}^{n} J_{(v)}(i)(\lambda, h_{(i)}, d_{(i1)}, d_{(i2)}|p) \tag{4.11}$$

subject to: $J_v(i) \leq J_{(v)}(max)$, and $d_{i1}+d_{i2} \leq L(max)$. where L(max) is the maximum length of the link and $J_{(v)}$ (i) is the diffraction loss associated with each link, n represents the number of paths. The rest of the parameters are as defined earlier. This objective function is used in the optimization process.

The problem is solved as an optimization problem in which the GA is used to generate the model parameters. The defined limits of the parameters, i.e. λ, d_{i1}, d_{i2} and h_i are used as constraints of the multi-objective function. The values of their limits form part of the information provided by the network operator and stored in the database of the radio devices or in a network database. The following subsection outlines the GA process.

4.4.4.1 The genetic algorithm framework

GA operation is a metaheuristic search and optimization technique based on the theory of evolution, in which the best species are allowed to reproduce [59]. The evolution process is based on inheritance, selection and crossover where species with the strongest genes are allowed to reproduce faster. GAs present a way of enabling self-organising capabilities in wireless networks by adding intelligence in the radio devices. The use of GA is proposed in this case due to its ability to simultaneously handle more than one variable This is required in determining the diffraction loss, whose value depends on the four SKED model parameters.

Solving optimization problems using GA requires identification of an initial population, from which the solutions are generated. The parameters are encoded into chromosomes. Each chromosome's fitness to reproduce and evolve to the next generation is evaluated against a fitness function. The continuous improvement of solutions is done through the processes of mutation, crossover and selection until the termination criteria is reached. A generic pseudo code for the GA is shown in Table 4.8.

The GA processes and terminology can be summarised as follows [59]. The initial population is a set of chromosomes representing the solution space, consisting of integer values, binary strings or other forms of encoding. Too large a population takes too long to converge, while too small a population leads to lack of solution diversity. The fitness function evaluation is the process of calculating the value of the objective function to determine the value of each chromosome. Good solutions are reproduced and bad ones discarded at each iteration. Selection is a fitness-based process for choosing chromosomes that must survive to the next generation. Common methods include roulette wheel, tournament and ranking. Crossover is the combination of two selected parents (Par_1, Par_2), to generate two new offspring (Ch_1, Ch_2) This is

Table 4.8: Pseudo code for GA

Input: $Population_{initial}$, P_c, P_m, **Output:** P_{best}
P ← Initialize diffraction point coordinates.
Evaluate the path loss on each link using the fitness function eqn(4.9).
P_{best} ← P get link with best path loss value.
Test for termination criteria.
While the no. of required links is not reached, do:
$P_{parents}$ ←(P select parent values of coords. from P)
$new\ generation_{initial}$←(Initialize coordinates set to 0)
For Par_1, $Par_2 \in P_{best}$,
Ch_1, Ch_2, ←crossover (Par_1, Par_2, P_c)
$new\ generationofnodes_{mutated}$←mutate($Ch_1$, Ch_2, P_m)
End
Evaluate population of diffraction points
P_{new} ← select diffraction points with least PL ($new\ set\ of\ diffraction\ points_{mutated}$)
P_{best} ← (replace $P_{initial}$ with P_{new}, $new\ generation_{mutated}$)
End
End GA

achieved by breaking each parent chromosome into two and recombining the resultant sections of the parent chromosomes. The ratio of the number of offspring to initial population size is the crossover probability (P_c). Mutation is the introduction of randomness in the population by changing the genes in the initial population. The ratio of mutated chromosomes to the initial population is the mutation rate (P_m). GA is a stochastic search method which requires definition of termination criterion. The algorithm can be terminated when a fixed number of generations is reached, at the end of allocated computation time, successive iterations can no-longer produce better results or a combination of any of these criterion.

4.4.4.2 Mapping the multiple-path problem parameters to genetic algorithm parameters

In order to use the GA, it is necessary to map its parameters to those of the objective function defined in equation (4.11). Each value represents a gene which is manipulated by the GA during the optimization process. The binary GA [95] is assumed in this

case since the values of the parameters are simple decimal values. In the optimization process, links with minimum diffraction loss are identified. The links are arranged in numerical order, starting with the link with the least diffraction loss. Only a predetermined number of links is stored in the network database.

The GA was implemented in MATLAB. The SKED model parameters set as follows: a frequency of 70GHz, expected to be used in small cell backhaul solutions was assumed, with a wavelength, λ, of 0.0043m. The baseline values of the rest of the variables were set to 40m, 190m and 0.18m for d_1, d_2 and h respectively. A line-of-sight distance of 200m, which lies within possible values defined for small cell backhaul links, was assumed. The NLOS paths would therefore be above this value. The model parameters formed part of the input variables to the genetic algorithm. The SKED model parameters were mapped to the GA parameters as follows: the number of possible diffraction paths, which correspond to the number of diffraction points, form the population size of the genetic algorithm, and was set to 20. The input variables were the wavelength and the distances between the radios and the diffraction points. The GA parameters were set as follows: The number of generations was set to 40 and was used as the stopping criteria. This value is used determines the number of times the GA attempts to find the minimum diffraction loss on a diffraction path. The crossover and mutation probabilities were set to 0.05 and 0.9 respectively. These values are not related to network parameters but determine the performance of the algorithm.

Since the initial values for the GA are generated randomly, there is a chance that the genetic operators are affected, i.e. the choice of initial parents, the crossover location and the probability of mutation. Values of diffraction loss for different diffraction points were recorded at the end of each cycle of 40 generations. The effects of the crossover and mutation rate on the performance of the GA was also determined.

4.4.5 Simulations results

The frequency of occurrence of a range of diffraction loss values was obtained for different values of d_1, d_2 and h. The results, as given in Table 4.9 illustrate the number of times the algorithm finds links with a diffraction loss within a specific range of values. The minimum, maximum and average values of diffraction loss obtained were 5.29dB, 34.37dB and 12.56 respectively. These values are important to network operators since they provide an overview of the performance of the selected propagation paths and are an important input to decision making at the initial planning stages. The results also that the algorithm does not find any links with diffraction loss below 4dB. This is expected since it can be difficult to find diffraction points with low values of diffraction loss given the fact that millimetre wave frequencies are easily absorbed by most of the diffracting surfaces. According to the ITU-R [86], the values can range from -0.02dB to 24dB for various values of the parameter V.

Table 4.9: Variation of the obtained number of diffraction points with diffraction loss

Diff. Loss (dB)	**Freq.**	**Diff. Loss (dB)**	**Freq.**
0-2	0	18-20	3
2-4	0	20-22	1
4-6	6	22-24	4
6-8	10	24-26	0
8-10	11	26-28	1
10-12	11	28-30	0
12-14	15	30-32	0
14-16	4	32-34	1
16-18	3	36-38	0

Fig. 4.18 illustrates the variation of the number of diffraction points obtained by the GA versus the diffraction loss calculated. The results show that the GA was able to obtain 15 diffraction points, i.e. NLOS paths, with a diffraction loss of between 10dB

and 15dB. This is a good number of paths for the SCB network design although a larger pool of points would increase the survivability of the network. The number of diffraction points with high diffraction loss is less compared to the number of points with low diffraction points. It can therefore be concluded that the GA can be used as part of the cognitive intelligence algorithms that can be installed in the radio devices to determine the suitable propagation paths under NLOS conditions.

Figure 4.18: Variation of success of GA in obtaining suitable diffraction points

4.4.5.1 Effects of varying GA operators on diffraction loss

Experiments to determine the effect of the mutation and crossover probability on the performance of the GA were also carried out. The results were taken for the network with 20 nodes, i.e. population size of 20 and 40 generations for three sets of values of mutation and crossover probabilities. For each set, the experiment was taken over 10 cycles. Table 4.10 shows the values of diffraction loss obtained for different values of mutation and crossover probability.

Fig. 4.19 shows the spreading of the results for the crossover probability. A crossover probability of 50% gives more points with lower diffraction loss compared to those of 90% and probability of 30%. Theoretically, a 50% crossover probability is preferred as explained in Chapter 2. It is also noted that an increase in the crossover probability results in more dispersion of the diffraction loss values.

Table 4.10: Values of diffraction loss for different mutation and crossover probabilities

Cycle	Mutation probability			Crossover probability		
	0.02	0.05	0.1	0.3	0.5	0.9
1	6.88	5.3	6.5	5.3	6.88	6.5
2	7.42	7.8	10.7	7.8	7.42	10.7
3	8.68	5.9	11.8	5.9	8.68	11.8
4	11.65	16.3	6.9	16.3	11.65	6.9
5	14.27	5.6	9.9	5.6	14.27	9.9
6	12.18	11.6	12.4	11.6	12.18	12.4
7	12.5	11.7	12.2	11.7	12.5	12.2
8	32.6	9.5	8.6	9.5	32.6	8.6
9	10.7	13.6	10.2	13.6	10.7	10.2
10	7.8	13.3	14.6	13.3	7.8	14.6

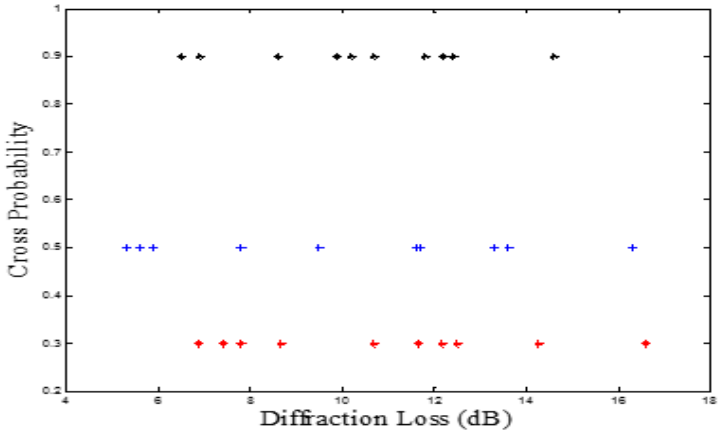

Figure 4.19: Diffraction loss spreading vs crossover probability

The GA was also run to determine the mutation rate that gives better values of diffraction loss. Fig. 4.20 shows that a mutation probability of 5% gives diffraction loss values that have a greater spread with more points of less diffraction loss. Values obtained for the 1% and 2% probability values have similar spread characteristics but less spread than those for 5%.

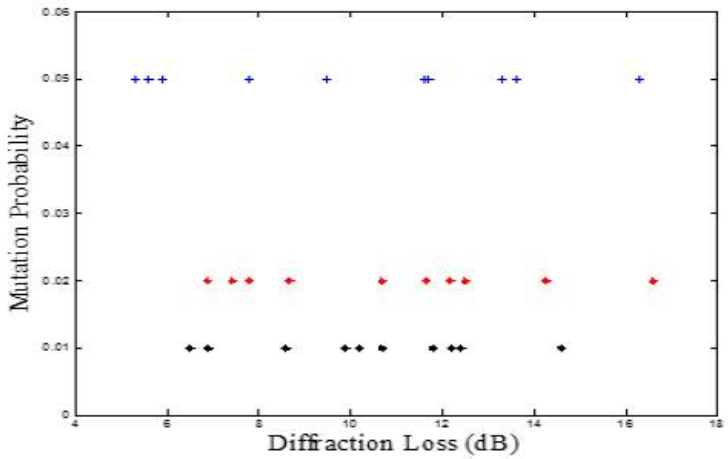

Figure 4.20: Diffraction loss spreading versus probability of mutation

4.4.6 Discussion

The results of the optimisation process showed that the GA, guided by the constraints, is able to generate locations of diffraction points that can be used as input in the establishment of connectivity by the radio devices. The algorithm therefore allows the radio devices to autonomously determine suitable transmission paths. Furthermore, the information about the identified paths is stored in a local database, which allows self-healing capabilities in the radio devices, by enabling them to autonomously access this information in the event of failure of the primary path.

The factors that affect the performance of a GA, hence the quality of solutions it produces include the crossover rate and mutation probability. Simulation results showed that a high crossover probability results in more dispersed diffraction loss values. The implication of this, is that the CNSCB system can therefore have access to more diffraction points with which to establish connectivity, compared to the case when there are few points with low diffraction loss or large number of points but with high diffraction loss. The same scenario was also observed when the mutation probability was varied. In the design of the optimization algorithm, it is therefore

important to select values of the crossover and mutation probabilities that give more points with lower diffraction loss.

4.5 SCBS Location Coverage Optimisation

The multiple-path selection and optimisation process discussed in the previous section focused on the multiple-path creation between a pair of backhaul radio devices. This section gives an in-depth analysis of how a SCBS location can be covered by a given set of diffraction points within its vicinity, with a focus on the the street-to-diffraction point segment of the NLOS path. This is because this is the most challenging segment of the street-to-rooftop level backhaul link that can suffer signal blockage by trees, traffic, and other urban structures. The problem is formulated as maximal covering location problem. Application of the concept in solving the SCBS backhaul coverage is explained. A coverage optimization model is proposed and results of simulations carried out are presented.

4.5.1 Related work

The use of device intelligence in backhaul radios to enable NLOS operation has been proposed in literature. GA is proposed in [96] to add reasoning intelligence in a cognitive radio network to enable NLOS operation. A drawback of the solution is the inability to use exact diffraction points in the establishment of the links, which can improve system reliability. In [97], GA is also proposed to improve the reliability of traditional wired and microwave links. The authors do not consider street-to-rooftop backhaul links. Software-defined networking (SDN) is another concept concept being proposed to address the NGMN requirement for service aware transport networks [98, 99]. SDN is expected to results in improved network utilization and user quality of experience. However, this approach assumes available connectivity between the

backhaul nodes. There is therefore a need to address the connectivity problem before the technology can be implemented.

4.5.2 Problem formulation

The potential location of a SCBS, hence a street level backhaul radio device, is determined by the network operator and depends on the demand for connectivity in the given location. However, finding suitable diffraction points capable of regenerating strong signals directed to the target SCBS location can be a challenge. Furthermore, the narrow beam-width of millimetre wave signals result in limited spatial spread. While automatic antenna steering can be used in refining the signal search, there is limitation in the degree of movement of the antennas. Ensuring that an SBR location is covered by at least a certain number of diffraction points for use in the link selection process can therefore be a challenge. Such a problem is know in research as location covering problem, which is formally defined as maximal covering location problem (MCLP).

The concept of the MCLP is concerned with ensuring that a set of demand points in a given area are covered by a facility providing the given service [100]. The solution to the problem seeks to maximize the number of demand points that are covered. The concept was initially introduced by Richard Church in 1972. However, its relevance and significance in solving location coverage problems is gathering momentum. This is illustrated by an increase in the number of citations recently recorded in research works [101]. Several applications of the concept in solving problems associated with optimal placement of devices in communication networks are emerging. For example sensor nodes in wireless networks, placement of security cameras in urban environments and optimal placement of base stations in mobile networks [102–105]. We propose to apply the concept in solving the NLOS location coverage problem in

the CNSCB system. In analysing the MCLP in the CNSCB system, the downlink is considered for simplicity. While the diffraction points are passive signal generators, retransmitting the signal from the radio devices, the area covered by a diffraction point depends on the field of spread of the signal and depth of coverage.

These factors are captured in visibility and spatial analysis modelling [102]. The visibility of a SBR location from a diffraction point depends on the distance between the location and the diffraction point. The study of an area illuminated by the diffraction point falls under a field of research known as visibility analysis. The visible area, known as a viewshed, is defined as a set of points specified by 3-D coordinates *(x, y, z)*. The illuminated area is formally defined as [102]:

$$Viewshed(\phi_{(q)}) = f(q, D, r) = \{\delta \in D | d(q, \delta)\} \leqslant r \tag{4.12}$$

where q is the source of the signal, δ is the point to be covered, with δ assumed to be visible from q; D is the surface that is visible from the point q and r is the extent of the visibility. The distance r can be obtained from equation 4.13, where a_1, b_1 and a_2, b_2 and are the x, y coordinates of the diffraction point and SBR location respectively.

$$r_{(i)} = \sqrt{(a_2 - a_1)^2 + (b_2 - b_1)^2} \tag{4.13}$$

While viewshed provides information that is used to analyse the visibility of a location from a given diffraction point, it does not provide enough information regarding the optimal combination of diffraction points that can cover the base station location and be used as part of the non-line of sight propagation paths. The small cell backhaul problem is therefore solved using the maximum covering set location model and the results of viewshed used as input to the optimization problem.

4.5.3 Optimization model

Modelling the optimal combination of diffraction points that can cover a small cell base station location can be achieved using the MCLP model. In the model, the objective is to maximise the number of sites that can be covered within a desired distance. The model is used in this research to formulate the backhaul coverage optimization problem, in which the objective is to maximise the number of diffraction points covering a base station location Z. In order to use the model, the parameters of the model must be mapped to those of the small cell backhaul problem. The MCLP is formally stated as [100]:

$$Z = max \sum_{i \in I} (a_i y_i) \tag{4.14}$$

subject to:

$$\sum_{j \in N_i} (x_j - y_i) \ \geqslant 0 \ \ \forall \ i \in I \tag{4.15}$$

$$\sum_{j \in J} x_j = P \tag{4.16}$$

$$x_j = (0, 1) \ \forall \ j \in J \tag{4.17}$$

$$y_i = (0, 1) \ \forall \ i \in I \tag{4.18}$$

where I denotes a set of nodes that must be covered, J denotes the set of sites that must provide the required service, d_{ij} is the shortest distance from node i to node j,

$$x_j = \begin{cases} 1 \ if \ a \ facility \ is \ allocated \ to \ site \ j \\ 0 \ otherwise \end{cases}$$

$$y_i = \begin{cases} 1 \ if \ a \ facility \ exists \ in \ the \ set \ N_i \\ 0 \ otherwise \end{cases}$$

$N_i = \{\text{j} \in J \mid r_{ij} \leq S\}$, N_i denotes the set of facility sites able to cover a demand point i, S denotes the distance beyond which a node is considered uncovered, a_i denotes

the set of base station locations to be covered, P denotes the number of facilities located, a_i denotes the population to be served at demand node i, x and y denote the decision variables in the optimization problem as explained below.

A base station location is considered covered if it is within a critical distance or time from a diffraction point, and the signal strength received by the radio device is above a given threshold. The objective of the optimization problem is to maximize the number of diffraction points covering a base station location. In this case the MCLP model parameters can be redefined as follows:

I = denotes the set of base station locations,

J =denotes the set of diffraction points,

a_i = denotes the set of diffraction points that can cover a base station location i,

$$x_j = \begin{cases} 1 \; if \; a \; base \; station \; is \; covered \; by \; a \; diffraction \;\; j \\ 0 \; otherwise \end{cases}$$

$$y_i = \begin{cases} 1 \; if \; a \; base \; station \; exists \; the \; set \; N_i \\ 0 \; otherwise \end{cases}$$

d_{ij} =is the shortest distance from a diffraction point i to base station location j,

P denotes the population of diffraction points that must be identified, i denotes the index of base station locations, j denotes the index of diffraction points, N_i {j $\in J \mid r_{ij} \leq S$}, S denotes the distance beyond which a SCBS location is considered uncovered.

The objective of equation 4.14 is to maximise the number of diffractions points serving a single base station location. The number of diffraction points determines the number of multiple-paths available for use by the backhaul radio nodes. Constraint 4.15 allows the location of a base station to be covered by diffraction points that are part of the set of diffraction points N_i, that are located within the defined maximum distance from the location. Constraint 4.16 provides a limit to the number of diffraction points that

can be identified. Constraints 4.17 and 4.18 specify the integer values of the decision variables x and y, $x_j = 1$, if j is a potential diffraction point for location j and x_j=*0* otherwise. $y_i = 1$, if the SBR location i is covered by a diffraction point and y_i =*0* otherwise.

The MCLP is NP-hard and is modelled as an integer programing problem. To solve the problem, it is necessary to apply relaxation and rounding [106]. This involves relaxing the problem to a linear programming problem and solving it in polynomial time to get feasible solutions. The constraints 4.17 and 4.18 can therefore be rewritten as follows:

$$0 \leqslant x_j \leqslant 1 : \forall_j \tag{4.19}$$

$$0 \leqslant y_i \leqslant 1 : \forall_i \tag{4.20}$$

From the previous discussions, it is clear that millimetre wave systems are distance limited, rather than interference limited. The location coverage problem is therefore solved using the distance-dependent propagation model proposed in this research, shown in equation 4.3, which includes diffraction loss. Euclidean distances determined using equation 4.13 are used to determine the distances between the diffraction points and radio locations.

Solving the location coverage problem of the CNSCB system involves obtaining spatial information about the area where the SCBS are installed, determination of viewsheds, assessment of the potential of a SBR location having the suitable number of diffraction points with which it can be associated with and hence establish multiple paths to the backhaul radio at the aggregation site and evaluation of the potential number of diffraction points to provide adequate signal strength to a street backhaul radio node.

4.5.4 Network deployment model

Fig. 4.21 illustrates the model of a network area consisting of diffraction points, two hub backhaul radios (HBR) and street backhaul radios (SBR), which are assumed to be co-located with the bases station and interconnected using Ethernet cable. The Manhattan grid deployment model is assumed due to the deployment pattern of small cell base stations which is expected to be along the streets. Two massive MIMO systems are assumed to be installed at opposite corners of the grid for better coverage of the SBR locations. The location information of the network nodes is provided by the network operator. A network area of 500m x 500m is considered. The inter-site distance between base station locations is assumed to be 100m, typical distances according to 3GPP specifications for deployment of pico cells. The number of diffraction points randomly generated is 200, and are assumed to be visible from the ABR. The height of diffraction points above ground is not taken into consideration, however, 3-D location information can be obtained using tools such as ArcView GIS.

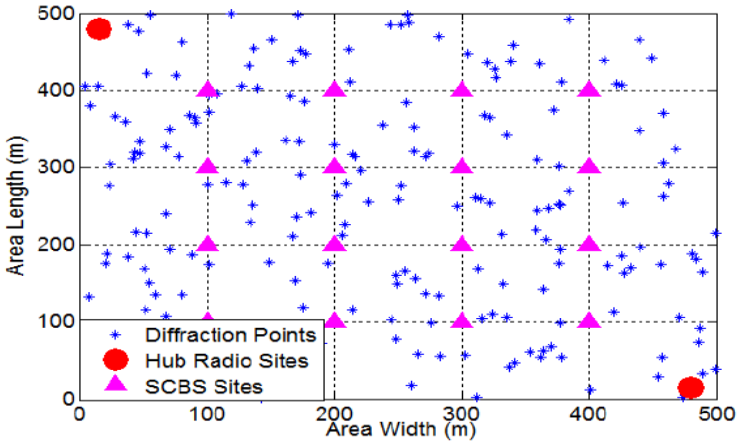

Figure 4.21: Network deployment model

4.5.4.1 Representation of the SCB MCLP using GA

To utilise the GA, various parts of the SCB coverage problem must be mapped to the GA components. The population of the GA is the coordinates of the DP locations covering a SCBS location and is set to *50*. Random values of the coordinates varying between 0m and 80m are generated and form the initial population. The feasibility of a DP is verified based on the evaluation results of the fitness function, represented in equation 4.12. 60GHz is one of the frequencies being proposed for SCB solutions, and a system using this frequency is assumed in the simulations. The value of d_0 used in the path loss model is 1m [8]. The number of x and y coordinates of the base station and diffraction points are used as input variables to the genetic algorithm and the number was set to 4. The mutation rate, selection rate and number of iterations (used as stopping criteria) were set to 0.2, 0.5 and 100 respectively. Since integers are used as chromosomes instead of bit strings, the algorithm switches indices of the locations of coordinates in the cross over process. A random value between 0 and 1 is used to create the new x values of the selected chromosomes while the y value is kept constant.

4.5.5 Simulation results

The coverage optimization algorithm was developed using GA and implemented in a MATLAB environment. This algorithm is part of the cognitive engine reasoning algorithms. The values of d_1 and d_2 for each diffraction point were determined using equation 4.16. The values of the coordinates of the diffraction points are randomly generated. In the calculations, the values of d_1 and d_2 were limited to 80m, typical values for SCB links. The locations of the radio devices are predetermined by the network operator, but the GA must determine the coordinate values of the diffraction

points that give the best link performance based on the strength the signal received from the diffraction point.

The simulations were used to determine the path loss and coverage ratio, which is defined as a ratio of the number of diffraction points capable of covering a SCBS location to the total number of diffraction points identified by the GA. The learning capability of the GA was also evaluated based on the rate at which the optimal number of suitable diffraction points covering a SCBS location were found. Two runs of 100 and 200 generations with a population size of 50 were carried out.

Fig. 4.22 shows the results of the best solution for the minimum and average path loss on the locations coordinates found by the GA for 100 generations using a mutation rate of 0.2. The best solution was found to be a diffraction point with coordinates [47.103m, 46.114m] and a distance of 66.562m from the SBR. The path loss was found to be 106.5dB. Fig. 4.23 shows the results for 200 generations with the mutation rate set to 0.5. The best solution was a diffraction point with coordinates [47.5m, 48m] and a distance of 67.53m from the SBR. The path loss was found to be 108dB.

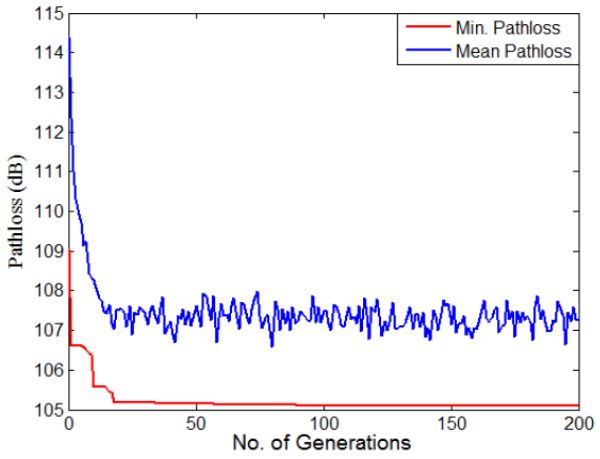

Figure 4.22: GA run for finding the minimum path loss with mutation rate 0.2.

As the best values of the population survive into subsequent generations, the value of the fitness function improves or remains the same. It is also noted that the

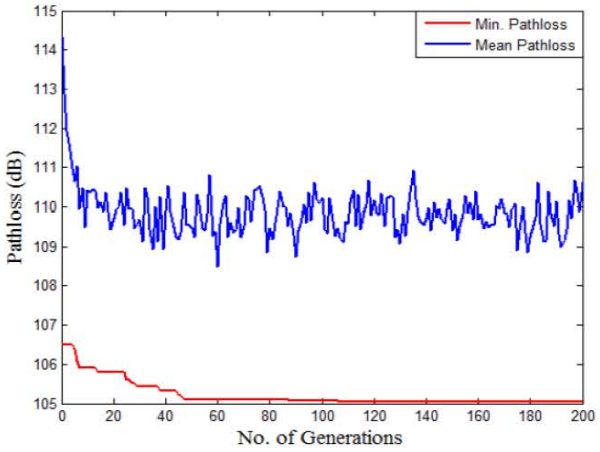

Figure 4.23: GA run for finding the minimum path loss with mutation rate 0.5

final solution of each run differs slightly from the other solutions as the number of generations increases. The minimum values of the path loss is found to be within the ranges obtained for a 60GHz system in [107]. Figs. 4.22. and 4.23 show that the algorithm finds the average path loss after about 20 generations and 10 generations when the mutation rate is set to 0.2 and 0.5 respectively. However, with the mutation rate set to 0.5, Fig. 4.23 shows that the algorithm consistently converges to a higher path loss value compared to the case in Fig. 4.22 when the rate is set to 0.2. It can therefore be concluded that a lower mutation rate is desirable if links of lower diffraction loss are to be established.

The variation of the number of generated diffraction points covering a SBR during each generation is shown in Fig. 4.24 The values were obtained over 10 iterations of 200 generations each. The results obtained show that all four SBR were covered by at least 60% of the generated diffraction points, with SBR2 having the highest number of covering diffraction points.

In Fig. 4.25, the GA's learning capability is demonstrated by the gradual acquisition of an optimal number of suitable diffraction points required to cover a SBR location. The algorithm was run four times for four different SBR locations. The results

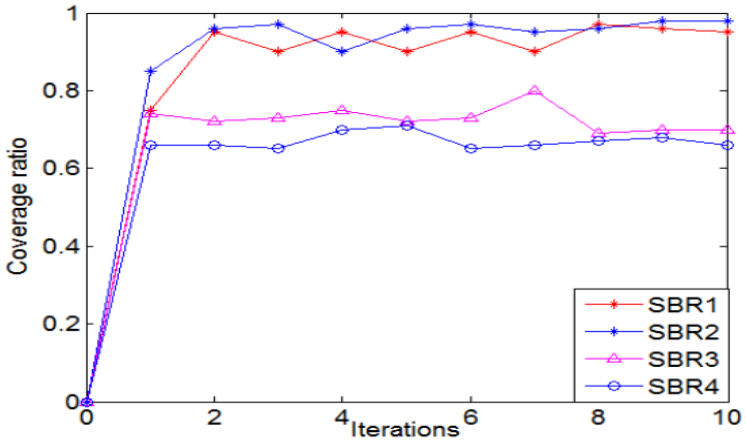

Figure 4.24: Achieved coverage ratio for different SBR locations

obtained show that the GA consistently achieves more than 40 diffraction points covering SBR locations before 20 generations. Overall, the obtained results show that algorithms can be used for autonomous network configuration and optimization, where the deployed radio devices determine the propagation path in real time, depending on quality of the wireless channel.

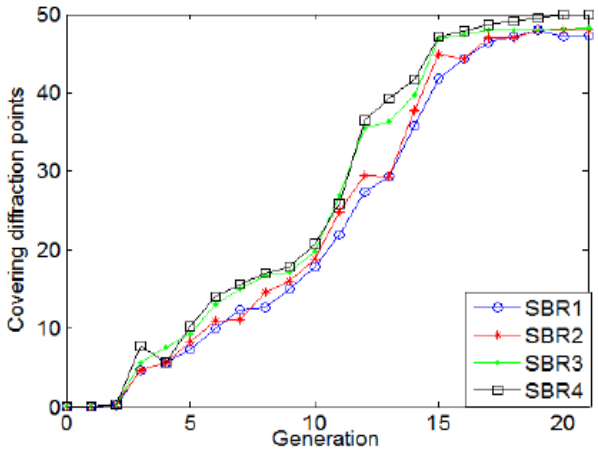

Figure 4.25: Covering diffraction points for different SBR locations

4.5.6 Discussion

The location of SCBS's is determined by network operators based on the demand for connectivity in the particular location. Obtaining suitable diffraction points capable of covering preselected locations can be a challenge. This section proposes an algorithm that enables the SBR devices to autonomously determine suitable diffraction points that can cover a SCBS location. The optimisation problem is modelled as a MLCP, in which the objective is to maximise the number of diffraction points that enable creation of NLOS propagation paths that meet the performance requirements of the backhaul links.

Simulation results show that the proposed GA is capable of finding suitable diffraction points for predetermined SBR locations. The results also show that a high mutation rate results in the GA obtaining diffraction points with higher path loss than when a lower mutation rate is used. The learning capability of the GA is also illustrated by the gradual increase in the number of diffraction points found around a given number of SBR locations. The results obtained show that the GA can identify at least 40 diffraction points per SCBS location, making it possible to have a wide selection of NLOS backhaul paths to the aggregation sites, hence improve system reliability.

4.5.7 Chapter Summary

Using mmW technologies for backhauling outdoor urban small cells allows Gbps data rates due to the inherent large bandwidth available in the systems. However, signal blockage in outdoor urban environments requires that techniques for enabling NLOS connections be developed. This chapter focused on addressing the problem of how to reliably connect SCBSs to roof-mounted backhaul aggregation sites where high-speed fibre links transport the traffic to core networks.

The street-to-rooftop links are modelled using the SKED geometry. The signal loss due to diffraction is analysed using the simplified Fresnel-Kirchoff integral, with values of the V determined using the SKED model parameters, which can be applied at any frequency, unlike other models which are frequency dependent. Results of the analysis show that the path loss due to diffraction increases with an increase in the operating frequency, when diffraction points are located beyond the near-side antenna distance, when points are located above the LoS path and with an increase in the angle between the LoS path and diffraction path.

The proposed CNSCB addresses the 5G specification of improved reliability through the use of multiple-paths between the street and aggregation backhaul radio devices. To realise this requirement, multiple-path selection algorithm based on genetic algorithm was proposed. The problem was formulated as an optimization problem, whose objective is to minimize the diffraction loss on a NLOS path. Diffraction loss on a selected path is determined using GA-generated SKED model parameters as input to objective function, thus automating the link selection process. The results obtained show that the GA can find an optimal number of diffraction points with diffraction loss values below the predefined threshold. The performance of the algorithm was also evaluated for different values of mutation and crossover probability rates. The results obtained show that a crossover probability of 0.5 gives more points with lower diffraction loss than those when the value is set to 0.9 and 0.3. The results show that a mutation rate of 0.05 gives more points with less diffraction loss than when the value is set to 0.01 and 0.02.

SCBS deployment locations will be determined by the network operators based on their requirement to provide access to end users in those locations. Most of the solutions proposed in the literature have provide backhaul coverage in locations where strong signals are detected. However, these locations may not be the ones desired

by network operators. This problem is addressed in this chapter by selecting an optimal number of diffraction points that are visible from a required SCBS location. The optimization process is modelled as a maximal covering location problem model, whose objective is to maximise the number of suitable diffraction points covering a SCBS location. The locations of the diffraction points are autonomously generated and a GA is used to determine suitable diffraction points based on the diffraction loss at each location. Simulation results show that each SCBS location can be covered by up to 50 diffraction points. A high mutation rate is shown to result in higher values of path loss. The GA is also shown to show learning capabilities by gradually finding the number of diffraction points around a SCBS location.

Chapter 5

Device Intelligence in the CNSCB System

5.1 Introduction

One of the requirements of small cell backhaul links is to be service-aware and be able to respond dynamically to changes in the performance characteristics of the transmission channel. This includes increasing channel capacity in response to increasing traffic or re-routing traffic to another link in the event of failure of the primary link. An emerging requirement is the capability to activate sleeping mode in response to reduced traffic from the base station in order to conserve energy on the network. The overall aim of this flexibility is to ensure uninterrupted service through reliable backhaul connections.The Cognitive Non-line-of-sight Small Cell Backhaul (CNSCB) system proposed in this research is based on millimeter wave and massive MIMO technologies for achieving Gbps data rates, flexible backhaul links and scalable link capacity. One of the capabilities of the system is to address the 5G backhaul requirement for reliable backhaul connections under NLOS conditions. Algorithms

for the establishment and performance optimization of of NLOS paths, and optimal coverage of SCBS locations were proposed in Chapter 4.

The main problem addressed in this chapter is how to ensure that the backhaul links provide reliable connectivity that is capable of responding to changes in the traffic patterns, traffic levels, changes in the operating environment; and still ensure reliable, uninterrupted service to the applications. The problem is addressed through a self-healing algorithm based on reinforcement learning, which can be implemented in the cognitive engine of the radio devices. The objectives of the algorithm are three-fold. Firstly, it must ensure that the data rate on a link is kept above a given threshold. Secondly, in the event of failure of a link that is currently in use, the backhaul radio must switch switches to an alternative path within a given time delay, and lastly, the path loss on a NLOS path is below a given threshold. If the conditions are not met, the controller in the aggregation site backhaul radio of the CNSCB initiates action to take corrective measures. The novel contribution of the chapter is the use of cognitive intelligence algorithms, based on reinforcement learning and implemented in the radio devices, to minimise the effects of NLOS propagation through self-organising network capabilities (SON).

Before the algorithm is presented, a review of related literature is presented, followed by the network model. A brief discussion on reinforcement and Q-learning is given. Simulation results are finally presented.

5.2 Related work

Cognitive radio technology has successfully been used for dynamic spectrum access and management in radio networks [110]. A number of applications are also emerging [109]. Methods for the evaluation of data rate and outage probability in cognitive radio networks are proposed in [108]. The main source of intelligence

in cognitive radios is the ability to learn and self-configure. These capabilities are implemented in in the algorithms that reside in the cognitive engine of the radio devices. A new application of cognitive radio technology proposed in this research is to improve reliability of of the proposed CNSCB system. The intelligence of the radio devices is achieved through a reinforcement learning algorithm.

5.3 Network model

Fig. 5.1 illustrates the network deployment architecture considered. The Manhattan grid grid, in which SCBSs are deployed along a rectangular area along the streets is assumed. The system consisting of two aggregation massive MIMO backhaul radios (ABR), several diffraction points and street backhaul radios (SBR) co-located with small cell base stations.

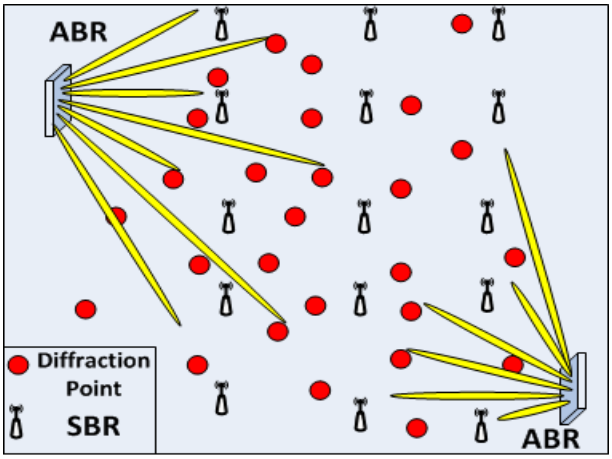

Figure 5.1: Network model

The massive MIMO system can assign individual beams to SBRs. Fixed beam switching and time division multiplexing (TDM) on the massive MIMO system allow a single beam to serve a number of SBR devices that are in close proximity to each other [114]. Electronic beam steering enables the radio devices to point the antennas to the individual diffraction points [114]. Electronic beam steering and fixed beam switching allow the system, through algorithms implemented in the controller

module of the CNSCB massive MIMO radio, to change the topology of the network in response to the changes in network configuration. The changes can be due to addition or removal of SBR devices, change in the diffraction point being used for signal retransmission or changes in proximity between SCBS locations which may render sharing of the MIMO beams impractical due to increased distance. Each SBR device can therefore be assigned a fixed beam or share with an adjacent device in fixed beam-switching mode depending on its location, the traffic available from the access network and the performance of the backhaul wireless channel. The use of multiple paths per backhaul link is designed to improve system reliability and scalability under non-line-of-sight conditions. It is also important to note that when sleep modes are implemented on the small cell base station to conserve energy, the SBR would also go into energy saving mode. Implementation of sleep modes is not part of the algorithms developed in this research, however, work which incorporates state-of-the-art sleep modes can be found in [55, 115–117]. The following subsection describes the proposed learning algorithm, which is based on reinforcement learning.

5.4 Reinforcement learning

Reinforcement learning (RL) is a dynamic learning programming technique in which agents in a given environment learn what to do and how to map situations to actions in order to maximize a numerical reward [118]. The process of learning, deciding and acting in RL is closely related to the basic principles of cognitive radio technology (CRT), i.e. ability to change operating parameters in response to changes in the operating environment. RL learning algorithms can, therefore, be used to implement artificial intelligence in the CNSCB system radio devices.

In RL, the agents observe the states in their operating environment, take action based on the results of their observation and get a reward based on the actions they have taken. The classic RL algorithm consists of three steps and is implemented as follows.

At time t, an agent observes a set of environmental states **S** and sets a state s_t; s_t $\in$ $\boldsymbol{S}$; the agent takes action a_t, from a set of possible actions **A**, $a_t \in \boldsymbol{A}$; and gets a reward r_t. At the next instance, the agent receives a new state s_{t+1}, performs another action a_{t+1} and gets the next reward r_{t+1}. Based on these interactions with the operating environment, the agent develops a policy $\xi : S \rightarrow A$, based on the Markovian Decision Process (MDP) model. The model provides a framework for modeling decision making in a situation where the outcome is partly random and partly under the control of a decision-maker. In reinforcement learning, it allows studying of optimization problems and allows a reward to be received on the basis of a discount factor γ, where: $0 \leqslant \gamma \geqslant 1$.

5.4.1 Q-learning

Q-learning (QL) is a reinforcment learning technique which is used to find and optimal action-selection policy for any given MDP. Implementation of QL in the CE of CNSCB system enables the radio devices to acquire information about the state of the NLOS transmission channel, i.e. the operating environment; change the radio operating system parameters such as increasing transmission power to improve data rates, and make decisions based on the outcome of the action. The basic operation of the algorithm is similar to that of the RL algorithm described above. The long-term rewards received by the learning agents are obtained by trying several possible states and actions. Like in RL, a QL agent starts in given operating state, tries an action, evaluates the consequences of the action based on the reward or penalty received, and estimates the value of this action. However, in QL, the action is assigned a value, called the Q-value [58]. The Q-value obtained for an expected reward $r(s_t, a_t)$ is calculated as follows:

$$Q_{(s,t)} \leftarrow Q_{(s,t)} + \alpha_t\{r_t + \beta max(Q_{(s(t+1),a(t+1)}, Q_{(s,t)}\} \tag{5.1}$$

where r_t is the immediate reward at time t, and $0 \leqslant \alpha_{(s,a)} \leqslant 1$. The state-action values of the learning process are stored in a Q-table. A detailed description of the QL process is given in [58].

QL algorithms require a global view of the operating environment with well formulated state-action pairs. However, this is difficult to obtain in distributed systems like communication networks. To overcome this drawback, single state QL (SSQL) algorithms have been used in communication networks. In SSQL, the algorithms model the behavior of individual wireless parameters [58]. The algorithm can then be applied to the system using parameters such as data rate, signal-to-interference-plus-noise ratio (SINR) and received signal strength (RSS). The SSQL is therefore used in the CNSCB system to model the learning algorithm.

5.5 Proposed Cognitive Q-learning model

Fig. 5.2 illustrates the proposed learning cycle of the CNSCB radio nodes. The learning agents are the radio devices. The operating environment consists of the wireless channel conditions, traffic conditions on the access network and other information available from the network database such as location information of the diffraction points and backhaul radio devices. The information database stores the results of the learning process and temporary information required for the proper operation of the radio device. A radio device senses or observes the conditions in the environment and takes action based on the sensing results. A reward or penalty is received based on the results of the action.

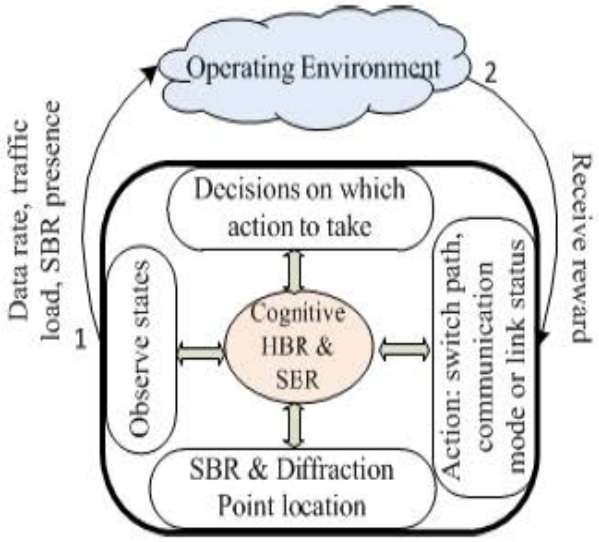

Figure 5.2: The cognitive Q-learning model

5.5.1 Cognitive QL in the CNSCB system

The CNSCB system can be modelled as a cognitive network with QL capabilities. Using the SSQL model, we formulate the system model as follows: the backhaul radio devices represent the learning agents; changes in the wireless channel, traffic variations from the SCBS and service requirements, represent the monitored operating environment; and the action taken to change internal parameters of the radio devices to improve the performance of the network, represent the QL action space. Each radio node observes the changes in network performance, variations in network traffic and service requirements; decides on the next best action to take, and gets a reward or penalty depending on the outcome of the action.

5.5.2 Cognitive Q-learning algorithm

The QL algorithm operates as shown in Fig. 5.3. The learning algorithm resides in the cognitive engine. The radio observes changes in the states and makes decisions to disconnect the link, change topology or switch propagation path. It takes the required

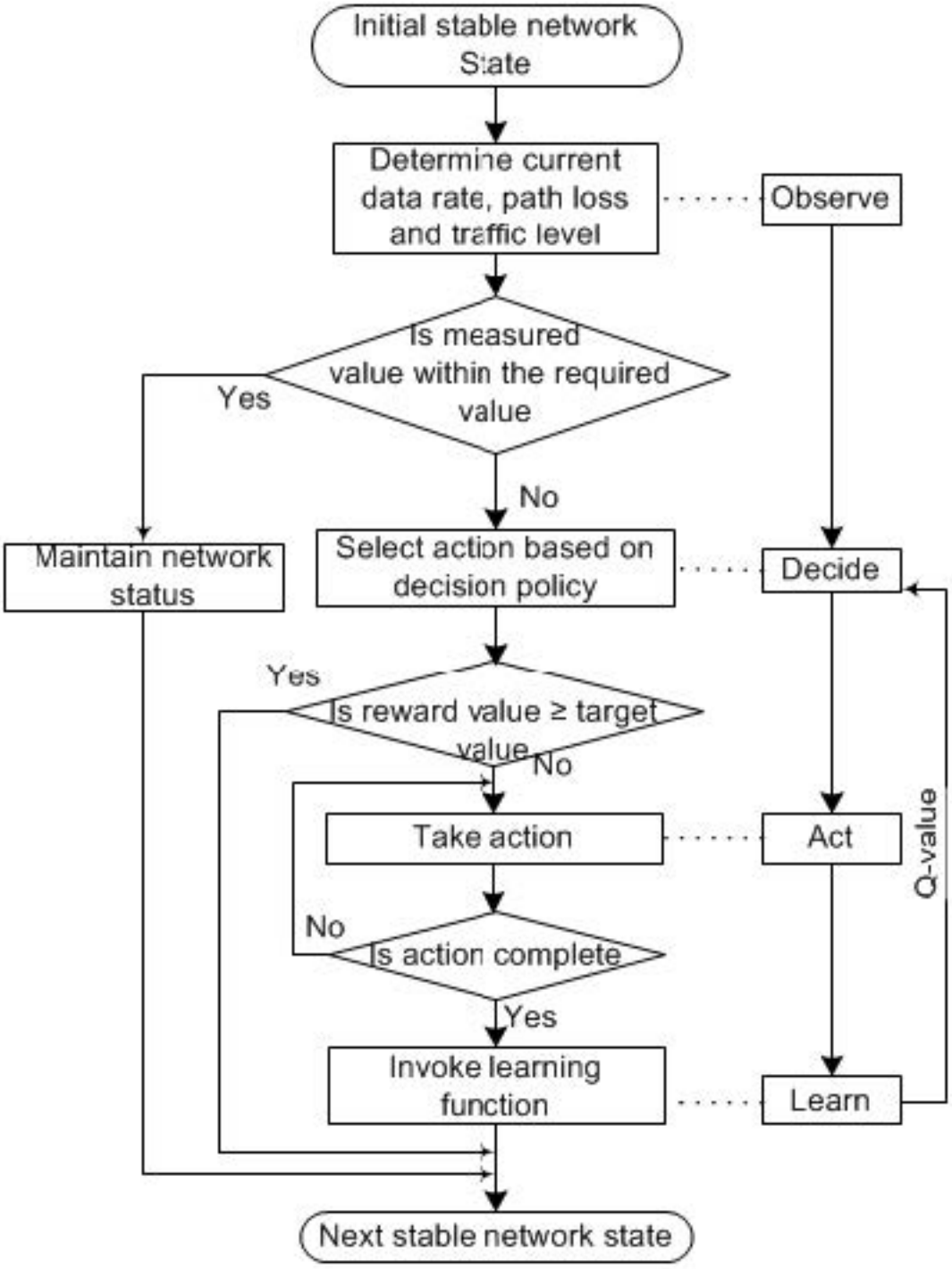

Figure 5.3: Q-learning Algorithm

action and updates the Q-value based on obtained reward. A positive reward will result in the reinforcement of the action taken.

5.5.3 QL implementation in the CNSCB radio devices

The current *state* $s_{(i)}$, of the performance requirements are stored in a Q-table and is defined by: $S = \{s_1, s_2, \cdots, s_n\}$, $s_i \in$ s, where s_1 to s_n are the states of each backhaul link. The current state of the contents of the Q-table considered in this research are the traffic level, data rate and received signal strength. The observed values of these parameters can be below or above the predefined threshold depending on the operating conditions. For example depending when a few users are connected on the network, the traffic level will be low. High data rates can be achieved under excellent channel conditions, such as high signal to interference plus noise ratio (SINR). The received signal strength can also vary depending on the weather conditions or variation in the characteristics of the diffraction point's surface. It is assumed that the radios get updates from a network database on the changes in the location information of the backhaul radio, the used diffraction path and addition or removal of a peer radio node. Any changes in the current state of the parameters result in a change from the current state to the next state.

Table 5.1 shows the state-action pair implementations proposed in this research. Four states are considered: changes in traffic levels, changes in data rate, changes in the received signal strength on the backhaul link and addition or removal of a SBR device on the network. The *action*, *'a'*, is the behaviour of a radio which allows it to change the state of the Q-table. During the operation of the CNSCB system, an action is taken when changes in the data rate, traffic level or received signal strength falls below a given threshold value; or a node is added or removed from the network.

A fall in data rate results in an action to increase transmission power or use higher order modulation scheme. A fall in traffic level below a predefined threshold results in an action to activate sleep mode result the radio devices. When the signal strength

on the wireless channel falls below the predefined threshold, the action would be to change a transmission path to one with better signal conditions. Addition or removal of SBR device results in an action to activate or deactivate an antenna on the ABR respectively.

Table 5.1: State-action pairs for learning algorithm

Change in state	**Action**
Change in traffic levels to lower or higher than threshold value	Activate/deactivate sleep mode in the SBR and SCBS
Data rate falls due to increase in path loss (or higher PLE) or dropping RSS	increase transmission power, change to higher modulation scheme or change transmission path by using alternative diffraction point
Detection of new SBR	If SBR is in close proximity to existing one, activate beam switching, otherwise assign antenna to new SRB
Deactivation of SBR due to removal of SCBS	Deactivate ABR in the case of the PtP mode or assigned antenna in the case of PtMP mode

The *reward*, *'r'*, received after an action has been completed is related to the performance of the network as follows: The target performance of the network when the traffic levels fall below a predefined threshold is to reduce the energy consumed in the network. Activating the sleep mode results in reduced overall network energy consumption since fewer devices would be active on the network. Lower traffic levels also result in reduced energy consumption due to less energy used to transmit the signals, as well as encoding and decoding processes in the radio modules. A reduction in the overall energy consumed on the network, therefore, results in a reward, whose value depends on the energy efficiency performance targets of the network. Algorithms for activating sleep modes are assumed to be available in the radio nodes [15, 55, 119] and are not developed in this research.

If the performance target for data rate is 10Gbps, a lower reward value is assigned if the achieved rate is below this value. If the RSS falls below the threshold, this

results in a change of the transmission path and use of the corresponding diffraction point. The reward can be predefined path loss exponent (PLE) of 6, a typical value for NLOS environments. If the determined PLE is above this value, the link gets a lower reward, prompting the algorithm to search for an alternative path until a value resulting in an acceptable reward is obtained. A reward for an action to activate a new antenna or fixed beam switching of an existing link in the point-to-multipoint mode can be defined in terms of switching delay. A target value can be set to 10ms.

5.6 Performance evaluation

This section describes a learning algorithm which can be implemented in the CE of the radio devices. In this implementation, the overall aim of the developed algorithm is to enable the hub radio, to obtain an optimal choice of data rate, traffic levels and path loss exponent for each backhaul link. The simulations were carried out using MATLAB. The results obtained are also presented.

5.6.1 Evaluation parameters

The state of the Q-table (s_t) at time t is given by: $s_t = \{\overrightarrow{ple}, \overrightarrow{dr}, \overrightarrow{tl}, \overrightarrow{swd}\}$, where $\overrightarrow{ple}$, $\overrightarrow{dr}$, $\overrightarrow{tl}$ and $\overrightarrow{swd}$ are the vectors for the path loss exponent, signal strength, traffic level and path or operating mode switching delay. The parameters $ple_{(i)}$, $dr_{(i)}$, $tl_{(i)}$ and $swd_{(i)}$ are the path loss exponent, data rate, traffic level and path or operating mode switching delay of the i^{th} SBR. The vectors used in the simulation are: $\overrightarrow{tl}_{(i)}$={0, 1}, $\overrightarrow{dr}_{(i)}$ = {0, 5, 10}, $\overrightarrow{ple}_{(i)}$ ={1.5, 3, 4.5, 6}, and $\overrightarrow{swd}_{(i)}$ = {0, 5, 10}. When the traffic level is above the defined threshold, the state in the Q-table would be *'1'*, otherwise it is *'0'* and the required action would be to activate sleep mode. According to [25], the data rate on the SCB must scale to 10Gbps peak value expected in 5G. This value used in this analysis as the target value for the system. However, since the average value can be 1Gbps, the value is allowed to fall below the 10Gbps value. Three states

are therefore considered, i.e. *'0'*, *'5'* and *'10'*. In the case of path loss exponent, the estimated value under NLOS conditions varies from *'3'* to *'8'* [8]. A maximum value of 6 is assumed in this analysis to ensure that the path would still be usable, and is allowed to vary from *'1.5'* to *'6'*. The reward value obtained for a link i, at time t for this scenario for the data rate, switching delay and path loss exponent can therefore be represented as follows:

$$r = \begin{cases} 10 Gbps\ data\ rate\ required\ to\ avoid\ disconnection \\ 10 ms\ maximum\ delay\ for\ switching\ operating\ mode \\ 6\ path\ loss\ exponent\ for\ NLOS\ path \end{cases} \tag{5.2}$$

The actions taken by the radio are given by $a_t = \overrightarrow{A_t}$, where $\overrightarrow{A_t}$ is a vector of actions at time t, and is given by:

$\overrightarrow{A_t}$= *{activate sleep mode, increase transmit power, switch propagation path}*

A radio device observes changes in the states and makes decisions to activate sleep mode, increase transmission power or switch propagation path. After taking the required action it updates the Q-value based on the obtained reward. A positive reward will result in the reinforcement of the action taken. Table 5.2 illustrates the single-state algorithm used to obtain values for data rate, traffic level and path loss exponent values for a link.

The Q-table contents are first reset to some random values. The radio observes the state of the traffic levels, data rate calculated value of the path loss exponent. The required actions are determined based on the results of the observation. If the value is less than a set value, the required action is carried out. After the required action has been carried out, a reward is recieved depending on the results of the action. The values of the Q-table are updated and the time incremented. The cycle is repeated at given time intervals. Action is taken if changes in the parameters are observed.

Table 5.2: Single State Q-learning Algorithm

Step	**Description**
1	At $t = 0$, reset random value to $Q_{(a)}$
2	Observe changes in states and measure performance parameters
3	Get set of actions $a \in \{A\}$
4	Generate a random number between 0 and 1
5	If number $< \epsilon$ (exploration probability)
6	Perform action a_t from available actions based on the parameters: dr_{th}, tl_{th}, ple_{th}
7	Assign action for increasing transmission power, activating sleep mode or switch propagation path
8	Receive reward (data rate, path switching delay or path loss exponent)
9	Update Q-value table as follows: $Q(s_t, a_t) \leftarrow Q(s_t, a_t) + \alpha_t \{r_t + \gamma \max Q(s_{t+1}, a_{t+1}) - Q(s_t, a_t) \}$
10	Update the time: $t = t+1$

The ϵ-greedy exploration algorithm where the learning agent explores a random action with probability ϵ, is applied. Threshold values of the performance parameters are applied to restore the system to the desired performance level. The learning variables used are the learning rate α, the discounting factor for subsequent rewards γ, and the exploration probability ϵ, where $\alpha = 1 - \epsilon$.

The system is assumed to operate at 60GHz, a typical backhaul frequency for 5G wireless systems. This gives a channel bandwidth of 3GHz, which translates to Gbps data rates for the backhaul links assuming a given set of adaptive modulation and coding scheme values. The achievable data rate is given by:

$$dr = \begin{cases} 0 \; for \; \eta \leqslant SINR_{min} \\ \mu B_r log_2(1+\eta) \; for \; SINR_{min} \leqslant \eta \leqslant SINR_{max} \\ Brdr_{max} \; for \; SINR_{max} \leqslant \eta \end{cases} \tag{5.3}$$

where dr is the data rate on each link, η is the signal to interference plus noise ratio (SINR) at the time t, dr_{max} is the maximum data rate and Br is the system channel

bandwidth. The value of the PLE on each link is determined based on the RSS obtained from routine sensing measurements done by the SBR and the value sent to the ABR. The maximum PLE value is set to 6, a typical value for NLOS links in urban environments. The delay in switching a path or operating mode can be obtained from the network performance monitoring system and is set to 10 in the simulations.

5.6.2 Simulation results

The performance of the QL algorithm was separately evaluated for three states.

5.6.2.1 Data rate

The performance evaluation parameters for data rate were defined as follows: number of states = 3, number of actions = 2, reward = 10, $\alpha = 0.7$ and $\eta = 0.3$. The simulations were run for three different values of the discount factor γ: 0.3, 0.5 and 0.9. The values of the reward obtained at intervals of 25 between 0 and 200 were plotted as a fraction of the target value of 10. The values of the learning rate and exploitation probability were kept constant at 0.7 and 0.3 respectively. Fig. 5.4 illustrates the simulation results obtained. The results obtained showed that a high discount factor results in the algorithm reaching the target value faster than lower values of the discount factor. This is because small values of γ attach more importance to near-term rewards. As a result the algorithm converges faster since near-term rewards are considered. For higher values of γ, future rewards are preferred. As a result the algorithm takes longer to converge. The impact on the performance of the system is that its operation can be slowed, thus possibly affecting user quality of experience for delay sensitive applications. In realistic scenarios, a high discount factor slows down the learning process. As a result, it may not be possible for the system to acquire the necessary knowledge to make the best decisions.

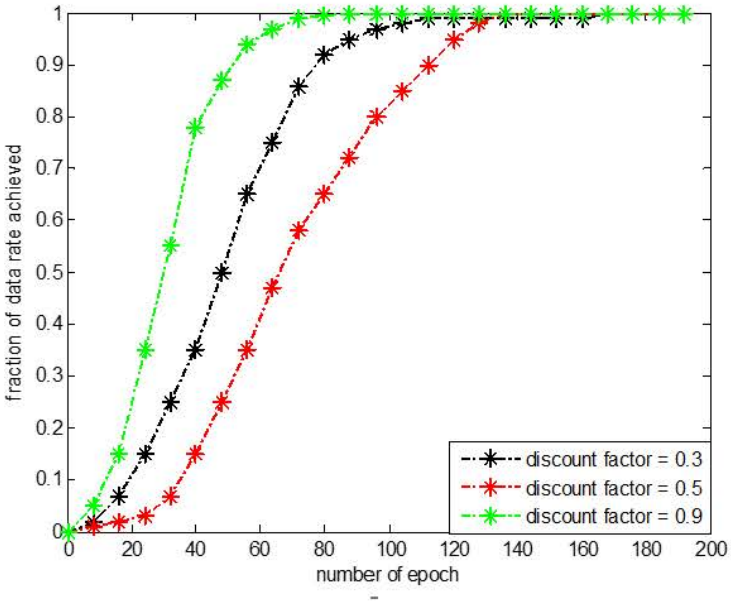

Figure 5.4: Data rate achievement for different discount factor values

5.6.2.2 Path or operating mode switching delay

The performance evaluation parameters for switching operating mode or propagation path were defined as follows: states = 2, action = 2, $\alpha = 0.5$, $\eta = 0.8$. The two states can take into account the condition when the traffic levels change, necessitating the action to change the operating mode. The algorithm's performance was evaluated for three different discount rates: 0.3, 0.5 and 0.9. The results obtained are illustrated in Fig. 5.5. The results show that a higher value of the discount factor results in the cognitive engine reaching the optimal value earlier than lower values. Like in the previous case, the higher discount factor results in the network quickly changing to a path with a value below 6. This is desirable to avoid packet loss during the switching period. A large buffer size in the nodes can be implemented to minimize the packet loss during the path switching period, however, this can result in increased device cost. A trade-off between the switching period and the buffer size would have to be considered.

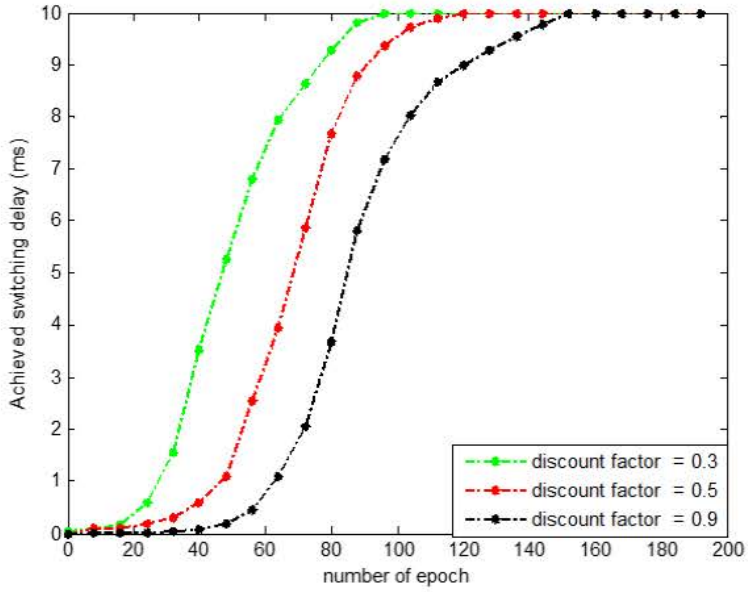

Figure 5.5: Switching delay for different values of discount factor

5.6.2.3 Path loss exponent for propagation path

The signal strength on a path is directly related to the PLE. NLOS conditions have a higher PLE compared to LoS conditions. It is used in this analysis to reflect the quality of the signal on a path. A decrease in the RSS can be reflected by a high value of PLE. The required action is either to switch to a new path or switch to a lower modulation index. The simulation parameters were set as follows: states = 3, action = 2, γ= 0.5, η = 0.5. In this simulation scenario, the performance of the algorithm was evaluated for three different learning rates corresponding to the above exploration rates: α = 0.10, 0.22 and 0.40.

The variation of the PLE with the number of generations is shown in Fig. 5.6. The results show that higher values of learning rate result in more exploitation of the algorithm. The target PLE is therefore achieved faster than with lower values of the learning rate. While this is desirable, high learning rates result in premature convergence of the algorithm. A higher learning rate also makes the agent consider

the most recent information about the network, which is desirable for increasing the speed of operation or response time of the system. A lower learning rate results in the algorithm taking more exploration time, resulting in the introduction of more diversity in the population. However, the algorithm takes longer to converge. This may have the effect of slowing down the network. This is because the longer exploration time increases the time taken for convergence of each GA computation for existing and incoming backhaul connections. This results in the SCBS taking longer to complete their transmissions. This increases the load on the network and therefore the service time for each SCBS. The benefit, however, is that each SCBS eventually gets the required QoS. A high PLE, hence low RSS, results in the system increasing the transmission power or switching a diffraction point to avoid data loss on the link. The algorithm therefore provides a self-healing capability, one of the key components in self-organising networks.

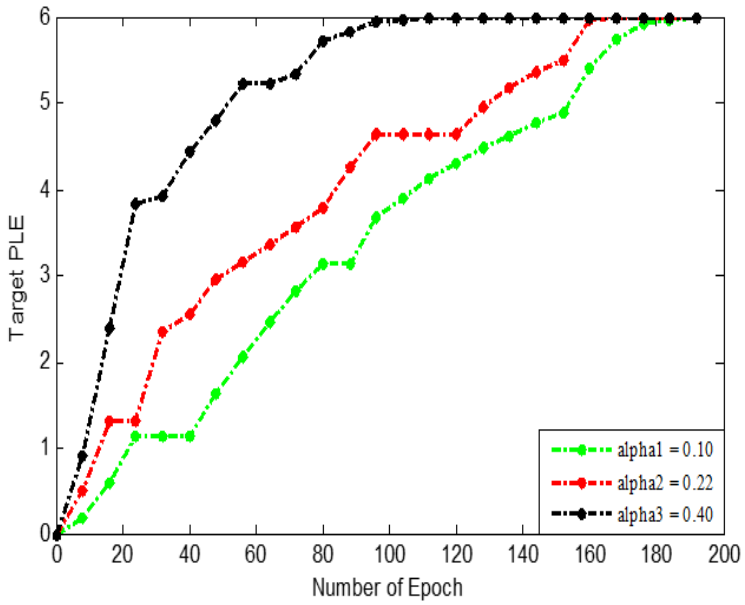

Figure 5.6: PLE for different learning rates (α)

5.7 Discussion

The capability to learn is one of the strengths and source of intelligence of the CNSCB system. In this chapter, a learning mechanism based on QL, a form of reinforcement algorithm was developed. The developed algorithm was used to determine the system's capability to maintain the link data rate above a given threshold; to ensure that in the event of a path failure the radio can switch to an alternative path within a specified time; to ensure that the path loss on the link is lower than a given threshold. Simulations were carried out to determine the system's capability to meet these requirements. The developed algorithm is part of the radio's CE learning algorithms.

The results obtained showed that the behaviour of the learning algorithm affects the way in which the radios respond to the changes in the operating parameters and environment. A high discount factor was found to achieve high data rates faster than low values. It can, therefore, be concluded that the performance of the radio devices can be improved by using high discount factor values than low values. This improves the overall network performance, hence user QoE.

Similarly, high values of the discount factor result in the algorithm making a radio device to switch to an alternative path or operating mode, faster than when a low value is used. This is required since it improves the performance of the network. The performance of the radio devices for different learning rates for different learning rates was also considered. Using path loss exponent as the performance parameter, the results showed that a high value of the learning rate enables a radio device to acquire more knowledge about the path loss on the path faster than low values. This enables the radio devices to make decisions to switch to alternative paths in the event of deteriorating propagation conditions on a path.

5.8 Chapter Summary

This chapter presented an algorithm for implementing cognitive intelligence in the CNSCB system, which enables the system to achieve some of the self-organising network capabilities required in 5G transport systems. Work related to achieving flexibility and scalability in SCB system is reviewed. The basic concepts of reinforcement learning and Q-learning were discussed. A Q-learning model for implementing the self-organising and and self-healing capabilities was presented. An algorithm that forms part of the radios' cognitive intelligence implemented in the cognitive engine is developed. An evaluation of the performance of the proposed algorithm, focusing on data rate, switching delay and path loss exponent is presented. Simulation results obtained show that high values of the discount factor result in improved performance of the learning algorithm. A high learning rate was also shown to improve the performance of the algorithm, hence a better performing network, in terms of response to changes in the operating environment.

Chapter 6

Energy Efficiency Analysis and Evaluation of the CNSCB System

6.1 Introduction

5G transport networks are required to be energy-efficient and energy-aware. These requirements have been taken into consideration in the design of the CNSCB architecture proposed in this research. The proposed use of diffraction points as opposed to daisy chaining radio devices to the core network reduces the number of deployed radio nodes, hence the energy consumed by the network. Furthermore, the proposed PtMP configuration also results in a reduced number of deployed backhaul radio devices, which will lower the energy consumed on the backhaul segment.

In the proposed CNSCB system, the street-level backhaul radio devices are co-located with small cell base station as illustrated in Fig. 3.5. This deployment strategy will allow the SCBS and backhaul radio devices to share the same power source and be connected using Gigabit Ethernet interfaces. Since sleeping modes are being proposed to be implemented in small cell base stations to conserve energy, it is also desirable for

the backhaul devices to have this capability in order improve overall network energy efficiency. However implementation of such algorithms for the SCB radio devices is beyond the scope of this research, and is recommended for future work.

The aim of this chapter is to determine the energy consumed on a small cell network, considering the access network, i.e. user equipment (UE) to SCBS and the backhaul segment. In the analysis, the energy used in transmitting data on the network, as well as the circuit power in the UE, SCBS and SCB radio devices is considered. The energy consumed in transmitting data is considered due to the expected increase in network traffic transmitted in 5G systems, and the energy can no-longer be ignored.

The novel contribution of the chapter is an analysis and comparison of the energy efficiency of two SCB configurations based on a framework that is used to evaluate energy efficiency in ultra-dense network deployments. The framework takes into consideration the energy required to keep the network equipment running, over a given period of time, and the energy required to transport a given number of bits over the same period of time. To the best our knowledge, this is the first time the power consumed on cellular network in ultra-dense network deployments under NLOS conditions is determined. Two possible configurations for the CNSCB system are considered, namely: PtP and PtMP. A review of related literature is first given. Emerging models for evaluating the energy efficiency in ultra-dense network deployments (UDN) are discussed. The proposed energy efficiency model is described, and analytical results of the energy efficiency analysis presented.

6.2 Related work

Sleeping modes are currently being proposed to improve energy efficiency in small cell networks [15, 55, 120]. Research into the impact of backhaul power consumption in HetNet network deployments is also emerging. Monti et al., study the power

consumption in fiber and microwave technologies [121]. The study does not also consider the power consumed on the UE, which is no-longer negligible under UDN deployments. Gao et al., analyse the energy efficiency of a HetNet including the backhaul segment [116]. The macro cell base station is assumed to operate at 5.8GHz, a frequency band with limited capacity in 5G small cell deployments. The authors do not take into account the circuit power of the radio devices. A major drawback of these solutions is the inability to consider the total power consumed on the network, taking into account the traffic presented to the backhaul networks for transmission. As discussed earlier, in UDN deployments, large volumes are generated on the access networks. Energy is used in the backhaul radio devices in the encoding and decoding of the data. This chapter addresses these drawbacks. Furthermore, non-line-of operation is taken into account.

6.3 Frameworks for evaluating energy efficiency in communication networks

A number of frameworks for evaluating the energy efficiency of communication networks have been developed in literature [55, 115–117]. One of the most recent is that proposed in the Earth Project for evaluating the energy efficiency in 5G networks [115]. The framework considers two metrics, namely: the power consumed per unit area and the energy consumed per bit transmitted over a given period of time. In terms of the power per unit area, the energy efficiency is expressed as:

$$\eta_{EE} = \frac{PT}{A},$$

where **P**, **T** and **A** are the consumed power, period of time considered and the area under consideration respectively. For the energy consumed per bit metrics, the energy efficiency is expressed as:

$$\eta_{EE} = \frac{E}{B},$$

where **B** is the number of bits transmitted in a given observation period and **E** is the energy consumed by the network over the same observation period. The energy consumed per bit can also be expressed as the average network power divided by the data rate, over a given period of time, in W/bps:

$$\eta_{EE} = \frac{PT}{R},$$

where **R** is the data rate.

The method used for evaluating the energy efficiency of the CNSCB system is based on energy consumed per bit. This is because in legacy networks, the energy consumed during data transmission could be negligible compared to that consumed for keeping the radio devices running. However, as explained earlier, in 5G networks, the amount of data transmitted is much larger and the energy consumed during data transmission must be taken into account.

6.4 Power consumption and traffic models for the CNSCB system

The energy efficiency evaluation model proposed in this research is based on power consumed by the backhaul radio devices and data transmitted on the network. In the analysis, reference is made to the power consumed by the devices and power consumed for data transmission. A period of one hour is assumed. In determining the energy efficiency, the power is then multiplied by time to obtained the energy consumed in the system. However, for the sake of simplicity, the analysis is carried out using power.

This model considered in this research takes into account the energy consumed by network devices and the amount of data transmitted, from the user devices to the

aggregation backhaul radio. This is because in traditional backhaul links, the energy consumed for data transmission was negligible. However, in ultra-dense network deployments, the amount of transmitted data is much and the energy consumed can no-longer be ignored. The model therefore best suites the dense deployment scenario in small cell networks. The following sections describe the mathematical analysis and evaluation frameworks. Two possible configurations are considered, i.e. point-to-point and point-to-multipoint. The network models and assumptions made in the analysis are given in the following sub-section.

6.4.1 Network model and assumptions

Fig. 6.1 illustrates the two possible deployment configurations. Fig. 6.1 (a) illustrates the point-to-point configuration. The backhaul links consist of two back

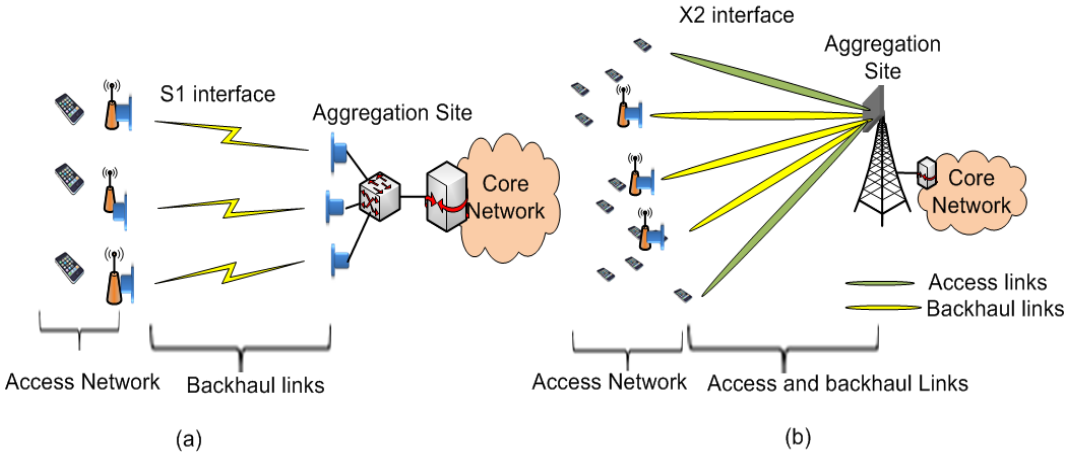

Figure 6.1: Small cell backhaul configurations (a): Point-to-Point, (b) Point-to-Multipoint

radio devices, one interconnected with the base station and the other interconnected to the aggregation equipment. User devices connect to the base stations on the access network and traffic is forwarded to the core network via the aggregation backhaul radio devices. The standard S1 interface is used on the backhaul links. Fig 6.1 (b) illustrates the point-to-multipoint configuration. The backhaul

link consists of radio devices interconnected to the base stations and a massive multiple-input-multiple-output (mMIMO) base station. A backhaul link is established by assigning a beam to each street backhaul radio device. The standard X2 interface is used on both the access and backhaul links. The *S1* and *X2* logical interfaces are defined by the 3GPP. The *S1* interface connect the base stations directly to the core network, while the *X2* interconnects base stations, allowing them to exchange management information such as handover signals.

In the analysis and evaluation of the energy efficiency of the system, the following assumptions are made:

1. Access network in point-to-point configuration is operated at a sub-6GHz frequency but the backhaul segment is operated at 60GHz.

2. Both access and backhaul in the point-to-multipoint configuration are operated at 60GHz. The radio devices are also assumed to be operating at 60GHz.

3. In the point-to-point configuration, the interface between the base station and the core network is the S1 interface, via the backhaul link, i.e. link between the street backhaul device and aggregation site backhaul device.

4. In the point-to-multipoint configuration, the base station connects to the core network using an X2 interface via the backhaul link..

5. The total number of backhaul links in the point-to-point and point-to-multipoint configurations is 300.

6. The access network traffic in the point-to-multipoint architecture is assumed to be negligible compared to the backhaul traffic.

7. In both configurations, non-line-of-sight-operation is based on propagation by diffraction

6.4.2 Power consumption model

This section presents an analysis of the power consumed by the systems during a given period of time. The total power consumed by a mobile network comprises base station operational power and power consumed during transmission and reception of data. The power can further be broken down into the power consumed by the network on the backhaul and access network segments. In the proposed energy efficiency analysis, we consider the total power consumed by the access and backhaul network segments, and the energy consumed for transmission and reception of data. The total power consumed by a cellular network, including the NLOS backhaul segment is defined in this research as follows:

$$P = \sum_{i=1}^{X} x_{(i)} p_{(i)} + \sum_{i}^{L} p_{bh(i)} \tag{6.1}$$

where:

X represents the total number of base stations in the network,

$x_{(i)}$ is the i^{th} base stations type,

$p_{(i)}$ is the total power consumed by each base station,

L represents the total number of backhaul links on the network, and

$p_{bh(i)}$ is the total power consumed on each backhaul link serving a base station.

The following notations are used to refer to the radio devices:

ABR: massive MIMO base station

SCBS: small cell base station

SBR: backhaul radio device co-located with and interconnected to the small cell base station

UE: User equipment, i.e. mobile phone devices

Fig. 6.2 shows the different network segments considered in the energy efficiency analysis. The end-to-end network considered consists of the access network segment consisting of the user devices and the small cell base station and the backhaul segment which consists of the street-level backhaul device and the aggregation point backhaul radio device. In the case of the PtP architecture, two radio nodes with an architecture shown in Fig. 3.2 form the backhaul segment. In the case of the PtMP architecture, the backhaul segment would consist of the street backhaul radio device and an antenna, which is part of the massive MIMO base station antenna arrays.

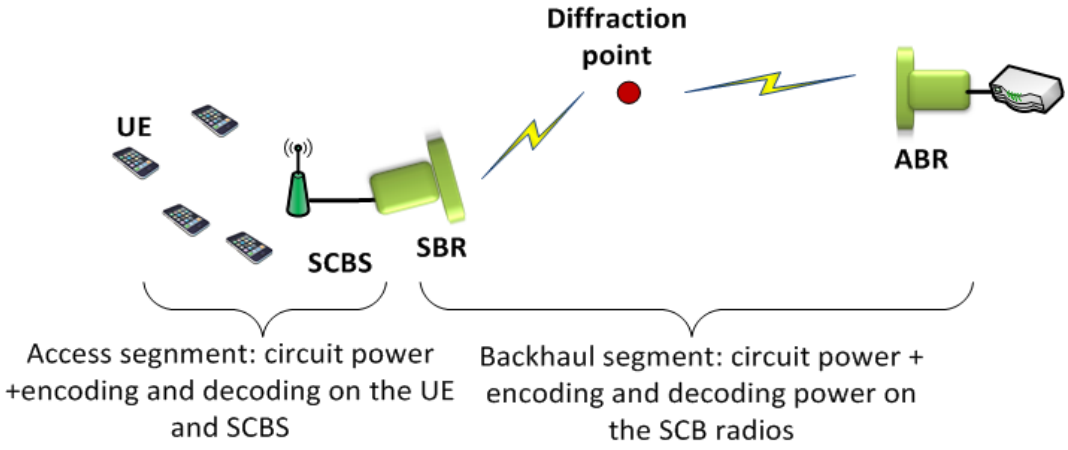

Figure 6.2: Network model for power consumption

The power consumed by a base station can be calculated as follows [117]:

$$p = \begin{cases} N_s(a_M p_{tx} + b_M) \text{ for a ABR station} \\ (a_{scbs} p_{tx} + b_{scbs}) \text{ for a SCBS station} \end{cases} \tag{6.2}$$

where:

N_s is the number of antennas at the ABR site,

p_{tx} is the transmission power,

a_M is amplifier power losses on the ABR,

a_{scbs} is amplifier power losses on SCBS,

b_M is a cooling and signal processing power consumption factor on the ABR,

b_{scbs} is a cooling and signal processing power consumption factor on the SCBS,

The ABR cooling power constitutes a major portion of the power consumed by the system since air-conditioning systems are required to cool the equipment due to the large number of circuits involved in running the base station. However, in the case of the SBR of the point-to-point and point-to-multipoint systems, and the ABR of the point-to-point system, the cooling power is zero, since they are air-cooled. The power consumption for SCBS in equation 6.2 reduces to:

$$p = a_{scbs} p_{tx} \tag{6.3}$$

6.4.2.1 Power consumption model for PtP system

A detailed breakdown of the power consumed by a SCBS can be represented as [117]:

$$\begin{aligned} p_{scbs} =& \tau_s.p_{tx} + (1-\tau_s).K_u.p_{ut} + p_f + K_u.p_{edDL}.R_{DL}.\tau_s \\ &+ p_{sf}.UE + p_{uf}.K_s + \tau_s.K_s.p_{edUL}.R_{UL}.(1-\tau_b) \end{aligned} \tag{6.4}$$

where:

τ_s is a fraction of time spent by the SCBS UE link on the uplink

K_u is the number of UEs per SCBS,

p_{ut} is the transmit power of the UE

p_{eDL} is the downlink encoding power

p_{uf} is the circuit power of the UE

p_{sf} is the circuit power of the SCBS

R_{DL} is downlink transmission power to the UE

R_{UL} is transmission power from the UE on the uplink.

By considering the power consumption for data transmission given in [117], the power consumption on the CNSCB links can also be derived. The power consumed on the backhaul segment can is therefore defined in this research as:

$$\begin{aligned} p_{bh} =& \tau_b.p_{bDL} + \{(1-\tau_b).K_s.p_{bUL} + \tau_b.K_h.K_u.p_{edDL}\}R_{bDL} \\ &+ p_{hf}.K_h + K_s.p_{stf} + \{(1-\tau b).K_u.K_s.p_{ed}\}R_{bUL} \end{aligned} \tag{6.5}$$

where:

τ_b is the fraction of time spent on the uplink of the backhaul,

p_{bDL} is the transmission power on the backhaul downlink,

K_b is the number of SBRs,

K_h is the number of ABRs,

p_{hf} is the circuit power of the ABR,

p_{uf} is the circuit power of the SBR,

p_{stf} is the transmission power at the SBR,

p_{eDL} is the encoding power on the SBR,

p_{dUL} is the decoding on the ABR downlink,

R_{bDL} is the data rate on the SBR downlink,

R_{bUL} is the data rate on the SBR uplink.

The total power consumed on the PtP architecture for both access and backhaul segments can therefore be determined from:

$$P_{PtP} = \sum_{i=1}^{L}(p_{scbs(i)} + p_{bh(i)}) \tag{6.6}$$

$p_{scbs(i)}$ is calculated from equation 6.4 and $pbh(i)$ is calculated from equation 6.5.

6.4.2.2 Power consumption model for PtMP system

As discussed earlier, the ABR in the PtMP architecture consists of a system of antenna arrays. Assuming a total of K antennas, with L antennas assigned to UEs, each UE being assigned one antenna, the number of antennas used for backhaul is K - L, with $K \gg L > 1$. The power consumed by a massive MIMO base station, p_{ABR}, is given by [116, 117]:

$$p_{ABR} = \frac{\frac{p_{tx}}{\eta(1-\sigma_{feed})} + p_c + p_{idle}}{(1-\sigma_{dc})(1-\sigma_{ABR})(1-\sigma_{cool})} \tag{6.7}$$

where:

η is the power amplifier efficiency,

p_c is the circuit power of the RF chains,

p_{idle} is the idle power consumption,

σ_{feed} is the lossy factor of the antenna feed,

σ_{dc} is the DC-DC power supply,

σ_{ABR} is the main power supply,

σ_{cool} is the active cooling power.

The circuit power is calculated from:

$$p_c = N_{(p_{dac}+p_{mix}+p_{filter})} + p_{syn} \tag{6.8}$$

where:

p_{dac} is the power consumed by the digital to analogue converter,

p_{mix} is the power consumed by the mixer,

p_{filter} is the power consumed by filter,

p_{syn} is the power consumed the synthesizer.

The power consumption of the PtMP system can therefore be broken down into the power consumption on the SCBS, SBR and ABR, and is represented as:

$$p_{PtMP} = p_{ABR} + \sum_{i=1}^{N} (p_{bh(i)} + p_{scbs(i)}) \tag{6.9}$$

with the components of the equation as defined before. A detailed breakdown of power consumption at the ABR site can be represented as follows:

$$\begin{aligned} p_{ABR} = \lambda_m.p_{tx} + (1-\lambda_m).K_m.p_{ut} + \lambda_m.K_m.p_{edDL}.R_{mDL} \\ + p_{mf} + (1-\lambda_m).K_m.p_{ed}.R_{mUL} \end{aligned} \tag{6.10}$$

where:

λ_m is the fraction of time spent on the downlink,

p_{tx} is the transmit power at the ABR site,

p_{ut} is the UE transmit power,

K_m is the number of UE's connecting directly to the ABR,

p_{edDL} is the encoding power on the ABR downlink,

p_{edUL} is the decoding power on the UE uplink,

R_{mDL} is the transmission rate on downlink,

$RmUL$ is the transmission rate on uplink,

p_{mf} is the circuit power consumed at each antenna on the ABR.

Similarly, the power consumption on the access network segment is determined from:

$$\begin{aligned} p_{scbs} = \lambda_{sc}.p_{stx} + (1-\lambda_{sc}).K_{sc}.p_{ut} + \lambda_{sc}.K_{sc}.p_{edDL}.R_{scDL} \\ + p_{sf}.M_{sc} + (1-\lambda_{sc}).K_{sc}.p_{ed}.R_{scUL} \end{aligned} \tag{6.11}$$

where:

λ_{sc} is the fraction of time spent on the downlink,

p_{stx} is the SCBS transmit power,

K_{sc} is the number of SCBS,

p_{edDL} is the encoding and decoding power on the SCBS downklink,

p_{edUL} is the encoding and decoding power on the UE uplink,

R_{scDL} is the transmission rate on downlink,

R_{scUL} is the transmission rate on the uplink,

p_{sf} is the circuit power consumed at each antenna on the ABR,

M_{sc} is the number of SCBS.

As in the case of the PtP configuration, the power consumption on the backhaul segment of the PtMP configuration including the transmitted data can be determined:

$$\begin{aligned} p_{bh} = \lambda_b.p_{mbtx} + (1-\lambda_b).K_b.p_{sb} + \lambda_b.K_b.K_{sc}.p_{edDL}.R_{scDL} \\ + p_{mf}.K_{sc} + (1-\lambda_b).K_b.K_{sc}p_{ed}.R_{scUL} + (p_b + p_{bc}).K_b \end{aligned} \tag{6.12}$$

where:

λ_b is the fraction of time spent on the downlink on the backhaul segment,

K_b is the number of SBR,

p_{sb} is the transmit power at the SBR.

The rest of the parameters are as defined above. The total power consumed on the PtMP architecture can, therefore, be represented as follows:

$$P_{PtMP} = \sum_{i=1}^{N}(p_{scbs(i)} + p_{bh(i)}) + \sum_{i=1}^{M} p_{ABR} \tag{6.13}$$

where M is the total number of antennas at the ABR and N is the total number of SCBS and their respective backhaul radios. In order to determine the energy efficiency of the two systems, the traffic carried on each of the systems must be determined. The following section presents the traffic models used to determine the traffic load on the systems.

6.4.3 Traffic models

The backhaul traffic generated by a SCBS can be determined using the Gauss-Markov models [27]. These models are used in this work to determine the traffic generated from the SCBSs. The traffic from a SCBS is predominantly user traffic, with control and signalling traffic negligible. Only user traffic is therefore considered.

6.4.3.1 Traffic model for PtP system

The traffic generated by a UE is assumed in this case, to be governed by a Pareto distribution with infinite variance [120]. The spatial traffic intensity of the UEs is assumed to be independently and identically distributed (i.i.d). The overall network traffic is also assumed to be self-similar and bursty. The average traffic on the network can, therefore, be determined from [120]:

$$T_{S1} = \lambda_{UE}.\pi.r^2.\frac{\theta\beta_{min}}{(\theta - 1)} \tag{6.14}$$

where:

λ_{UE} is the number of mobile subscribers,

β_{min} is the minimum rate of traffic preserved for a UE required for the UE to maintain its QoS,

$\theta \in \{1, 2\}$ is a reflection of the heaviness of the traffic distribution tails,

r is the small cells radius.

The area of the circle is assumed to be approximately that of a circle of radius r. The values of β and θ are assumed to be 10.75 and 1.8 respectively [128]. From equation 6.14, it can be concluded that the backhaul traffic increases as the radius of the base station increase. An increase in the number of users connected to the SCBS also results in an increase in the backhaul traffic.

6.4.3.2 Traffic model for PtMP system

The offered load for a UE in PtMP configuration can be represented as:

$$r_{UE} = RTp_{ue} \tag{6.15}$$

where:

R is the data rate,

T is the transmission time,

p_{ue} is the probability that a UE is in active session and is given by:

$$p_{ue} = \frac{\alpha}{\alpha + \gamma}$$

where α is the user arrival rate and γ is the duration of the session of a user. If there are K different UEs, the traffic on the *X2* link can be defined using a random vector:

$q = \{q_1, q_2 \cdots, q_K\}$,

where q denotes the transmission rate of a single UE. The total traffic emanating from a SCBS and placed on the backhaul link can therefore be determined from:

$$T_{X2} = \sum_{k=1}^{K} r_{ue(k)} q_{(k)} \tag{6.16}$$

where $r_{ue(k)}$ and $q_{(k)}$ are the data rate and traffic generated by the k^{th} UE respectively.

The volume of traffic on the *X2* interface can also be expressed as a fraction of the *S1* traffic as follows:

$$\psi = \frac{T_{x2}}{T_{s1}} \tag{6.17}$$

To evaluate the traffic on the *S1* and *X2* interfaces of the point-to-point and point-to-multipoint architectures respectively, default values recommended by the 3GPP, and also used in [122] are considered.

6.5 Energy efficiency evaluation

The energy efficiency of the PtP and PtMP architectures is determined from the energy consumed by the network for various network traffic loads. A duration of one hour is considered, and the energy consumed is obtained by multiplying the power by the time, in seconds, i.e. $Energy(J) = Power(W) \times Time(s)$. For the PtP architecture the energy efficiency is determined from:

$$\eta_{EE_{PtP}} = \frac{P \times Time}{R} = \frac{P_{PtP} \times 1hr}{T_{S1}} = \frac{E_{PtP}}{T_{S1}} \tag{6.18}$$

where P_{PtP} and T_{S1} are determined from equations 6.6 and 6.14 respectively.

For the PtMP architecture it is determined as follows:

$$\eta_{EE_{PtMP}} = \frac{P \times Time}{R} = \frac{P_{PtMP} \times 1hr}{T_{X2}} = \frac{E_{PtMP}}{T_{X2}} \tag{6.19}$$

where P_{PtMP} and T_{X2} are determined from equations 6.13 and 6.16 respectively.

6.5.1 Simulation results

This section presents simulations results of the energy efficiency analysis for the two deployment scenarios under study. The simulation parameters used are shown in Table 6.1. The energy consumed by the networks is considered for a period of one hour, assumed to be the peak period.The energy efficiency for the two PtP and PtMP architectures was determined using equations 6.18 and 6.19 respectively.

6.5.1.1 Simulation results of PtP architecture

Fig. 6.3 shows a plot of the energy efficiency (Bits/J) versus number of backhaul links for the PtP architecture with traffic load at 30%, 50% and 100%. The minimum

Table 6.1: Simulation Parameters

System Configuration		**Power values**	
Backhaul P_{tx}	60W	P_{mb}	60W
No. SCB links	300	Pb_{UL}	40W
No. SCBS links	300	$P_{(scbs)tx}$	0.23W
UEs per SCBS	10	P_{ut}	0.05W
R_{DL}/R_{UL}	300/75Mbps	$P_{(scbs)f}$ / b_{bf}	5.2W
τ	0.5	P_{mf}	225W

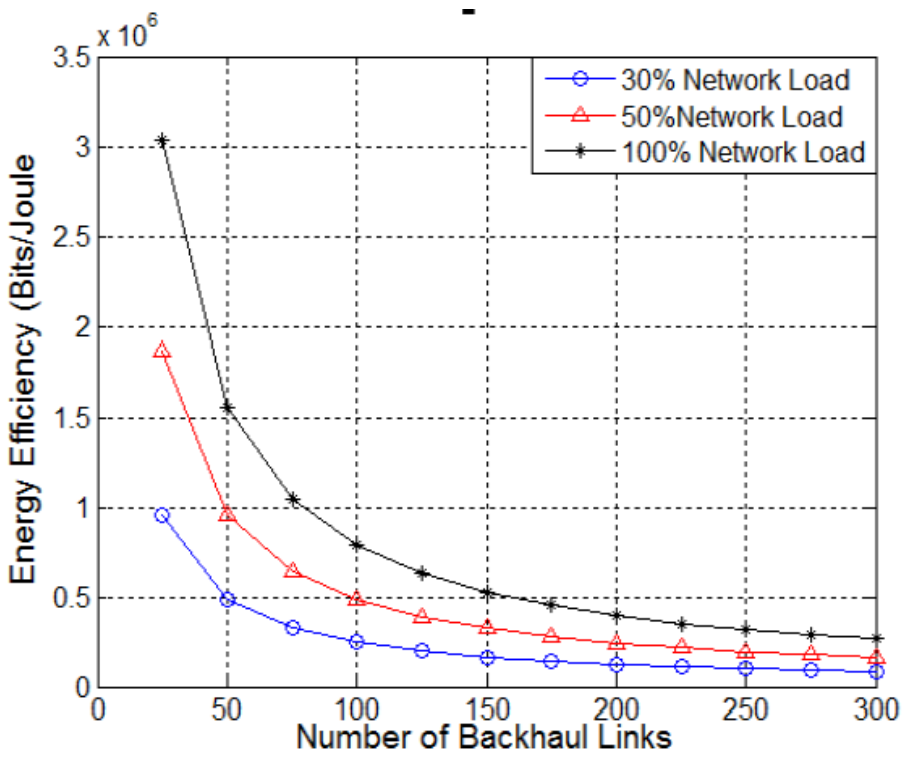

Figure 6.3: Energy efficiency for PtP system as a function of the number of SCB links for varying network loads with no SBR circuit power

number of backhaul links required to provide minimum connectivity under the lowest traffic loads is assumed to be 25. The energy efficiency of the system decreases as the number of backhaul links increases. This is due to increased energy consumption on the network caused by a higher number of deployed devices. The aim of the CNSCB system is to provide backhaul coverage to SCBS deployed to provide access in locations where they are required by netowrk operators. Decreasing the number

of backhaul links to achieve a high energy efficiency can therefore result in failure to meet the traffic throughput requirements of the access networks in a given area. There is, therefore, need to balance the achievable energy efficiency and the network QoS.

6.5.1.2 Simulation results for PtMP architecture

Fig. 6.4 shows a plot of the variation of energy efficiency versus the number of backhaul links for the PtMP system. As in the case of the PtP scenario, the energy

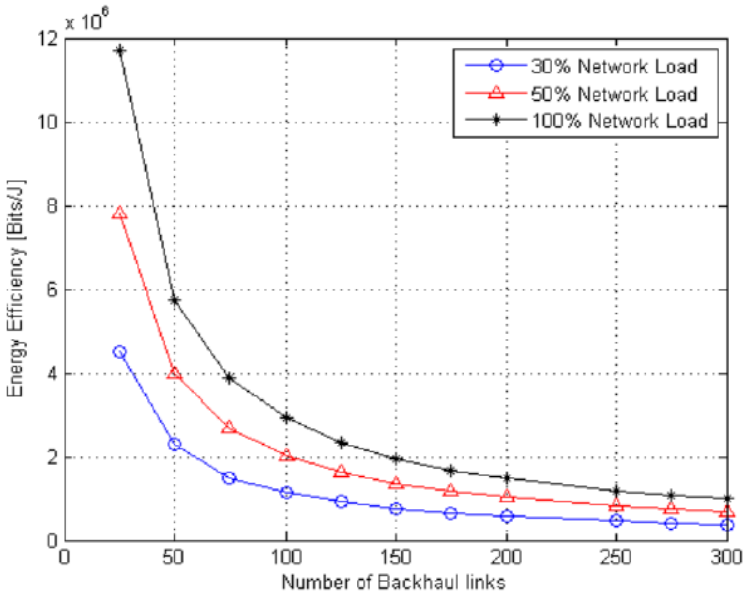

Figure 6.4: Energy efficiency for PtMP system as a function of the number of SCB links for varying network loads.

efficiency is also observed to decrease as the number of backhaul links increase, even though the architectures differ significantly. This is because, irrespective of the architecture, energy is consumed for transmitting traffic on the backhaul segment and operation of the radio devices. The use of in-band backhauling eliminates the need for additional radio devices. However, in-band backhauling has capacity limitations given the high data rate capabilities of 5G UEs. Furthermore, given the rapid increase in the number of users per given area in ultr-dense network deployments, a scalable

backhaul system would be required. For example, in the PtP case, higher energy efficiency is preferable, but this must be achieved under the constraint of meeting the network QoS and user quality of experience. Energy efficiency can be increased by reducing the number of network devices, hence backhaul links. However, this can cause some areas not to have good network coverage and could reduce achievable user data rates per unit area, and can result in reduced user quality of experience and eventually loss of revenue.

6.5.1.3 Comparison of energy efficiency of the PtP and PtMP architectures

Fig. 6.5 shows a comparison of the energy efficiency performance of the two systems with 100% traffic load. The results show that the PtMP architecture performs better than the PtP architecture. The increased energy consumption on the PtP architecture is due to additional fixed power consumption of backhaul radio devices. On the other hand, the use of phased antenna arrays to provide backhaul links in PtMP systems eliminates the need for additional radio devices at the aggregation site. However, while the massive MIMO systems provide higher energy efficiency, deployment in areas where fewer links are required may not be cost effective compared to PtP links. A trade-off between the required coverage and energy efficiency may determine the eventual architecture adopted for the SCB.

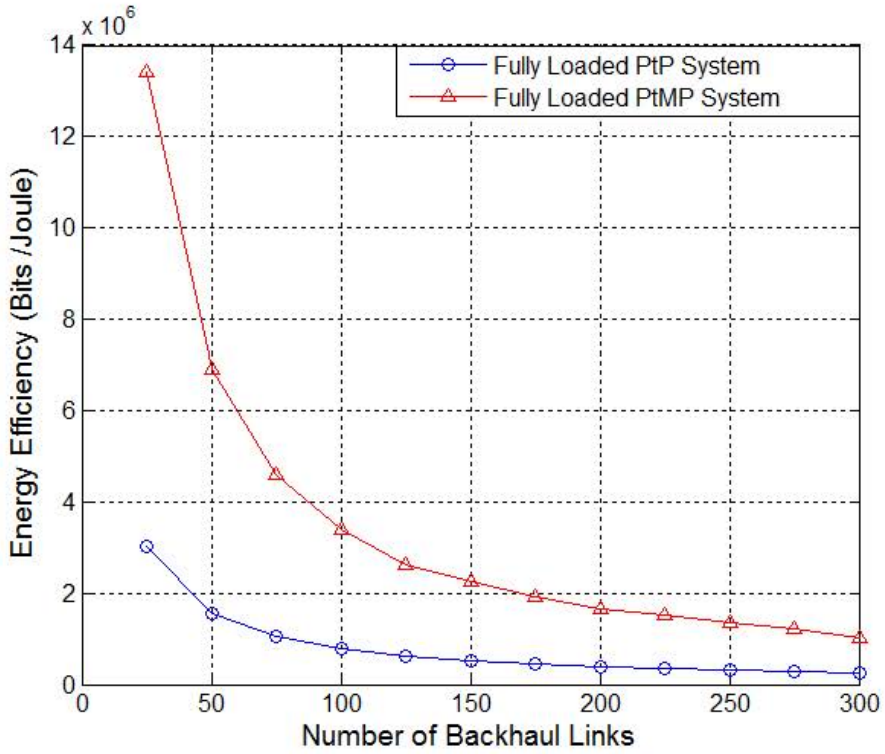

Figure 6.5: Comparison of energy efficiency of PtP and PtMP systems at varyig number of deployed backhaul links.

6.6 Discussion

An analysis and evaluation of the energy efficiency of the CNSCB system when deployed in PtP or PtMP configuration was carried out. By including the contribution of the data transmitted on the networks, the analysis catered for the large amounts of data expected to be transmitted on small cell networks. The number of deployed devices was also taken into consideration due to the expected UDN deployment in 5G. It was observed that the energy efficiency of the network in decreased as the number of backhaul links increased. This is attributed to the increase in energy used by a large number of radio devices. This means that more radios would require more energy for operation. The proposed CNSCB architecture is based on massive MIMO technologies which allows the PtMP configuration. This configuration reduces the

number of deployed devices since only antenna arrays are used at the aggregation site and a single module for the network and processing modules. This makes the CNSCB more energy efficient than than a PtP architecture. Furthermore, the use of diffraction points for redirecting signals to the radio devices also reduces the number of deployed radio devices compared to the strategic node placement or daisy chaining strategies proposed in literature to address the NLOS problem.

The deployment of a small number of backhaul links has been shown to increase energy efficiency. However, reducing the number of backhaul links can lead to the inability of the backhaul system to provide backhaul coverage in all the SCBS locations where this is required. Conversely, increasing the number of backhaul links makes it possible to place more SCBSs, resulting in providing access to more users. However, high traffic volumes result in reduced energy efficiency since more energy is used by the radio devices for encoding and decoding processes. It is therefore necessary to strike a balance between the required energy efficiency and the traffic allowed on the network. One of the benefits of in-band backhauling is the complete elimination of the backhaul radio devices. While this will result in very high energy efficiency, the network throughput will not scale to 5G requirements. The CnSCB system therefore provides a middle ground between the in-band backhaul solutions and the strategic node-placement solutions.

While the PtMP configuration was found to be more energy efficient than the PtP configuration, it should be noted that the deployment of the massive MIMO system will not be cost-effective in an area with few SCBS locations. The PtP architecture would therefore be cost-effective and can result in reduced energy consumption, hence higher energy efficiency. A trade-off between the required throughput per unit area and achievable energy efficiency would be needed. This is because reducing the

number of deployed devices will improve energy efficiency, however, this results in achievable throughput per unit area.

6.7 Chapter Summary

This chapter presented an analysis and evaluation of the energy efficiency of the CNSCB system in PtP and PtMP configuration. A review of existing energy efficiency models showed that most of the proposed solutions consider the energy consumed on the access network only. This is because the energy consumed on the backhaul segment has always been considered as negligible. However, in 5G systems, the number of backhaul links is expected be large, and contribute significantly to network energy consumption. Furthermore, the backhaul traffic is also expected to be high.

Analytical power consumption and traffic models that take into account the power consumed on the backhaul nodes, the SCBS and user devices were considered. Furthermore, the energy consumed in the encoding and decoding of traffic on all the network nodes was also considered. The energy efficiency of two possible deployment configurations for SCBS systems was analysed and a compared. An analysis of the shows that the PtMP architecture is more energy efficient than the PtP architecture. However, the deployment of the PtMP architecture may not be cost-effective in cases where a SCBS is in an isolated location. A trade-off between the energy efficiency and the need for ensuring backhaul coverage is therefore required.

Chapter 7

Conclusions and Recommendations

Ultra-dense network deployment of heterogeneous wireless access networks was identified as one of the strategies for meeting the increasing demand for capacity and coverage on the access network. Most popular among these are densely deployment small cell networks with base stations deployed 3-6m above ground. This thesis found that backhauling the small cell traffic to core network networks is a challenging task. Using existing roof-mounted aggregation sites will reduce operational costs. However, deploying wired solutions to these sites will be costly and time-consuming. Traditional microwave backhaul solutions have capacity and coverage limitations. Millimeter wave technologies are the preferred technologies due to their cost-effectiveness, flexibility and Gbps achievable data rates. However, like all wireless systems, they suffer from signal blockage.

Existing literature on backhaul architectures for outdoor urban small cells was reviewed and classified into three categories namely: in-band, strategic node-placed, and SON-based solutions. These strategies show a fragmented approach in addressing the outdoor urban small cell backhaul problem. In-band backhaul solutions involve the use of macro cell access links for backhauling traffic from small cell networks. While these solutions are cost effective, they result in reduced capacity available for

backhaul. Furthermore, complex radio resource management schemes would need to be in place. Strategic node-placement solutions involve the use of intermediate nodes purposely placed between street-level and rooftop radio devices to enable NLOS links. These solutions can be costly due to the use of additional radio equipment. In addition to this, implementation and operational costs can also be high, especially in UDN deployment scenarios.

The reviewed SON-based solutions address the issues of dynamicity and flexibility. However, the NLOS connectivity is not addressed. It was therefore concluded that a small cell backhaul solution that addresses the connectivity problem through NLOS coverage is required. Furthermore, an architecture based on propagation by diffraction would result in fewer deployed devices, hence reduced capital costs. Most of the proposed solutions do not make use of device intelligence to mitigate the effects of NLOS coverage. SON technologies have been proved to in access networks to reduce operational costs, a key requirement in densely deployed backhaul links. A solution incorporating mmW and massive MIMO technologies would also address the capacity and cost problems.

The overall goal of this research was to design a non-line-of-sight (NLOS) backhaul architecture that solves the limitations of existing backhaul solutions and addresses the current and future backhaul requirements of outdoor urban small cells. The developed solutions allow autonomous creation and establishment of street-to-rooftop backhaul links, based on propagation by diffraction, using diffraction points in predefined locations between the backhaul radio devices. The main difference between this thesis and existing literature is that most of the researchers have proposed the use of wireless solutions due to their cost-effectiveness and flexibility. However, they have assumed line-of-sight operation, which will have limited application in outdoor urban environments. This thesis does not make this assumption, but proposes to

use carefully selected diffraction points to guide the radio beams to backhaul radio devices located at street level and aggregation sites. A number of algorithms are proposed to enable the radio devices to establish multi-path backhaul links, determine their performance characteristics, rank the links according to this performance and use the best performing as the primary links. A coverage model and reasoning algorithm for ensuring that a SCBS location is covered by a minimum number of diffraction is proposed and its performance evaluated. The use of diffraction points for NLOS backhaul coverage, and incorporation of algorithms for enabling autonomous capabilities in the radio devices fulfils the main goal of this research.

In addition, other key issues such as feasibility studies on the effectiveness of the proposed architecture were explored. Furthermore, due to the demand for more energy-aware communication networks, an analysis and evaluation of the energy efficiency of the proposed architecture is carried out. While a number of schemes have been proposed in this thesis to address the requirements for cost-effective, reliable and high capacity of NLOS backhaul links, there is scope for improving the work. The first section summarises the research done in each chapter, and the second section discusses possible future work related to the contributions in each of the chapters in order to identify extensions and potential approaches for further improvements.

7.1 Conclusions

The major conclusions that can be drawn from the solutions proposed throughout this thesis are as follows:

Chapter 2 gives a description of the fundamental challenge of backhauling outdoor urban small cells, major requirements, enabling technologies and existing solutions. An investigation into the SCB problem reveals that providing reliable connectivity to the street-level SCBS locations is the major challenge that must be addressed

first, since most SCBS locations will not have communications infrastructure. Wireless solutions are preferred because of their cost-effectiveness, flexibility and short deployment times. However, the backhaul solutions must be able to meet the current 180Mbps minimum capacity requirement, and be scalable to the 1Gbps requirements of 5G backhaul systems. Furthermore, the systems must incorporate SON capabilities to reduce deployment and operational costs by minimising human intervention.

A review of backhaul technologies being proposed for small cells showed that the four major technologies are mmW, massive MIMO, SON and cognitive radio technology. However, ensuring NLOS operation at mmW spectrum bands is the key enabler of outdoor urban small cell backhaul connectivity. The CNSCB system proposed in this research is based on these technologies, and is designed to operate under NLOS conditions.

A major drawback of existing solutions was the inability to properly address the NLOS coverage problem. In-band solutions, in which backhaul links and user equipment links share linsk on the base stations do not meet the capacity requirements and cannot scale to 5G capacity requirements. Where super-6GHz frequency bands were proposed, the NLOS problem was not addressed. Solutions that proposed strategically placing intermediate nodes between the street and aggregation nodes would not be cost-effective since this increases the number of deployed devices. Furthermore, costs associated with installation costs and energy consumption would also increase. SON-based solutions addressed the issues of reducing operational costs by employing SON techniques. However, even though mmW technologies are proposed to meet the capacity requirements, the problem of NLOS connectivity is not addressed.

A backhaul architecture designed mainly to address the coverage and capacity problems is proposed in **Chapter 3.** It is based on mmW frequency bands and is capable of operating under NLOS conditions. In the proposed solution, each

backhaul link consists of a street backhaul radio collocated with a SCBS, and another aggregation backhaul radio collocated with routers or switches at the aggregation site located on a rooftop.

Termed the cognitive NLOS small cell backhaul (CNSCB) system, the architecture can be implemented in PtP or PtMP configurations depending on the operator's requirements. PtMP configuration is achieved through the use of massive MIMO technology. NLOS links are established by simultaneously pointing the antennas of the street and rooftop radio devices at a diffraction point. Learning and optimization algorithms implemented in the cognitive engine of the radio devices are proposed to minimize operational costs through SON capabilities. Multiple-path propagation is proposed to ensure network resilience and reliability. The proposed architecture, therefore, bridges the gap between existing architectures and 5G transport requirements for small cell backhaul.

This research focused on ensuring SCBS location coverage under NLOS conditions by using cognitive intelligence implemented in the radio devices in the form of learning, reasoning and optimisation algorithms. The cognitive intelligence gives the radio devices the ability to autonomously create NLOS multiple-paths between the backhaul radio devices, and ensure that the links operate within the specified QoS performance requirements.

Chapter 4 is dedicated to studying and defining the models and algorithms for ensuring NLOS coverage. Due to signal blockage at mmW frequencies, diffraction was the proposed mode for signal propagation between the backhaul radio devices. The single knife edge diffraction (SKED) geometry was found to be most suitable for representing the street-to-rooftop path topology. The SKED model was therefore used in the design of the architecture. Furthermore, unlike other existing models, it is frequency independent and can therefore be used for mmW spectrum bands.

In order to gain more insight into the behaviour of mmW signals under NLOS conditions in the framework of the proposed architecture, a numerical analysis of diffraction loss of radio signals at 15GHz-90GHz frequencies was carried out. The results obtained show that diffraction loss increases with increase in operating frequencies, decrease in the distance between the transceivers and at points less than 40m from the radio antennas. The small wavelength of mmW signals was also found to contribute to the high diffraction loss due to the small radius of the first Fresnel zone of the signals. Identifying diffraction points suitably located between the transceivers was therefore found to be key in the performance of the proposed solution.

Studies to determine the feasibility of the proposed architecture were carried out in a typical outdoor urban environment using prototype 17GHz and 60GHz backhaul radio devices. Results of the propagation measurements showed that signals above the usable threshold could be detected below the roof edge used as anchor points for the diffracted signals. Furthermore, link quality tests to determine the QoS values of the established links showed that data rates above the current of 180Mbps can be achieved. Links performance characteristics within the those defined by the ITU for voice, video, and data applications were obtained.

The establishment of NLOS links in the proposed CNSCB system is based on the fact that an identified diffraction point has line-of-sight visibility of both the street level radio location and the aggregation site. The experiments using the 60GHz radio equipment were therefore carried out to determine the ease with which these radio device can establish line-of-sight links, given the narrow beam width of the radio signals and the need to carefully align the transmitting and receiving antennas. The results of the propagation tests show that the signal strength rapidly decreased with an increased in the transmitter-receiver distance. The sensitivity of the signal to atmospheric absorption was shown by the difference in the signal strength of the

uplink and downlink channels, which was approximately 10dB. The signal strength was also observed to drop by 0.9dB per meter from 2m to 46.9m. The received signal strength was observed to be sensitive to the antenna pointing of the radio devices, which required boresight-to-boresight alignment for maximum signal strength. Slight misalignment resulted in the degradation of the received signal strength.

Autonomous creation of multiple-path between the backhaul radio device differentiates the CNSCB architecture from existing architectures. In the third section of chapter 4, the NLOS backhaul problem is formulated and an algorithm for the creation of multiple paths is proposed. Each path is represented using the SKED geometry. The genetic algorithm is used to solve the path selection optimisation problem, which minimizes the diffraction loss on a NLOS path as the main objective. Simulation results showed that up to 15 possible path can be identified using the GA-generated SKED model parameters. An evaluation of the proposed algorithms showed that a high crossover probability results in more dispersed diffraction points, implying that more points with which to establish connectivity would be available. A high mutation rate also gave the same result.

The last section of the chapter is dedicated to developing a genetic algorithm for maximizing the number of diffraction points that can cover a SCBS location. The concept of maximal covering location problem (MCLP) was used in the optimization model. The GA is used to generate the location coordinates and to determine the distances between the SCBS locations and the diffraction points. Simulation results showed that the algorithm can identify between 60% and 98% of potential points for covering a base station location. A comparison of four SCBS locations showed that each location could be covered by up to approximated 98% of the identified diffraction points. The learning capabilities of the GA are also shown by the gradual process of obtaining the points observed. The results of the learning capability tests showed

that the algorithm gradually identified up to 50 diffraction points after just about 15 generations.

Results of the link selection and location coverage algorithms show that the GA can be used as reasoning algorithms in the cognitive engine of the backhaul radio devices.

Learning is the source of intelligence of the CNSCB system radio devices. In **Chapter 5**, a novel learning algorithm based on Q-learning was developed. The algorithm allows the radio devices to gather information from the operating environment, i.e. the wireless channel; compare this with information stored in the radio database, and make decisions based on whether the current conditions meet the required performance conditions or not. Specifically, three parameters were used in the model: data rate, traffic level, and conditions on the wireless channel represented as levels of path loss exponent. The proposed algorithm enables the radio devices to take various actions; to switch to a better performing path, increase transmission power to increase data rate or activate or deactivate sleeping mode in the event of detecting low traffic levels to save energy.

The results obtained show that the algorithm can achieve the target data rate, switch to an alternative path or operating mode within the prescribed time. Furthermore, the results show that a large discount factor improves the performance of the learning algorithm, enabling to achieve the required target faster than low values. This is important as it improves the overall performance of the system. Using a high learning rate is also shown to improve the performance of the GA by achieving the target values earlier than using a lower learning rate.

This thesis also studied the energy efficiency in SCB solutions based on mmW and massive MIMO technologies. The focus was to develop a framework for analysing and evalauting the energy efficiency of the proposed CNSCb system. Specifically, **Chapter 6** provides insight into the energy consumption on the networks, which takes

into account not only the energy required to keep the radio equipment active, but also also the energy used in the encoding and decoding of data traffic from the user device, SCBS and backhaul equipment up to the aggregation site. The framework takes into account the high traffic volumes expected in 5G wireless transport networks and a large number of backhaul devices expected to be deployed which results in increased energy usage on the backhaul networks. The energy efficiency of the proposed PtMp architecture is compared with that of the PtP configuration. Simulation results obtained show that as the backhaul traffic increases, the energy efficiency of the networks decreases. The energy efficiency is also shown to decrease with an increase in the number of backhaul links. A comparative analysis of the two configurations shows that when both systems are fully loaded, the PtMP system is more efficient than the PtP configuration.

7.2 Recommendations

There are a number of research issues and related avenues that need to be investigated based on the work presented in this thesis. This section describes possible future work related to the contributions of each of the chapters.

7.2.1 State-of-the-art research for 5G backhaul

Small cell deployment is already under way. However, suitable backhaul solutions still top the priority list of network operators. This research revealed the key candidate backhaul technologies for small cells. To reduce operational costs, heterogeneous backahul systems are being proposed. An open research is integration of these technologies with other emerging technologies such G.Fast in order to realise heterogeneity in the backhaul.

7.2.2 5G Backhaul architectures

This research proposed an architecture for NLOS connectivity at mmW frequencies. The issue of scalability was addressed through the proposed use of massive MIMO. However emerging architectures include virtualisation of the backhaul service. SDN-based architectures also being proposed for dynamic resource allocation in the backhaul. Combining the device intelligence introduced in this research with the concepts of SDN will improve network performance by allowing the radio devices to use their intelligence to pro-actively minimize the effects of link malfunctioning on the services. In cases where the device fails, SDN can re-route traffic away from the failed device. Realising these architectures under NLOS conditions can be challenging.

7.2.3 Development of databases for the backhaul radio devices

Learning and optimization algorithms were developed and implemented in this research. The information used as the basis for comparing current network conditions was assumed to be available in the radio's databases. Furthermore, the schemes for storage of the information of the learned information was not covered in this research study. Developed of such schemes suitable for use on radio devices with limited storage and processing capacity is an interesting area of research.

7.2.4 SON in the small cell backhaul segment

The overwhelming growing size of backhaul networks dictates the use of SON to automate network organisation and optimisation in a distributed manner. This has the advantage of fast network adaptability, to dynamic changes in the network, compared to centralized solutions. Algorithms for achieving some SON capabilities were developed in this research. However, the development of more algorithms is still required to realise full SON capabilities. Furthermore, research into the design of

efficient low complex algorithms is still required to avoid an increase in the cost of the equipment and energy consumption.

7.2.5 Joint access and backhaul energy management

A framework for analysing and evaluating the energy consumed on the backhaul systems was developed in this research study. Energy management using sleeping modes on the backhaul has also been proposed in literature. However, coordinating the energy management process on the access and backhaul can be done jointly to improve overall energy efficiency on the network. The development of such algorithms presents an opportunity for further research as joint access and backhaul energy management in 5G small cell networks

Appendix A

A.1 Propagation characteristics of mmW frequencies

This section provides details on propagation at mmW frequency bands and genetic algorithms. Propagation by diffraction involves the bending of radio signals when they encounter obstacles. The effects of an obstruction on a radio signal depend on the wavelength of the signal and radius of curvature of the obstacle [125]. The energy loss at a point of diffraction, i.e. diffraction loss, is inversely proportional to the wavelength of the signal, and hence directly proportional to the operating frequency [125]. Radio signals at sub-6GHz frequencies have longer wavelength compared to that of 10-100GHz spectrum bands and are therefore less prone to diffraction loss. Signals in the latter frequency bands, therefore, suffer severe diffraction loss.

The diffraction loss is also determined by the radius of curvature of the obstruction, with a larger radius of curvature (R) giving rise to less energy loss compared to a smaller R. Most of the obstructing objects in urban areas have small radii of curvature. Radio signals at mmW frequencies are therefore more prone to energy loss compared to those outside urban environments. Furthermore, radio signals with smaller wavelength are more likely to suffer more energy loss since the small wavelength of the signals is comparable to the size of R for most obstructing objects

in urban environments [125]. Diffraction loss in the received signal results in reduced signal strength, hence the quality of the wireless link. Excessive diffraction loss may result in link outage and unavailability, hence packet loss.

The concept of Fresnel zone is useful when describing diffraction loss in wireless systems. The Huygens-Fresnel principle, which states that *"each point on a wavefront acts as a signal source"* , is used to explain the concept of propagation by diffraction. Radio signals can, therefore, propagate round obstructions as long as there exists a portion of the Fresnel zone visible between the transmitter and the receiver [126]. Objects should be kept off the first Fresnel zone to avoid causing destructive interference between transmitted signals. For sub-6GHz frequencies, buildings are located within the first Fresnel zone, which results in minimal diffraction loss. For higher frequencies, however, the radius of the first Fresnel zone is small, and most of the signal power is absorbed by obstructing objects. However, experimental tests at mmW frequencies conducted in [9] have shown that by carefully pointing the signal beam at the correct angle and at the edge of a building or roof at higher frequencies, signals with a high signal strength can be detected at the other side of the obstructing edge. Since Fresnel zones affect signal strength, this has an impact on both capacity and coverage. The concept of point the antenna at diffraction point is used in this research to establish NLOS links.

Antenna polarization is another factor to be considered when communication links are based on propagation by diffraction. Diffraction loss varies depending on whether the transmitting antenna is horizontally or vertically polarized. When the transmitting antenna is vertically polarized, and diffraction is over a vertical edge, diffraction loss is less than if the diffraction was over a horizontal edge and vice versa [125]. Antenna polarization, therefore, has an impact on coverage and capacity due to the effects on

signal strength. The effects of antenna polarization are not considered in this research study.

Propagation models for wireless systems exist [82, 123]. However, most of them have been developed for frequencies below 30GHz. The Walfisch-Bertoni model is useful in predicting the effects of rooftops and building edges on radio signal strength, but it is valid for UHF frequency bands only [85]. The Deygout method, which is based on the concept of treating diffraction points as knife edges, was developed to estimate the path loss due to diffraction in urban areas. The model used is called the single knife edge diffraction (SKED) model [86, 87] and can be used at any frequencies including mmW spectrum bands. This method is used in this research to analyze propagation losses due to diffraction in street-to-rooftop SCB links. The expected wide adoption of mmW frequencies for commercial purposes has led to new initiatives to develop propagation models for mmW frequencies bands [8]. With limited knowledge of the propagation characteristics of radio signals at mmW frequencies, recent research efforts have also focused on feasibility studies on the mmW frequency bands, results of which are now being used to develop propagation models for the 30-90GHz frequency bands [8].

The main reason for the differing propagation characteristics is the short wavelength associated with mmW frequencies, which equates to the diameter of atmospheric gasses, making the wireless signals more prone to atmospheric absorption. This results in high propagation losses and therefore shorter transmission distances compared to sub-6GHz frequencies. In the V-band i.e. 57-66GHz, attenuation is mainly due to oxygen absorption, whereas in the E-band i.e. 70-80GHz, attenuation is due to rain. Fig. 1 illustrates the signal attenuation at different frequency bands [123]. Frequencies in the white region are less prone to atmospheric attenuation and have therefore been popularly used in mobile networks. The attenuation in the green

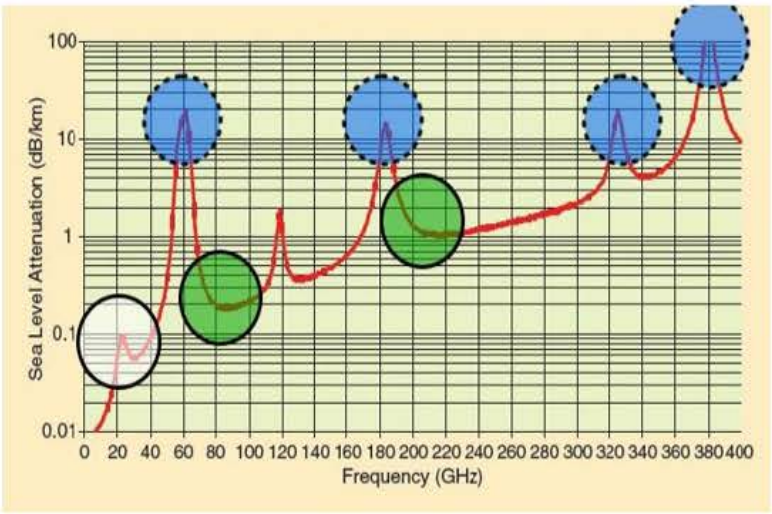

Figure 1: Signal attenuation at high frequencies [123]

regions (70/90GHZ) is higher than in the white circle, but short hop links up to 2km, with improved spectral efficiency and reduced inter-system interference are possible. However, high gain antennas can be used to compensate for the losses as illustrated in link budget calculations, using equation 1.

$$P_{rx} = P_{tx} + G_{tx} + G_{rx} - 92 - 20log_{10}(d) - 20log_{10} - 20log_{10}(f) - L_f - L_{NLOS} \quad (1)$$

where P_{rx} is the received power, P_{tx} is the transmitted power, G_{tx} and G_{rx} are transmitter and receiver antenna gains respectively, d is the distance separating the transmitter and receiver in km, f is system operating frequency in GHz, L_f represents any losses due to fading, L_{NLOS} is the additional loss due to NLOS deployment [18].

A.2 The genetic algorithm elements and processes

The elements of GA are the initial population, chromosomes, and genes. The solution of optimization problems involves selection of the initial population, which consists of a number of randomly generated chromosomes representing the optimization parameters. Each individual chromosome's fitness to reproduce is evaluated against some fitness function. The next generation of chromosomes is selected based on the value of its calculated fitness. A summary of the GA processes is given below. The

description is based on a binary-GA (bGA), in which the chromosomes are made up of binary digits [59].

1. Initial population generation: The initial population can be randomly generated or predefined by the user. The size of the population must be taken into consideration. Too large a population may result in the algorithm taking too long to converge and too small a population may result in a lack of diversity in the solution.

2. Termination: A stopping criteria for terminating the GA must be defined since it is a stochastic search method. Terminating criteria can be the number of generations, a computer clock or a threshold to the diversity of the population.

3. Crossover: Crossover involves the combination of selected parent chromosomes to generate new offspring. This is achieved through the selection of a cut-off point on each of the parent chromosomes, breaking it into two. The first half of the first chromosome is moved to the second half of the second one, creating the first child chromosome. Next, the second half of the first chromosome is combined with the first half of the second one resulting in the second child chromosome. The process is most suited in cases where the chromosomes are represented by binary digits. The probability of crossover Pc is defined as the ratio of the number of offspring to the population size.

4. Mutation: The mutation process produces random changes in the chromosomes by replacing chromosomes lost in the selection process and introducing new chromosomes. This introduces more diversity in the population, resulting in a better solution. The probability of mutation Pm is the ratio of mutated chromosomes to the population size.

5. Selection: The selection process involves choosing the chromosomes that must survive into the next generation. Several methods for selecting the surviving chromosomes are available, the most commonly used are roulette wheel, tournament, and ranking.

6. Fitness Evaluation: Fitness evaluation is the process of checking the calculated value of the objective function subject to constraints. At each generation, good solutions are reproduced and bad solutions are discarded.

7. Inversion: Inversion is the process in which the locations of genes in a chromosome are reversed to create more diversity in the population. For example, a gene in the first position is moved to the last position and the gene in the last position is moved to the first position. Next, a gene in the second swaps positions with a gene in position n-1, where n is the number of genes in the chromosome, and so on.

Bibliography

[1] Cisco, "Cisco visual networking index: Global mobile data traffic forecast update, 2015-2020," *Cisco White Paper*, 2016.

[2] L. Militano et al., "Device-to-device communications for 5G Internet of things", *EAI Endorsed Transactions on Internet of Things*, Vol. 15, Issue 1, 2015.

[3] R. N. Clarke, "Expanding mobile wireless capacity: The challenges presented by technology and economics," *Elsevier*, vol. 38, no. 8-9, pp.693-708, 2014.

[4] Small Cell Forum "Backhaul technologies for small cells: Use cases, requirements and solutions" *Small Cell Forum*, 2013. Available online, https://ytd2525.files.wordpress.com/2013/03/049-backhaul-technologies-small-cells.pdf, 2012.

[5] J. Robson, "Small cell backhaul requirements" *NGMN Alliance*, white paper, 2012.

[6] Small Cell Forum, "Small cell deployments market status report," *Small Cell Forum White Paper*, 2016.

[7] SenzaFili Consulting, "Backhaul for small cells Finding the right cost/performance tradeoffs to meet the backhaul challenge ", Available online, http://www.senzafiliconsulting.com/Portals/0/docs/Reports/SenzaFili_SMCLBKH_FullReport.pdf?ver=2015-06-06-040838-000, 2012.

[8] T. S. Rappaport et al., "Wideband millimeter-wave propagation measurements and channel models for future Wireless Communication System Design ", *IEEE Trans, on Comm.*, Vol. 63, issue 9, pp.3029-3056, 2015.

[9] M. Coldrey et al., "Non-line-of-sight small cell backhauling using microwave technology," *IEEE Comm. Mag.* , Vol. 51, issue 9, pp.78-84, 2013.

[10] J. Karjalainen et al, "Challenges and opportunities of mm-wave communication in 5G networks," *IEEE CROWN*, 2016. pp.372-376, 2014.

[11] S. Tombaz et al., "Impact of densification on energy efficiency in wireless access network" *IEEE Globecomm Workshop*, pp. 57-62, 2012.

[12] 4G Americas, "Self-optimizng networks: the benefits of SON in LTE", *4G Amercias*, Available online, http://www.4gamericas.org/files/2914/0759/1358/Self-Optimizing_Networks-Benefits_of_SON_in_LTE-July_2011.pdf, 2011.

[13] CLAdirect "Connectivity: Why would 5G connectivity be dominant by 2020", *CLAdirect*, Available online, http://cladirect.com/en/2016/01/07/connectivity-why-would-5g-connectivity-be-dominant-by-2020/, 2016.

[14] E. Yaacoub et al, "An overview of research topics and challenges for 5G massive MIMO antennas",*IEEE MECAP*, pp.1-4, 2016.

[15] S. Samarakoonet et al., "Opportunistic sleep mode strategies in wireless small cell networks" *IEEE ICC*, pp.2707-2712, 2014.

[16] G. Zhang et al., "Fundamentals of heterogeneous backhaul design, analysis and optimization" *IEEE Trans. on Comm.*, Vol. 64, Issue 2, pp. 876-889, 2016.

[17] J. Mitola, "Cognitive radio an integrated agent architecture for software defined radio",*KTH* Available online, http://www.diva-portal.org/smash/get/diva2:8730/FULLTEXT01.pdf, 2000.

[18] J. Hansryd et al., "Non-line-of-sight microwave backhaul for small cells", *Ericsson Review*, 2013.

[19] B. Malila et al., "Design of a Cognitive Small Cell Backhaul System for Non-Line-of-Sight Deployment in Urban Canyons", *SATNAC*, 2014.

[20] B. Malila et al., "Performance analysis of NLOS small cell backhaul using 17GHz point-to-point prototype radio", *IEEE MELECON*, pp1-6, 2016.

[21] M. Jaber, "5G backhaul challenges and emerging researching directions: a survey" *IEEE Access*, Vol. 4, pp.1743-1766, 2016.

[22] Small Cell Forum, "Urban small cells in the real world" *Small cell Forum*, June 2014.

[23] B. Li et al, "Small cell in-band wireless backhaul in massive multiple-input multiple-output systems", *IEEE ICC*, pp.1838-1844, 2015.

[24] J. S. Lu et al, "Measurement and characterization of various outdoor diffracted and scattered paths", *IEEE Milcom*, pp.1238 - 1243, 2013.

[25] 5PPP, "The 5G Infrastructure public private partnership: the next generation of communication networks and services", *5GPPP*, Available online: https://5g-ppp.eu/wp-content/uploads/2015/02/5G-Vision-Brochure-v1.pd, 2015

[26] A. H. Jafari, et al., "Small cell backhaul: challenges and prospective solutions", *J Wireless Com Network*, 206. doi:10.1186/s13638-015-0426-y, 2015.

[27] X. Ge et al., "5G Wireless backhaul networks: challenges and research advances" *IEEE Network*, Vol. 28 issue 6, pp. 6-11, 2014.

[28] ITU-R, "IMT Vision: Framework and overall objectives of the future development of IMT for 2020 and beyond", *ITU*, Nov. 2015.

[29] J. Monserrat et al, "METIS research advances towards the 5G mobile and wireless system definition", EURASIP JWCN vol. 2015, p. 53, Mar. 2015.

[30] NGMN, "5G", White Paper. . Available online, http://www.3gpp.org/technologies/presentations-white-papers, 2015.

[31] E. Dahlman et al, "5G radio access", *Ericsson Review,* June 2014.

[32] M. Jeong et al., "8-10Gbps terrestrial optical free-space transmission over 3.4 km using an optical repeater", *IEEE Photon. Technol. Lett.*, vol. 15, issue 1, pp. 171-173, 2003.

[33] P. Wainio and K. Seppanen, "Self-optimizing last-mile backhaul network for 5G small cells" *IEEE ICC*, pp. 232-239, 2016.

[34] E. Karamad et al, "Optimizing placements of backhaul hubs and orientations of antennas in small cell networks", *IEEE ICC*, pp.68-73, 2015.

[35] Real Wireless, "Techniques for increasing the capacity of wireless broadband networks: UK, 2012-2030", *Real Wireless*, white paper, Available online, https://www.ofcom.org.uk/static/uhf/real-wireless-annex1.pdf, 2012.

[36] 3GPP, "Self-Organizing Networks (SON): Concepts and requirements", *3GPP*, Available online, https://5g-ppp.eu/wp-content/uploads/2015/02/5G-Vision-Brochure-v1.pd, 2011.

[37] A. Imran et al, "Challenges in 5G: how to empower SON with big data for enabling 5G", *IEEE Network*, Vol. 28, issue 6, pp.27-33, 2014.

[38] T. K. Vu et al, "Joint in-band backhauling and interference mitigation in 5G heterogeneous networks", *European Wireless conference*, pp.1-6 2016.

[39] Z. Gao et al, "Millimeter wave massive-mimo-based wireless backhaul for the 5G ultra-dense network", *IEEE Wireless Comm.*, Vol. 22, issue 5, pp.13-21, 2015.

[40] A. Ahmed and D. Grace, "Energy-aware topology management for 5G dual-hop ultra-high capacity backhaul networks exploiting path diversity", *IEEE ICUFN*, pp.1020-1025, 2016.

[41] P. Demestichas et al, "5G on the horizon", I*EEE Vehicular Tech. Mag.*, Vol. 8, issue 3, pp.47-53, 2013.

[42] 5G PPP, "View on 5G architecture", *5G PPP*, 2016.

[43] W. Feng et al, "Millimetre-wave backhaul for 5G networks: challenges and solutions", *Journal on Sensors*, 16, 892; doi:10.3390/s16060892, 2016.

[44] N. Bhushan et al., "Network densification: the dominant theme for wireless evolution into 5G," *IEEE Commun Mag.*, Vol. 52, issue 2, pp. 82âĂŞ89, 2014.

[45] J. Laskar et al, "CMOS, Cognitive and mmW: A Wireless Revolution," *IEEE RWS*, 2016. pp.211-214, 2012.

[46] H. Zhao, et al, "28 GHz Millimeter wave cellular communication measurements for reflection and penetration loss in and around buildings in New York City", *IEEE ICC*, pp.5163-5167, 2013.

[47] T. S. Rappaport et al.,"Millimeter wave mobile communications for 5G cellular: it will work!" *IEEE Access*, Vol. 1, pp. 335-349, 2013.

[48] S. Rangan et al., "Millimeter wave cellular wireless networks: potentials and challenges", *IEEE Proceedings*, Vol. 102, issue 3, pp.366-385, 2014.

[49] Y. Niu, et al., "A survey of millimeter wave (mmW) communications for 5G: Opportunities and challenges", *Wireless Netw*, doi:10.1007/s11276-015-0942-z, 2015.

[50] P. Moorhead, "Intel And Qualcomm Partner (Yes, Really) To Move WiGig 60 GHz 802.11AD Wi-Fi Forward", *Forbes*, Available online, http://www.forbes.com/sites/patrickmoorhead/2016/02/03/intel-and-qualcomm-partner-yes-really-to-move-wigig-60-ghz-802-11ad-wi-fi-forward/#5d6c94cb13c4, 2016.

[51] Samsung, "Samsung electronics develops key RF technology for smaller 5G equipment and devices", Available online, https://news.samsung.com/global/samsung-electronics-develops-key-rf-technology-for-smaller-5g-equipment-and-devices, 2016.

[52] FP7, "5G Radio network architecture", *Future Networks Cluster*, Available online, http://www.ict-ras.eu, October 2015.

[53] J. Haikun et al, "Research on CMOS mm-wave circuits and systems for wireless communications," *China Communications*,Vol 12, Issue 5, pp 1-13, 2015.

[54] T. E. Bogale and L. B. Le, "Massive MIMO and mmWave for 5G wireless HetNet", *IEEE VT Mag.*, Vol. 11, issue 1, pp.64-75, 2016

[55] Y. Gao et al., "Energy efficient cooperative sleep control using small cell for wireless networks", *International Journal of Distributed Sensor Networks*, Vol. 11, issue 8, 2015.

[56] J. Mitola, "The Software Defined Radio", *IEEE Comm. Mag.*, pp. 26-38, 1995.

[57] W. Lifeng and W. Shengqun, "Cognitive engine technology", Available online, wwwen.zte.com.cn/endata/magazine/ztecommunications/.../t20090630_173458.html, 2016.

[58] C. Jiang et al, "Machine learning paradigms for next-generation wireless networks", *IEEE Wireless Comm.*, Vol. 23, issue 99, pp.2-9, 2016.

[59] R. L. and S. Haupt, "Practical genetic algorithms" *John Wiley & Sons, New Jersey*, 2004.

[60] N. Abbas et al, "Recent advances on artificial intelligence and learning techniques in cognitive radio networks", *Eurasip JWCN*, 174, 2015.

[61] A. Holzinger et al, "Darwin, Lamarck, or Baldwin: Applying evolutionary algorithms to machine learning techniques", *IEEE Comsoc*, Vol. 2m pp 449-453, 2014.

[62] NGMN, "5G NGMN", *NGMN*, Available online, https://www.ngmn.org/uploads/media/NGMN_5G_White_Paper_V1_0.pdf, 2015.

[63] S. Khan, et al, "The benefits of SON in self-organising backhaul networks", *Ericsson Review*, 2013.

[64] N. Wang et al, "Backhauling 5G small cells: A radio resource management perspective", IEEE Wireless Comm., Vol. 22, issue 5, pp.41-49, 2015,

[65] H. Tabassum et al, "Massive MIMO-enabled wireless backhauls for full-duplex smalls", *IEEE GLOBCOM*, pp.1-6, 2015.

[66] R. Taori and A. Sridharan, "In-Band, point-to-multi-point, mm-Wave backhaul for 5G networks" *IEEE ICC Workshop on 5G Technologies*, pp96-101, 2014.

[67] Ericsson Review, "Wireless backhaul in future heterogeneous networks", *Ericsson Review*, Nov. 2014.

[68] K. Balachandran et al, "Capacity benefits of relays with in-band backhauling in cellular networks", *IEEE ICC*, pp.3736-3742, 2008.

[69] U. Siddique et al, "Adaptive in-band self-backhauling for full-duplex small cells", *IEEE ICC*, pp.44-49, 2015.

[70] Y. Shi, "A flexible backhaul architecture for small cell networks", *IEEE PIMRC*, pp.1679-1684, 2014.

[71] M. N. Islam et al., "Wireless backhaul node placement for small cell networks", *IEEE CISS*, pp.1-6, 2014.

[72] C. Bojic et al., "Advanced wireless and optical technologies for small cell mobile backhaul with dynamic software-defined management", *IEEE Comm. mag.*, Vol. 51, issue 9, pp.86-93, 2013.

[73] R. Villar et. al, "Wireless backhaul architecture for small cells deployment exploiting Q-band frequencies", *IEEE Future Network and Mobile Summit* , pp.1-11, 2013.

[74] M. Zolotukhin et al, "On optimal relay placement for improved performance in non-coverage limited scenarios", *ACM MSWiM*, pp127-135, 2014.

[75] A. Sayenko et al, "On optimal placement of low power nodes for improved performance in heterogeneous networks", *IEEE/IFIP NOMS*, pp.349-357, 2016.

[76] K. Lakhani et al., "Optimization of cognitive radio in NLoS backhauling of small cells", Available online www.diva-portal.org/smash/get/diva2:831362/FULLTEXT01.pdf, 2013.

[77] J. Ala-Laurinaho et al, "MM-wave lens antenna with an integrated LTCC feed array for beam steering", *4th EuCAP*, pp.1-5, 2010.

[78] A. Karttunen et al, "Using optimized eccentricity rexolite lens for electrical beam steering with integrated aperture coupled patch array", *Progress In Electromagnetics Research*, Vol. 44, issue B, pp. 345âĂŞ365, 2012.

[79] J. Ala-Laurinaho et al, "A mm-wave integrated lens antenna for E-band beam steering", *9th EuCAP*, pp.1-2, 2015.

[80] R. Kalimulin et al, "Impact of mounting structures twists and sways on point-to-point millimeter-wave backhaul links", *IEEE ICCWSHOPS*, pp. 19-24, 2015.

[81] M. Cudak et al, "Experimental mm wave 5G cellular system", *IEEE GLOBECOM WSHOPS*, pp.377-381, 2014

[82] P. K. Sharma and R.K Singh, "Comparative analysis of propagation pathloss models with field measured data", *IJEST*, Vol. 2, issue 6, pp.2008-2013, 2010.

[83] C. Phillips et al., âĂIJThe efficacy of path loss models for fixed wireless rural wireless linksâĂİ, *Springer*, Vol 6579, pp42-51, 2011.

[84] C. Akkash, "Methods for path loss prediction", Available online: https://pdfs.semanticscholar.org/6228/24c07fb8c08cb8714d399ad81010c55635dc.pdf, 2009.

[85] J. Walfisch and H. L. Bertoni, "A theoretical model of UHF propagation in urban environments", *IEEE Transactions on Antennas and Propagation*, pp1788-1796, 1988.

[86] ITU-R, "Propagation by diffraction", *ITU-R*, 1999.

[87] G. M. Galvan-Tejada, "Wimax urban coverage based on the Lee model and Deygout diffraction method", *IEEE CCE*, pp. 294-299, 2010.

[88] P. Sankaro, "Performance analysis of diffraction gain (Gd) due to presence of knife-edge as compared to free space e-field and identifying position of obstacle in a fresnel zone", *IJSRP*, Vol. 3, issue 1, 2013.

[89] ITU-R, "Characteristics and applications of fixed wireless systems operating in frequency ranges between 57 GHz and 134 GHz", *ITU-R Report F.2107-2*, 2011.

[90] G. Y. Delisle et al., "Propagation loss prediction: a comparative study with application to the mobile radio channel", *IEEE Transactions on Vehicular Technology*, Vol. 34, issue 2, pp.86-96, 1985.

[91] M. Bennai et al., "Medium range backhaul feasibility under NLOS Conditions at 60GHz", *IEEE GSMM*, pp1-3, 2015.

[92] P. Okvist et al., "15GHz Propagation properties assessed with 5G radio access prototype", *IEEE PIMRC*, pp22-26, 2015.

[93] F. Letourneux, et al, "Small-cell wireless backhaul and access networks: Realistic modeling and holistic analysis", *10th EuCAP*, pp.1-5 2016.

[94] C. Ranaweera et al, "Cost-optimal placement and backhauling of small cell networks", *Journal of Lightwave Technology*, Vol. 33, issue 18, pp.3850-3857, 2015.

[95] M. Gen et al, "Network models and optimization: a multi-objective genetic algorithm approach", *Springer, ISBN:1848001800 9781848001800*, 2008

[96] R. Kumar et al, "Topological design of communication networks using multi-objective genetic optimization", *IEEE CEC*, Vol. 1, pp.425-430, 2002.

[97] P. K. Tripathy, et al, "A genetic algorithm based approach for topological optimization of interconnection networks" , *Elservier, ICCCS*, Vol. 6, pp.196-205, 2012.

[98] R. Santos and A. Kassler, "A SDN controller architecture for small cell wireless backhaul using a LTE control channel", *IEEE WoWMoM*, pp. 1-3, 2016.

[99] J. Nunez-Martinez et al, "WiseHAUL: An SDN-empowered wireless small cell backhaul testbed", *IEEE WoWMoM*, 2016, pp.1-3, 2016.

[100] R. Church and C. Revelle, "The maximal covering location problem", www:geog:ucsb:edu=forest=G294download=maxcoverrlccsr:pdf, Available on-line accessed Sept 2016.

[101] A.T Murray, "Maximal coverage location problem: impacts, significance and evolution", *Journal on International Regional Science Review*, Vol. 39, pp5-27, 2016.

[102] A.T Murray, "Coverage optimization to support security monitoring", *Elservier: Journal on Computers, Environment and Urban Sytems*, Vol. 31, pp.133-147, 2007.

[103] K. Tutschku, "Demand-based radio network planning of cellular mobile communication systems", citeseerx.ist.psu.edu/viewdoc/download, Available online, accessed Sept 2016.

[104] S. Indhumathi and D. Venkatesan, "Improving coverage deployment for dynamic nodes using genetic algorithm in wireless sensor networks", *India Journal of Science and technology*, Vol. 8, issue 16, 2015.

[105] M. Aadhil and J.R Roselin, "Maximizing coverage problem using genetic algorithm in wireless sensor network", *IJETAE*, Vol. 4, Issue 2, 2014.

[106] L.V Snyder, "Covering Problems", www.lehigh.edu/lvs2/Papers/CoveringProblemsFINAL.pdf, Available online, accessed Sept 2016.

[107] J. Carr, "30GHz and 60GHz angle-dependent propagation for cellular peer-to-peer wireless communications", *IEEE ICC*, pp4568-4573, 2012.

[108] A. D. Le et al, "Achievable rates and outage probability of cognitive radio with dynamic frequency hopping under imperfect spectrum sensing", *IET Communications*, Vol 9, issue 17, pp. 2160-2167, 2015.

[109] S. Agarwal and S. De, "Cognitive Multihoming System for Energy and Cost Aware Video Transmission", *IEEE Trans. on CCN*, Vol 2, issue 3, 2016.

[110] L. Le and E. Hossain, "A mac protocol for opportunistic spectrum access in cognitive radio networks", *2008 IEEE WCNC*, March 2008, pp. 1426–1430.

[111] P. Ohlen et al., "Flexibility in 5G transport networks: the key to meeting the demand for connectivity", https://www.ericsson.com/en/publications/ericsson-technology-review/archive/2015/flexibility-in-5g-transport-networks-the-key-to-meeting-the-demand-for-connectivity

[112] E. Grass et. al, "Dynamically reconfigurable optical-wireless backhaul/fronthaul with cognitive control plane for small cells and cloud RANS (5G-Xhaul", http://cordis.europa.eu/project/rcn/197339_en.html, Available online, accessed August 2016.

[113] D. Chen et al., "5G self-optimizing wireless mesh backhaul: A proof-of-concept demo on interconnected small cell wireless backhaul", *IEEE INFOCOM*, pp. 23-24, 2015.

[114] J. S. Kim et al., "System coverage and capacity analysis on millimeterwave band for 5G mobile communication systems with massive antenna structure", *Hindawi, IJAP*, Vol. 2014, Article ID 139063, 11 pages, 2014.

[115] G. Auer et. al, "Energy efficiency analysis of the reference systems, areas of improvements and target breakdown", Available online, https://www.ict-earth.eu/publications/deliverables/deliverables.html, accessed 2016.

[116] X. Ge et al., "Energy efficiency of small cell backhaul networks based on Gauss-Markov mobile models", *IET Network*, Vol. 4 issue 2, pp. 158-167, 2015.

[117] D. Ha et al., "Energy efficiency analysis with circuit power consumption in massive MIMO systems", *IEEE PIMRC*, pp. 938-942, 2013.

[118] R. S. Sutton and A. G. Barto, "Reinforcement learning: An introduction", http://people.inf.elte.hu/lorincz/Files/RL_2006/SuttonBook.pdf, Available online, accessed Aug 2016.

[119] B. Partov et al., "Dynamic idle mode control in small cell networks", https://www.scss.tcd.ie/Doug.Leith/pubs/Small_Cell_FP_V4.pdf, Available online, accessed Aug 2016.

[120] S. Tombaz, "Impact of backhauling power consumption on the deployment of heterogeneous moile networks", *IEEE Globecom*, pp.1-5, 2011.

[121] P. Monti et. al, "Mobile backhaul in heterogeneous network deployments: technology options and power consumption", *IEEE ICTON*, pp.1-7, 2012.

[122] I. Widjaja and H. Roche, "Sizing X2 bandwidth for inter-connected eNBs", *EEE VTC*, pp. 1-5, 2009.

[123] G. R. MacCartney Jr., et al, "Path loss models for 5G millimeter wave propagation channels in urban microcells", *IEEE GLOBECOM*, pp.3948-3953, 2013.

[124] F. Iqbal, and F. Kuipers, "Disjoint paths in networks," Available online, https://www.nas.ewi.tudeflt.nl, 2015

[125] ITU-R, "Propagation by diffraction", *ITU*, November 2013.

[126] Lecture notes, "Wireless system design: fresnel zones and diffraction", Available online, www.ece.ubc.ca/~edc/7860/exams/midterm.pdf, 2013.

[127] B. Malila et al, "Small cell backhaul design using genetic algorithm", *Procdeedings of SATNAC2015*, pp.15-20, 2015.

[128] 3GPP, "User equipment (UE) radio transmission and reception (FDD)", *3GPP TS 25.101 V14, 3GPP*, June 2016.